Investigating the effects of inflammatory mediators on the neuroinflammation response

X Sawkulycz

2022

Investigating the effects of inflammatory mediators on the neuroinflammation response

A thesis submitted in partial fulfilment of the requirements of Manchester Metropolitan University for the degree of Doctor of Philosophy

Xenia Sawkulycz

Department of Life Sciences Manchester

Centre for bioscience

Metropolitan University

2022

COVID-19 IMPACT STATEMENT

The progress of this PhD project was significantly affected by the covid-19 pandemic, upon the announcement of the national lockdown in March of 2020 my university closed the campus, including research labs, to all staff and students. With the easing of the restrictions in August of 2020 my university began to gradual re-open and welcome back staff and students. Several restrictions were put in place to mitigate any risks to people attending the university, these extended to the research labs. These restrictions included the labs operating at a 50% occupancy and students being advised to attend up to three days a week. When a second lockdown was announced in January of 2021, lab work was halted for up to 12 weeks, impeding my experiments and my ability to generate data for my thesis.

Acknowledgments

Thank you to Dr Xianwei Zeng for the financial support for this PhD and being a part of the supervisory team.

I would like to thank my supervisory team, Professor Mark Slevin, Dr Baoqiang Guo, and Dr Chris Murgatroyd for giving me the opportunity to do a PhD at MMU. To my director of studies, Professor Mark Slevin. Without your guidance, encouragement, and expertise, I could never have completed this PhD and become the scientist I am today. It was a real pleasure being a part of your research team over the last three years. To Chris Murgatroyd, my scientific career started when I did a Master of Research with you. You believed in me and gave me all the opportunities to become the research scientist I am today. I am appreciative of all the advice that you have given me over my career at MMU.

I would like to thank everybody in the Centre of Bioscience, especially members of staff which include Dr Stuart Fielding and Glenn Ferris. Your continued support in the labs and advice has made be a better researcher. Thank you to all my colleagues and friends on the first, third and fourth floor of the labs. I would like to thank Helen, Laura, Lauren, Azzia, Amelia, Nirali and Annelia for making me smile every day and driving me forward to succeed when I was in my darkest days.

Finally, I would like to thank my grandmother (Helga Tamanis) and I dedicate this PhD to you. You may no longer be here with me, but you are in my heart every day. The support you gave me every step of the way made me who I am today. None of this would have been possible without you. We were supposed to be celebrating this day together, but I know you are watching. Caring for you, every single day and completing this PhD was the hardest time of my life. However, what I will take away from it will make my life better. Rest in peace grandma, this PhD is for you.

Abstract

Ischemic stroke is a devastating event which further stimulates a cascade of inflammatory events in the brain, known as neuroinflammation to occur which is important for repair. However, this neuroinflammation is a double-edged sword that can also have a detrimental impact within the brain. Numerous inflammatory markers are known to be stimulated following an ischemic event and one of interest for this study is C reactive protein (CRP) and its isoforms monomeric c reactive protein (mCRP) and native c reactive protein (nCRP). Several different cell types were used throughout this work which included U937 monocytes which were also differentiated into M0 macrophages. Finally, human microglia cell line HMC-3 cell were also used. Lipopolysaccharide (LPS) was used as a positive inflammatory mediator through this work. Pro-inflammatory effects were observed when different cell types were treated with mCRP or nCRP to test for any inflammatory effects. The liver x receptor agonist (GW3965) was selected for its anti-inflammatory properties and current promising research as a therapeutic in ischemic stroke. Micro-fragment adipose tissue (MFAT) conditioned media was used to test its potential anti-inflammatory effect. Levels of inflammatory activity were measured by several different methods including enzyme-linked immunosorbent assay (ELISA), immunofluorescent staining, aggregation analysis and qPCR. Results from this study showed that mCRP can alter the morphology and physiological function of both U937 monocytes and HMC-3 microglia cells. Increased expression of important pro-inflammatory cytokines was observed, including interleukin 1 beta (IL-1β), interleukin 6 (IL-6), tumour necrosis factor alpha (TNFα), highlighting mCRP pro-inflammatory activity. The LXR agonist (GW3965) significantly reduced key pro-inflammatory proteins after HMC-3 microglia cells were stimulated with either LPS or mCRP inflammatory mediators. However, no up regulation or down regulation was observed in gene expression at any time point after treatment. This study demonstrated that mCRP acts as a pro-inflammatory mediator on HMC-3 and U937 monocytes. MFAT, was also seen to have key anti-inflammatory properties with secreting key cytokines and chemokines. An in vitro inflammatory cell model was used to determine MFAT condition medium can attenuate inflammatory cytokine up regulation. MFAT attenuated the up regulation of protein and gene expression levels of key cytokines (TNFα, IL-1β, IL-6, and IL-10) which are involved in neuroinflammation after an ischemic event such as stroke. In conclusion, this study demonstrated that mCRP could cause morphological and behaviour changes in either U937 monocytes or HMC-3 microglia

cells. Further to this mCRP demonstrated pro-inflammatory activity, whilst the use of GW3965 inhibited its pro- inflammatory activity, therefore reducing TNF-α, IL-6, IL-1β, MCP-1, RANTES. On another note, MFAT secreted key cytokines and chemokines into conditioned media (IL-1ra, Il-1β, IL-4)

Table of Contents

Acknowledgments ***4***

Abstract ***5***

List of figures ***10***

List of tables ***11***

Author ***12***

List of abbreviations ***15***

Chapter 1 – Introduction ***17***

1.1 Ischaemic stroke **18**
1.1.1 Epidemiology and pathophysiology of Ischaemic stroke 18
1.1.2 Risk factors for ischemic stroke 18
1.1.3 Current stroke treatments 20

1.2 Neuroinflammation **21**
1.2.1 Concept of neuroinflammation 21
1.2.2 Monocytes 23
1.2.3 Microglia and other brain macrophages 23
1.2.4 Cytokines in neuroinflammation after ischemic event 24
1.2.5 Chemokines 34
1.2.6 Inflammatory mediators 36

1.3 Therapeutics targets for the inflammatory response after ischemic stroke **39**
1.3.1 Existing anti-inflammatory compounds 39

1.4 Overview of stem cells **41**
1.4.1 Mesenchymal stem cells 42

1.5 Aims and objectives. **48**

Chapter 2 – Materials and methods ***49***

2.1 Materials **50**

2.2 Methods **53**
2.2.1 Tissue culture 53
2.2.2 Preparation of C reactive protein isoforms 58
2.2.3 Microscopy 60
2.2.4 Flow cytometry 63
2.2.5 RNA analysis 64
2.2.6 Protein analysis 67
2.2.7 Statistical analysis 73

Chapter 3 – The impact mCRP plays on the morphology and physiology of monocytes. ***74***

3.1 Introduction **75**
3.1.1 The Role of mCRP in the vascular pathology and atherothrombosis 75
3.1.2 Effects of mCRP on monocytes. 76

3.2 Aims and objectives. **77**

3.3 Results **78**
3.3.1 mCRP causes morphological changes in U937 monocytes. 78
3.3.2 mCRP affects the cell viability of U937 monocytes. 80
3.3.3 mCRP promotes U937 monocytes necrosis. 81

3.3.4 mCRP treated monocytes cells exhibit apoptosis and necrosis characteristic under scanning electron microscope. 87
2.3.5 mCRP induced expression of MCP-1 and IL-8 by U937 monocytes in vitro over time. 89

3.4 Discussion 94
3.4.1 Monomeric c reactive induces U937 monocyte physiological and morphological changes. 94
3.4.2 Monomeric c reactive protein promotes cell death and necrosis. 95
3.4.3 MCP-1 and IL-8 gene expression levels are altered after treatment of monomeric c reactive protein. 96

Chapter 4 – Targeting LXR pathway with a Liver X receptor agonist (GW3965) as a potential anti-inflammatory therapeutic target for neuroinflammation. 98

4.1 Introduction 99
4.1.1 Clinical problems of neuroinflammation 99
4.1.2 The role of mCRP in neuroinflammation 100
4.1.3 Agonist compound GW965 as potential treatment for inflammation 101

4.2 Aims and objectives. 103

4.3 Results 104
4.3.1 mCRP causes morphological changes to HMC-3 microglia cells. 104
4.3.2 Holographic quantifiable cell morphological and proliferative features after treatment with CRP isoforms 108
4.3.3 Determine the kinetic dose response for GW3965. 110
4.3.4 Determine the kinetic dose response for GSK4112. 113
4.3.5 LPS and mCRP modulated IL-6 protein levels in HMC-3 microglia cells. 116
4.3.6 mCRP activated IL-6 and regulated through NfKb signalling pathway. 118
4.3.7 LPS and mCRP modulated IL-1β protein levels in HMC-3 microglia cells but not TNFα. 120
4.3.8 The Effects of the GW3965 on LPS/mCRP-Stimulated HMC3 microglia cells expression of chemokines 122
4.3.9 Inflammatory mediators LPS/mCRP significantly increase key anti-inflammatory cytokines levels with GW3965 agonist have no effect. 125
4.3.10 Inflammatory mediators have no effect on IL-1β, IL-6 and TNFα gene expression levels over time course. 127

4.4 Discussion 132
4.4.1 mCRP promotes morphological changes with resident microglia brain cells 132
4.4.2 mCRP causes pro-inflammatory cytokine to increase with GW3965 potentially acting as an inhibiting compound. 133
4.4.3 mCRP does not alter gene expression is several markers at selected time points. 135

Chapter 5 - Determine the potential anti – inflammatory potential of Adipose derided MSCs. 137

5.1 Introduction 139
5.1.1 Anti-inflammatory benefits of MSCs derived from micro-fragmented adipose tissue. 139
5.1.2 Current use of adipose-derived mesenchymal stem cell in a clinical setting 139

5.2 Aims and objectives. 142

5.3 Results 143
5.3.1 Characterisation of key cytokine, chemokine, and growth factor secretion from MFAT samples 143
5.3.2 Differentiation of monocytes into M0 macrophage 147
5.3.3 The Effects of the MFAT Conditioned Medium on the LPS-Stimulated Macrophage Expression of Pro-Inflammatory Cytokines 150
5.3.4 The Effects of the MFAT Conditioned Medium on the LPS-Stimulated Macrophage gene expression. 151

5.4 Discussion 153
5.4.1 Characterisation of Cytokine Secretion from MFAT Samples 153

5.4.2 The Effects of the MFAT Conditioned Medium on the LPS-Stimulated Macrophage Expression of Pro-Inflammatory Cytokines 154
Chapter 6 Conclusions and future work *155*
6.1 Conclusion **155**
6.2 Future work and limitations **156**
Chapter 7 - References *158*
Appendix *172*

List of figures

Figure 1 – Mechanism of neuroinflammation post ischemic stroke 22
Figure 2 – IL-1 signalling pathway. 27
Figure 3 - IL-6 signalling pathway 29
Figure 4 – TNF α signalling pathways. 30
Figure 5 - IL-4 signalling pathway. 32
Figure 6 – Interleukin 10 signalling pathway 33
Figure 7 -Chemokine and receptor function. 35
Figure 8 - Chemical structure of nCRP 37
Figure 9 - LXR activators and effects on gene regulation and pathways 40
Figure 10 - Differentiation on potential of both adult and embryonic stem cells 42
Figure 11 - Location MSC can be harvested. 43
Figure 12 – Mechanism of lipogems device for adipose tissue processing 46
Figure 13 – Morphology of high density U937 monocytic cells. Images were taken using an Axiovert 10x inverted phase contrast microscope. 54
Figure 14 - Morphology of confluent HMC-3 microglia cells. Images were taken using an Axiovert 10x inverted phase contrast microscope. 56
Figure 15 - MFAT sample 10 - Geimsa stain to determine colony count. 57
Figure 16 - Gene of interest temperature gradient 64
Figure 17 - Housekeeping genes temperature gradient 65
Figure 18 - Diagram of the mechanism of multiplex analysis 70
Figure 19 – Cell aggregation induced by CRP isoform (mCRP 100 μg/mL) 79
Figure 20 – The effects of mCRP stimulation on U937 monocytes were examined. 80
Figure 21 – Flow cytometric analysis of apoptosis and necrosis in 3-hour mCRP treated U937 monocytes. 82
Figure 22 - Flow cytometric analysis of apoptosis and necrosis in 6-hour mCRP treated U937 monocytes. 84
Figure 23 - Flow cytometric analysis of apoptosis and necrosis in 24-hour mCRP treated U937 monocytes. 86
Figure 24 - Scanning electron microscopic observation on the effects of mCRP on cellular and nuclear morphology in U937 Cells. 88
Figure 25 – Housekeeping reference gene (TBP + PABC4) stability plot. 89
Figure 26 - IL-8 gene expression from U937 monocytes over 24-hour period 91
Figure 27 – LPS and mCRP alter MCP1 gene expression in U973 monocytes. 93
Figure 28 – Overview of the positive and negative aspects of neuroinflammation 100
Figure 29 - GW3965 chemical structure 102
Figure 30 - Observing HMC-3 morphological changes caused by mCRP. 105
Figure 31 – mCRP causes morphological chances to HMC-3 microglia cells. 107
Figure 32 - Holographic imaging of cells reveal the impact of culture extracellular environment on cell migration and cell motility. 109
Figure 33 – HMC-3 single cell 2D movement trajectories after GW3965 drug treatment displayed as a rose plot. 111
Figure 34 – Kinetic response of GW3965 treated HMC-3 microglia cells for 24-hour period. 112
Figure 35 - HMC-3 single cell 2D movement trajectories after GSK4112 drug treatment displayed as a rose plot. 114
Figure 36 - Kinetic response of GSK4112 over 24-hour period. 115
Figure 37 -GW3965 2.5 μM significantly reduces IL-6 protein levels after treatment with pro-inflammatory mediators (LPS and mCRP) 117
Figure 38 - GW3965 (2.5 μM) reduced pro-inflammatory IL-6 levels in inflammatory mediator stimulated HMC-3 microglia cells. 119
Figure 39 – GW3965 agonist reduced IL-1β levels but not TNF alpha after treatment with LPS and mCRP. 121
Figure 40 – Chemokine protein analysis after treatment with LPS or mCRP plus or minus GW3965 123
Figure 41 – Regulation of monocyte and macrophage chemokines after microglia cells treated with LPS or mCRP. 124
Figure 42 – LPS and mCRP pro inflammatory mediators increases key anti-inflammatory protein expression levels in microglia cells 126
Figure 43 - Gene expression analysis of HMC-3 cells at 3 hrs. 127

Figure 44 – Pro-inflammatory gene expression analysis after 6 hr treatment with inflammatory mediators and anti-inflammatory agonist. 129
Figure 45 - gene expression analysis of HMC-3 microglial cells stimulated with LPS and mCRP for 24 hrs to induce an inflammatory in which to test GW3965 as a potential anti-inflammatory therapeutic target. 131
Figure 46 - Cytokines and growth factors in the MFAT condition medium in a serum free culture for 24hrs and 5 days. 144
Figure 47 – MFAT secretion levels of TGFβ1-3 secretion 145
Figure 48 - Observation of 24 hour and day 5 culture MFAT media for secretion of several important cytokines and growth factors in culture media for one day and five days. 146
Figure 49 - Morphology of U937 cells before and after treatment with PMA at 50 ng/mL for 72 hours to differentiated monocytes to macrophages. 147
Figure 50 - Flow cytometry confirming U937 monocytes differentiation into M0 macrophages 149
Figure 51 - MFAT condition medium attenuated LPS (10 ng/mL) mediated cytokines secretion of IL-1ß and IL-6 150
Figure 52 – Housekeeping gene stability plot for PABC4 and RPLPO 151
Figure 53 – MFAT conditioned media attenuates the upregulation of key-pro-inflammatory cytokines after LPS treatment.C 152
Figure 54 – MFAT conditioned media attenuates the upregulation of key-pro-inflammatory cytokines after LPS treatment. 152
Figure 55 – MFAT conditioned media attenuates the upregulation of key-pro-inflammatory cytokines after LPS treatment. 152

List of tables

Table 1 - Overview of cytokines 25
Table 2 – Extraction and culture of MSCs derived from various tissues 44
Table 3 - Materials 50
Table 4 -Equipment and software 52
Table 5 - U937 cell line complete media recipe 53
Table 6 - HMC-3 microglia complete cell media recipe 53
Table 7 - Adipose derived mesenchymal stem cells complete media recipe 53
Table 8 - Dilution table of standard 59
Table 9 - Forward and reverse primers 66
Table 10 - Serial dilution example preparation taken from IL-8 sigma ELISA kit used during this work. 69
Table 11 - Inflammatory cytokines and chemokines observed. (Bio-Rad 27-plex human cytokine kit) 71
Table 12 - Inflammatory cytokines and chemokines observed (Quantikine multiplex system (R&D Systems Inc, Oxford, UK) 72
Table 13 - IL-8 gene expression analysis of LPS /mCRP treated U937 monocytes. 91
Table 14 - MCP1 gene expression analysis of mCRP treated U937 monocytes. 93
Table 15 – The use of adipose derived stem cell in clinical trials. 140

Author

The author has published the following manuscripts during this PhD.

Publication

1. Sawkulycz X, Bradburn S, Robinson A, Payton A, Pendleton N, Murgatroyd C. Regulation of interleukin 6 by a polymorphic CpG within the frontal cortex in Alzheimer's disease. Neurobiology of Aging. 2020 Aug; 92:75-81. doi: 10.1016/j.neurobiolaging.2020.04.008. Epub 2020 Apr 15. PMID: 32408055

I designed and conducted all experiments which are outlined in this paper. Further to this, I put this paper together with the help of Dr Chris Murgatroyd who is the corresponding author on this paper.

2. Combes L*, Sawkulycz X*, Fang W-H, Guo B, Slevin M. Potential of adipose derived stem cell preparations in neurological repair and regeneration. Biophysics Reports, 2021, 7(2): 81-90. doi: 10.52601/bpr.2021.200025)(*Joint first authorship with Laura Combs)

The planning and writing of this mini review were shared 50/50 with fellow author Laura Combes (Joint first author). This mini review added value to my introduction and chapter 5 in which a large part focuses on repair and regeneration.

3. Guo, B.; Sawkulycz, X.; Heidari, N.; Rogers, R.; Liu, D.; Slevin, M. Characterisation of Novel Angiogenic and Potent Anti-Inflammatory Effects of Micro-Fragmented Adipose Tissue. International Journal of Molecular Sciences 2021, 22, 3271. https://doi.org/10.3390/ijms22063271

I designed and preformed several experiments which were included in these papers and present in chapter 5 of my thesis. (Measuring TGF beta 1 and 3 levels in MFAT conditioned media and observe reduction in IL-6 and IL-1β levels after treatment with and with conditioned media with U937 differentiated macrophage treated with inflammatory stimulant 10 ng/ml of LPS

4. Slevin.M, **Sawkulycz X,** Combes L, Guo B, Wen-Hui Fang, Zeinolabediny Y, Liu D, Ferris G, Ludlaim A. Laser-Capture microdissection for measurement of angiogenesis after stroke. Stroke biomarkers 2020, DOI: 10.1007/978-1-4939-9682-7_7,

   Jointly wrote the methods section with G Ferris for this chapter entitled Laser-Capture microdissection for measurement of angiogenesis after stroke.

5. García-Lara, E.; Aguirre, S.; Clotet, N.; **Sawkulycz, X**.; Bartra, C.; Almenara-Fuentes, L.; Suñol, C.; Corpas, R.; Olah, P.; Tripon, F.; et al. Antibody Protection against Long-Term Memory Loss Induced by Monomeric C-Reactive Protein in a Mouse Model of Dementia. *Biomedicines* **2021**,*9*,828. https:// doi.org/10.3390/biomedicines9070828

Provided mCRP protein.

Presentations

Poster presented at the inaugural Geoffrey Jefferson brain research centre symposium 2022.

Title - mCRP pro-inflammatory risk factor in neuroinflammation after ischemic Stroke

Oral presentation at the centre of bioscience seminar, Manchester metropolitan university 2019

Title - A new potential culprit of dementia: Monomeric C – reactive protein

Oral presentation at the centre of bioscience seminar, Manchester metropolitan university 2022

Title - mCRP pro-inflammatory risk factor in neuroinflammation after ischemic Stroke

List of abbreviations

AdMSC	Adipose-derived mesenchymal stem cells
ATP	Adenosine triphosphate
BBB	Blood brain barrier
BSA	Bovine serum albumin
BCA	Bicinchoninic acid assay
$CaCl_2$	Calcium chloride
DAMPS	Damage associated molecular pattern
ddH_20	Double distilled water
EDTA	Ethylene diamine tetra acetic acid
ELISA	Enzyme linked immunosorbent assay
FITC	Fluorescein isothiocyanate
HMC-3	Human microglia cells line
ICAM	Intracellular adhesion molecule
IL	Interleukin
iNOS	Inducible nitric oxide synthase
IF	Immunofluorescence
IFN α	Interferon-alpha
IFN γ	Interferon-gamma
Ig	Immunoglobin
LPS	Lipopolysaccharide
LXR	Liver X receptor
L-Glut	L-glutamine
MFAT	Micro-fragmented adipose tissue
MAPK	Mitogen-activated protein kinase
MCP	Monocyte chemotactic protein
mCRP	Monomeric C reactive protein
MMPs	matrix-metalloproteinases
MSC	Mesenchymal stem cells
MEMα	Minimum essential medium alpha
qPCR	Quantitative polymerase chain reaction

PI	Propidium iodide
PMA	Phorbol 12-myristate 13-acetate
ROS	Reactive oxygen species
RT-PCR	Real time polymerase chain reaction
SDS	Sodium dodecyl sulphate
SEM	Scanning electron microscope
SDS-page	SDS – polyacrylamide gel electrophoresis
TEMED	N, N, N, N tetramethylenediamine
TGF β	Transforming growth factor beta
TNF-α	Tumour necrosis alpha
TYK2	Tyrosine Kinase-2
tPA	Tissue plasminogen activator
VCAM-1	Vascular cell adhesion molecule -1
VEGF	Vascular endothelial growth factor

Chapter 1 – Introduction

1.1 Ischaemic stroke

1.1.1 Epidemiology and pathophysiology of Ischaemic stroke

In the UK, ischemic stroke is the most common type of stroke and accounts for 85% of cases with the other 15% due to haemorrhagic stroke. In the UK each year, more than 100,000 people suffer a stroke with 38,000 leading to death (King et al., 2020). There is a significant impact on the socioeconomic burden and the aggregated cost of stroke, including long-term healthcare, rehabilitation, and loss of employment, is estimated to be £25.6 billion per year (Hurford et al., 2020). An ischemic stroke happens when a blood vessel which supplies the brain becomes blocked and impairs the flow of blood to the brain. Due to the lack of nutrients (glucose) and oxygen not reaching the brain, cells and tissue begin to die within minutes (Donkor, 2018). Ischemic strokes can be subdivided into thrombotic and embolic strokes. Thrombosis is caused by a clot which develops in a blood vessel within the brain. The build-up of plaques within the blood vessels constricts the vascular chamber, and a clot is formed, causing a thrombotic stroke (Kuriakose and Xiao, 2020). Embolic stroke is caused by a clot or plaque debris which has developed outside the brain and has travelled to one of the blood vessels in the brain (Diener et al., 2020). The other classified stroke is haemorrhagic, which is due to bleeding into the brain caused by a rupture of a blood vessel. Haemorrhagic stroke can be further subdivided into either intracerebral haemorrhage (ICH) or subarachnoid haemorrhage (SAH) (Shao et al., 2019).

1.1.2 Risk factors for ischemic stroke

Non-modifiable risk factors for ischemic stroke include age, sex, and race/ethnicity. At younger ages, males are at an increased risk of having a stroke compared to women. However, this is reversed in older age groups whereby women are at a higher risk (Wajngarten and Silva, 2019). There are also effects of ethnicity with some ethnic groups such as black or South Asian families being more prone to having a stroke (Gezmu et al., 2014). Modifiable risk factors are important and intervention strategies can be put in place to reduce stroke risk. Modifiable risk factors include hypertension, diabetes mellitus, atrial fibrillation, lifestyle issues and obesity (Boehme et al., 2017). Most ischemic strokes occur in patients with cardiovascular disease (Arboix and Alio, 2010). The following conditions increase the risk of embolic stroke: arrhythmias, valvular

heart disease, thrombus and structural lesion and structural heart disease (Chugh, 2019). Hypertension is a major risk factor for stroke; the increased pressure damages arteries throughout the body leading to them becoming more easily blocked or burst. Weakening of blood vessels in the brain leads to a higher risk of having a stroke (Wajngarten and Silva, 2019). Making changes to reduce blood pressure can decrease the risk of having a stroke (Law et al., 2003). People who present with high blood pressure will be recommended to change to a healthy lifestyle with tests carried out to decide treatment. There are several types of medication available to control blood pressure and many are taken in combination (Dusing et al., 2017). According to NHS guidance, if you are under 55 years of age, ACE inhibitor or an angiotensin-2 receptor blocker will be used for treatment. For people aged 55 or older and of African or Caribbean descent, calcium channel blocker will be used for the treatment (BHF, 2022). Diabetes is a well-known risk factor for stroke as it can cause pathological changes within blood vessels. In patients who have poorly controlled glucose levels, post stroke outcomes are poorer, and mortality is greater (R. Chen et al., 2016). Diabetes is characterised by too much sugar within your blood (Lopes et al., 2021). This increase in sugar can lead to damage of blood vessels causing various microvascular and macrovascular changes leading to greater risk of stroke. The factors which are at play include vascular endothelial dysfunction, increased arterial stiffness, systemic inflammation and thickening of the capillary basal membrane (R. Chen et al., 2016). These changes can lead to a blood clot and risk of breaking off and travelling to the brain causing a stroke (Fadini and Cosentino, 2018). Atrial fibrillation is a risk factor for ischemic stroke and results in a 5-fold increased risk of having a stroke as well as a 2-fold increase in mortality (Migdady et al., 2021). Atrial fibrillation is when there is an irregular and rapid heart rhythm intern lead to blood clot formation in the heart and increased risk of stroke (Baman et al., 2021).

1.1.3 Current stroke treatments

Tissue-type plasminogen activator (tPA) cleaves plasminogen on the surface of thrombus to form plasmin, a powerful endogenous fibrinolytic enzyme (Chevilley et al., 2015). tPA is licensed to improve functional outcome in acute ischaemic stroke up to 4.5 hours after symptom onset (Marko et al., 2020). UK guidelines recommend all patients with disabling symptoms should be considered for Recombinant tissue-type plasminogen activator (rtPA) treatment within 3 hours of symptom onset, and up to 4.5 hours in those aged under 80. Patients presenting at 4.5–6 hours should be considered on an individual basis for treatment, recognising that the benefits are smaller than if treated earlier, but that the risks of a worse outcome, including death, are not increased (Hurford et al., 2020). A limited number of severe ischaemic strokes can be treated by an emergency procedure called a thrombectomy which removes blood clots and restores blood flow to the brain (Tawil and Muir, 2017). This treatment is effective at treating ischaemic strokes caused by a blood clot in a large artery in the brain. The procedure entails a catheter which is placed into an artery, which is often the groin, and a small device is passed through into the artery in the brain (X. Guo and Miao, 2021). The blood clot will be removed either by the device or suction. There are several distinct types of device which can be used for thrombectomy which include guide catheters, stent-retrievers, microcatheters, aspiration catheters, and aspiration pump systems (Jesus, 2022). Haemorrhagic strokes are treated in a separate way to ischemic stroke and treatments are outlined below. There are several different treatment options available for haemorrhagic stroke. Blood pressure management is a key treatment with medication. Another acute treatment is reversal of antithrombotic medication such as warfarin. Reversal can be achieved with prothrombin factor concentrate and vitamin k. Surgical interventions are another possibility for the treatment of ICH where evacuation of the haematoma is necessary (McGurgan et al., 2020).

1.2 Neuroinflammation

1.2.1 Concept of neuroinflammation

Neuroinflammation presents in several types of brain injuries with the focus of this work looking at ischemic stroke (Liu 2017). Neuroinflammation is when inflammatory response occurs within the spinal cord or the brain because of stimuli and is a protective response (Sochocka et al., 2017). The response is mediated by cytokines, chemokines, reactive oxygen species (ROS) and secondary messenger production (Kempuraj et al., 2017). These mediators are made by the glia cells within the central nervous system (CNS) like microglia and astrocytes, endothelial and peripherally derived immune cells (DiSabato et al., 2016). After an ischemic stroke there is a significant inflammatory response which plays a pivotal role in worsening the brain injury (Jin et al., 2010). There is evidence that post ischemic inflammation can cause acute blood brain barrier (BBB) disruption, vasogenic edema, haemorrhagic transformation and worsen the outcomes of patients neurologically. In the preliminary stages of an ischemic stroke, inflammation can contribute to brain damage (S. Chen et al., 2021). However, during the late stages, inflammatory response is important for recovery by helping neurogenesis, angiogenesis, and neuronal plasticity. A better understanding of the mechanism by which neuroinflammation translates from injury to repair is vital to help look for novel therapeutic strategies (Candelario-Jalil et al., 2022). During this event, damage-associated molecular pattern (DAMP) is produced, leading to the activation of different cell types including the resident macrophage (microglia) and endothelial cells (Land, 2015). DAMPS also cause the disruption of the BBB by the release of several pro-inflammatory cytokines and chemokines (interleukin 1β (IL-1β), tumour necrosis factor-alpha (TNF-α), and interleukin-6 (IL-6), MCP-1, Interferon gamma-induced protein 10 (CXCL10), matrix-metalloproteinases (MPPS) and ROS (Takata et al., 2021). After damage of the BBB, circulatory cells can infiltrate and lead to migration immune cells which cause brain edema and haemorrhage. This in turn leads to further neuroinflammation and tissue damage (Li et al., 2018). There is a switch in microglia activation from cytotoxic to phagocytic phenotype. This change leads to recovery and repair through tissue clearance, and expression of anti-inflammatory mediators' examples include Interleukin 4 (IL-4) and interleukin 10 (IL-10). This recruitment leads to the initiation of the brain repair mechanisms, including neurogenesis and angiogenesis (Rajkovic et al., 2018).

Neuroinflammation is critical after an ischemic event and figure 1 is a representation of the mechanism of a post ischemic inflammation. Focusing on how inflammatory cascade of events cause BBB disruption and neuronal injury (Rajkovic et al., 2018; Yang et al., 2019).

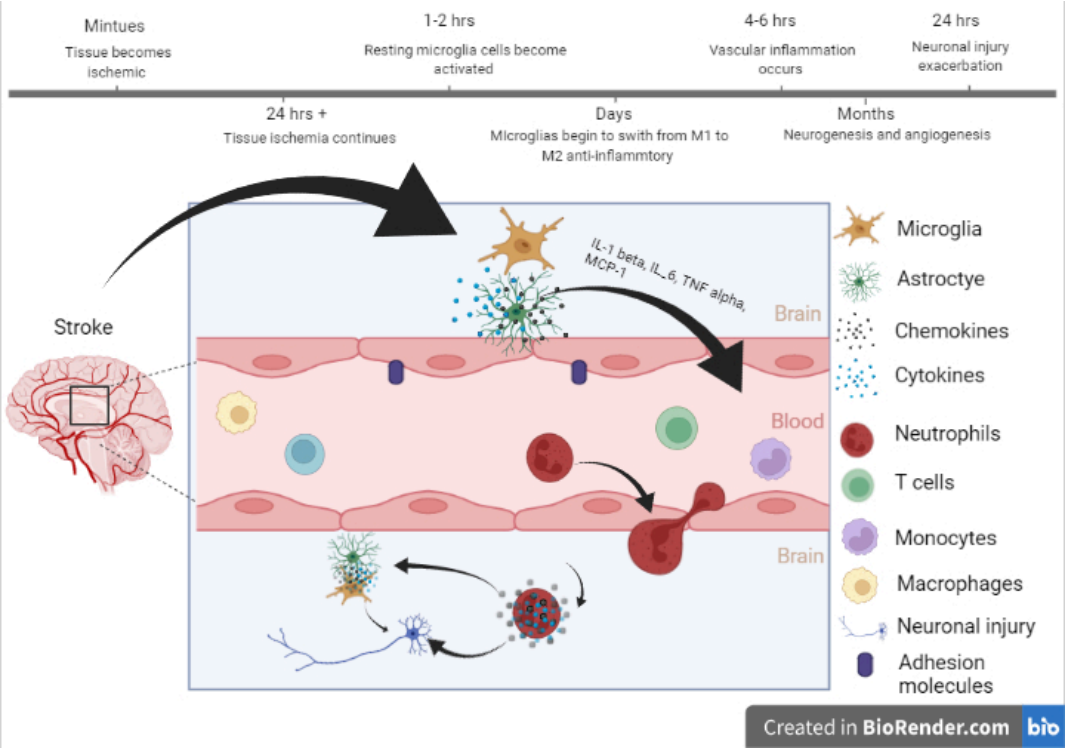

Figure 1 – Mechanism of neuroinflammation post ischemic stroke

Mechanisms of neuroinflammation are caused by acute stimuli leading to the production of DAMPS. This leads to activations on microglia and endothelial cells leading to breakdown of blood brain barrier, through release of major mediators like pro-inflammatory cytokines, chemokines, ROS and MMPs. Degradation of the extracellular matrix in both the parenchyma and basement membrane induces astrocyte end feet and pericytes lifting from the endothelium. Damage of the BBB enables infiltration of circulatory cells with transmigration of neutrophils and immune cells. This damage can lead to brain oedema and haemorrhage, causing further neuroinflammation and tissue damage. This figure has been adapted from blood brain barrier simple longitudinal zoom by biorender.com 2022). Retrieved from https://app.biorender.com/biorender-templates/t-5e6170876b78a20088805178-blood-brain-barrier-simple-longitudinal-zoom (2022) and information included from (Rajkovic et al., 2018; Yang et al., 2019)

1.2.2 Monocytes

Monocytes come from the hematopoietic system within the bone marrow and play a pivotal role in the innate immune response. Monocytes have several mechanisms which include scavenger receptors, low-density lipoprotein receptors, toll-like receptors, chemokine/cytokine receptors, Fcγ receptors and adhesions molecules (ElAli and Jean LeBlanc, 2016). Monocytes are distributed throughout the body systematically and when they leave the circulatory system and reach the targeted tissue, they then differentiate into macrophages (D. Han et al., 2020). There are 3 subsets of monocytes which are classical, intermediate, and non-classical. Monocytes are characterised by their cluster differentiation (CD) markers which are CD11c, CD14, CD16 and CD115 expression (ElAli and Jean LeBlanc, 2016; Marimuthu et al., 2018). During the onset of an ischaemic stroke, circulating monocytes infiltrate into the brain through the compromised BBB because of neuroinflammation (J. Park et al., 2020). In human ischemic stroke there is an increased number of total monocytes in the blood circulation. Interestingly, the number of classical monocyte subset (CD14++ CD16−), significantly increased in blood circulation, while the number of the non-classical monocyte subsets (CD14+ CD16++), significantly decreased (ElAli and Jean LeBlanc, 2016).

1.2.3 Microglia and other brain macrophages

The resident innate immune cells within the brain are microglia cells and they represent between 5-20% of the glial cell population (Jayaraj et al., 2019). Microglia cells are highly specialized, dynamic, and play a key role in the physiology of the CNS (Yu et al., 2020). The most widely used markers are ionized calcium-binding adapter molecule 1 (IBA1), CD11b, CD14, CD45, CD68, CD80, and CD115 (Jurga et al., 2020). In a healthy human brain, microglia cells display a ramified morphology and constantly check the microenvironments in the CNS. Microglia cells in response to stimuli move towards the site of injury and transform into an amoeboid shape helping their movement (S. X. Zhang, 2019). Classic (M1) or alternative (M2) activation has been mostly reported for macrophage responses during peripheral inflammation, and, recently, microglia were found to have a similar activation process upon ischemic insult (S. C. Zhao et al., 2017). M1 macrophages are induced by interferon gamma (IFN-γ) or lipopolysaccharides (LPS) and involved in the acute pro-inflammatory response with

several different signalling pathways contributing to M1 macrophage polarization (Orihuela et al., 2016). The alternative activation of macrophages (M2) is usually induced by IL-4 or IL-10 and IL-13 and is involved in the anti-inflammatory response (Eldahshan et al., 2019). Microglia are the first line of defence against brain injury (ischaemic stroke) and respond to alterations in the brain microenvironment (Dong et al., 2021). When microglia cells turn towards M1 phenotype they release different cytokines such as IL-1β, TNFα, IL-6, other inflammatory cytokines, and ROS into circulation. M2-polarized microglia, by producing anti-inflammatory factors (IL-4, IL-10, IL-13, or TGF-β), contribute to the resolution of inflammation and have important roles in tissue remodelling and repair as well as angiogenesis by producing insulin-like growth factor-1 (IGF1), which suppresses apoptosis and increases proliferation and differentiation of neural precursor cells (Jurcau and Simion, 2021). Microglia become activated rapidly, initiate migration, and activate downstream cell signalling during the first stages of an ischemic stroke. Microglia, are an integral part of the immune system, produce inflammatory factors, alter the permeability of the BBB, phagocytose vascular endothelial cells, and lead to BBB breakdown after stroke, which can result in reduced brain recovery following infarction. After ischemia occurs, microglia become activated, and produce detrimental and neuroprotective mediators (Dong et al., 2021).

1.2.4 Cytokines in neuroinflammation after ischemic event

Cytokines have a vital role in the activation, proliferation, and they also range in size (8-26 kDa). Cytokines can mediate the inflammatory response or act as anti-inflammatory molecules which stop the inflammatory response (Jayaraj et al., 2019). Cytokines can broadly be classified by immune response but also have their individual characteristics which are briefly outlined in table 1.

Table 1 - Overview of cytokines.

IL-1	B cells, dendric cells, activated monocytes macrophages	B+T cells, natural killer cells	Pro-inflammatory, proliferation, differentiation
IL-4	T helper cells	Macrophages B+T cells	B and cytotoxic T cells proliferation, MHC class II expression, IgG + IgE production stimulation.
IL-6	T helper cells, macrophages, fibroblasts	Activated B cells and plasma cells	Differentiation into plasma cells, IgG production, B +T cell growth factors, stimulation of acute phase response, haematopoiesis, and Immune reactions
TNF-α	Macrophages Monocytes	Macrophages Tumour cells	Phagocyte cell activation, Tumour cytotoxicity, Vasodilatation, Leukocyte adhesion by expression of adhesion molecules
IFN-γ	T helper cells	Various	Anti-viral, macrophage activation, increase neutrophil, monocyte function, MHC-I+II expression on cells
G-CSF	Fibroblasts Endothelium	Bone Marrow stem cells	Granulocyte production, survival, proliferation, differentiation, function of neutrophil precursors, mature neutrophils
GM-CSF	T cells, macrophages, fibroblasts	Stem cells	Granulocyte, monocyte, and eosinophil production
TGF-β	T+B cells	Activated T+B cells	Inhibit proliferation of B+T cells, inhibit haematopoiesis, wound healing, angiogenesis, and immunoregulation is promoted via TGF-β

Brief discussion of source, target cell and function of cytokine important in neuroinflammation. This table presents information from (Idriss and Naismith, 2000; Prud'homme, 2007; Tanaka et al., 2014; Turner et al., 2014)

1.2.4.1 Pro-inflammatory cytokines

There are three major cytokines linked to neuroinflammation after an ischaemic stroke and they are IL-1β, TNF-α, and IL-6 (Jayaraj et al., 2019).

1.2.4.1.1. Interleukin 1 beta

IL-1 is a general name for two distinct proteins, IL-1α and IL-1β which have a significant role in the up-regulation and down-regulation of acute inflammation (Dinarello et al., 2012). Human IL-1α and IL-1β are synthesized as 31-33 kDa cytokines (Fields et al., 2019). In a pro-inflammatory response IL-1β isoform has a significant role and this cytokine presents in several cell types including keratinocytes, fibroblasts, synoviocytes, endothelial, neuronal, immune cells such as macrophages, mast cells, and glial cells such as Schwann cells, microglia, and astrocytes (Ren and Torres, 2009; Lambertsen et al., 2019). IL-1β is present in the CNS and expressed constantly which is important as this cytokine exerts neurotrophic factors (Lambertsen et al., 2019). IL-1 receptor antagonist (IL-1Ra) is the endogenous inhibitor and has been the most studied in stroke. IL-1β is a pro-inflammatory cytokine and has a key role in both acute and chronic inflammatory disorders (Denes et al., 2011). Stroke and traumatic brain injury lead to the up-regulation of IL-1β, IL-1Ra, IL-1 receptor (IL-1r) (Murray, Parry-Jones, and Allan, 2015). It has been shown that mRNA levels of IL-1β are seen to be increased in the first 15/30 minutes after the ischemic event (Wang Q, 2007). After the event of an ischemic stroke, IL-1β is upregulated and is seen to peak at around 12 to 24 hours in macrophages (microglia) and long term astroglia (Lambertsen et al., 2012). There are constituently low levels of IL-1β protein and mRNA expressed within the brain and this is regulated by transcriptions, translation and cleavages and cellular release. IL-1β stays inactivated until it is cleaved by caspase 1 and is then consequently activated. Binding to (IL-1r) occurs when IL-1β is biologically activated and this is linked with the interleukin 1 receptor accessory protein which mediates intracellular signalling. After an ischemic event, there is an increase level of ATP circulating which contributes and promotes cleavage and cellular release of IL-1β (Doll et al., 2014). Signalling pathway of IL-1 is presented above in figure 2 highlighting the activated pathway though LPS stimulation via transcription of encoding gene IL-1β (Murray, 2015).

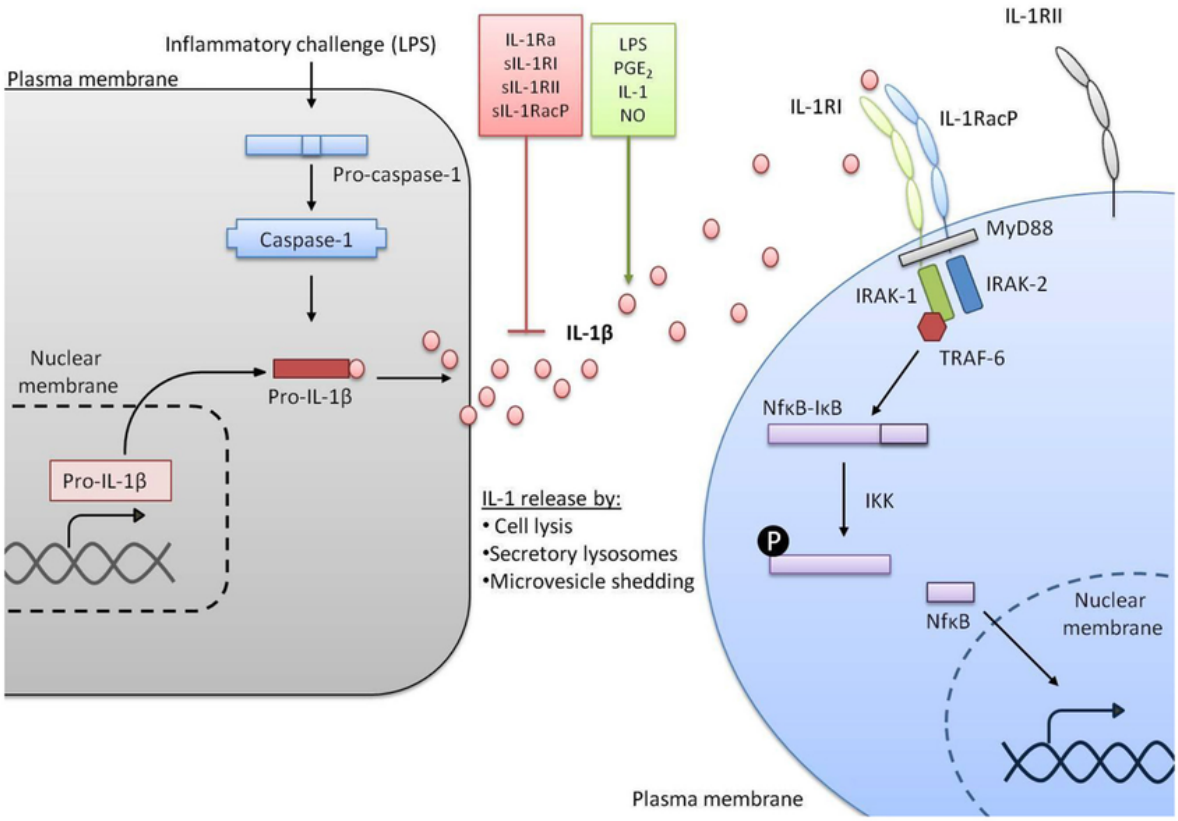

Figure 2 – IL-1 signalling pathway.

Image taken from (Murray, 2015) which depicts IL-1 signalling pathway activation from a stimulus like LPS. A stimulus will activate the transcription of the gene encoding IL-1β. IL-1β is an inactive precursor protein and caspase-1 cleaves this pro-IL-1β to make the active form called IL-1β. A variety of factors can promote or inhibit the release of active IL-1β. IL-1β binds to IL-1Ri alongside IL-1 receptor accessory protein (IL-1RAcP). Signal transduction is triggered by MyD88, IL-1 receptor associated kinase (IRAK-1) and IRAK-2, recruitment of TNF receptor associated factor 6 (TRAF-6) and NFκB from complex with IκB.

1.2.4.1.2 Interleukin 6

A well-studied cytokine of interest is IL-6, which is a pro-inflammatory cytokine (Tanaka et al., 2014). The dysregulation of IL-6 is closely related to the occurrence and outcome of many clinical diseases, including coronary heart disease, leukaemia, hypertension, ischemic stroke (Erta et al., 2012). IL-6 is produced by several different activated cells including microglia and astrocytes in the different regions of the brain (Sanchis et al., 2020). Further to this, IL-6 itself can potentially stimulate microglia and astrocytes leading them to releasing a cascade of pro-inflammatory cytokines and acute phase protein such as CRP and promote recruitment of macrophages. The events outlined are essential for the inflammatory reaction resolution and starting the acquired immunity response (Camporeale and Poli, 2012). Levels of IL-6 have been seen to be reported in stroke patients (Gertz et al., 2012) but there is still doubt on whether IL-6 plays a significant role in ischemic stroke and further research is needed. IL-6 is produced by many different cells which include neurons, microglia, endothelial cells, and astrocytes and at different amounts depending on stimulation. IL-6 stimulates the inflammatory response in several diseases which include diabetes, atherosclerosis, Alzheimer's disease, multiple myeloma, rheumatoid arthritis, and depression. Due to this response in several different diseases, there is an interest in developing the anti-IL-6 agent as a potential therapeutic for these diseases. Levels of IL-6 are increased in stroke and the plasma levels have been seen to correlate with increased severity of the infarcts volume size and with the outcome becoming less favourable (Gertz et al., 2012). Figure 3 represents an overview of IL-6 signalling. IL-6 cytokine has pro-inflammatory and anti-inflammatory properties and is encoded by the *IL-6* gene in humans. Inflammation driven by IL-6 allows for *IL-6* trans signalling. This signalling allows the up-regulation ICAM-1, VCAM-1, CXCL1, CXCL5, CXCL6, IL-8 and MCP-1 which are key pro inflammatory mediators(Tanaka et al., 2014)

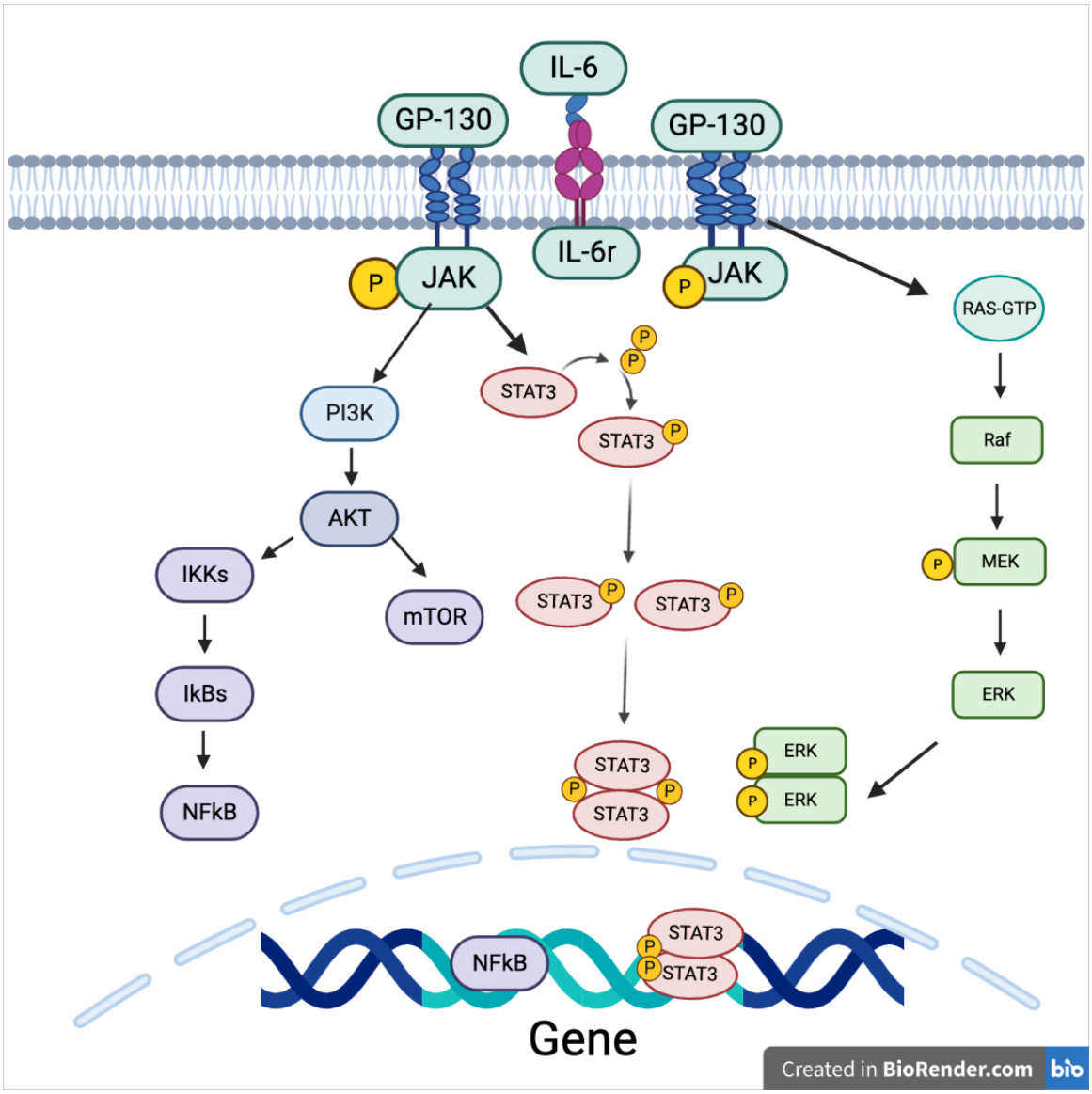

Figure 3 - IL-6 signalling pathway

IL-6 cytokine has pro-inflammatory and anti-inflammatory properties and is encoded by the IL-6 gene in humans. IL-6 binds to IL-6R to initiate cellular events including activation of JAK kinases, Ras and PI3k-mediated signalling which lead to activation of several transcription factors. SOCS and PIAS proteins negatively regulate IL-6 activity. Schematic created with BioRender.com and adapted from (Bio-techne, 2023a).

1.2.4.1.3 Tumour necrosis factor alpha

TNF is a cytokine that can be generated in the brain and many different cells can synthesize this which include macrophages and microglia (Doll et al., 2014). TNF-α is made up of 35 amino acids, a cytoplasmic domain, 21 amino acid transmembrane segments and a 177 amino acid extracellular domain. It presents with a molecular weight of 17.3kDa (Webster and Vucic, 2020). TNF-α has a role in the acute inflammatory response and seen to exacerbate stroke pathology and identified as a key regulator of the inflammatory response. Levels of TNF-α are not normally detectable in healthy humans but are seen to be elevated in serum and tissues when found in inflammatory and infectious conditions (Bradley, 2008). TNF-α can move across the BBB via a receptor-mediated transport system that is upregulated due to inflammation and trauma in the CNS. TNF-α gene is located on chromosome 6 and consists of four exons and 3 introns (Parameswaran, 2010). In stroke research, TNF is one of the most studied cytokines due to it being both an immune regulator and a pro-inflammatory mediator. After an ischemic event microglia, the resident brain macrophages lead to the production of TNF-α causing further damage due to the pro-inflammatory effects (Jayaraj et al., 2019).

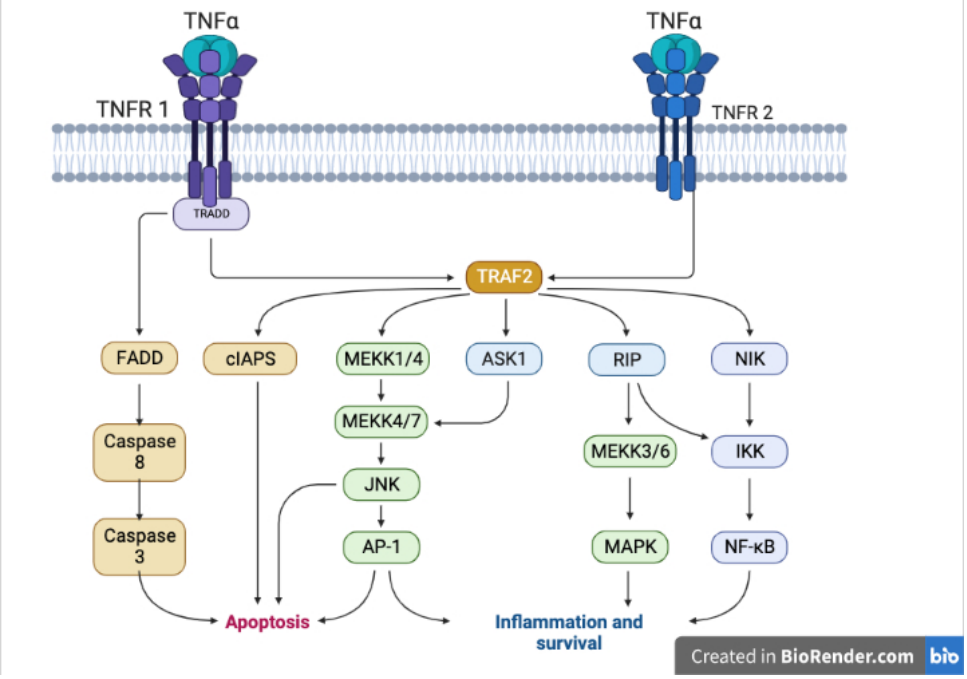

Figure 4 – TNF α signalling pathways.

TNFα signalling pathway (Created with BioRender.com) and adapted from (Rolski and Blyszczuk, 2020). Downstream signalling is media by two receptors with are TNFR1 or TNFR2. TNFα is a precursor bound membrane and is cleaved by TNFα converting enzyme, releasing either TNFR1 or TNFR2 which are the soluble forms.

1.2.4.2 Anti-inflammatory cytokines

Anti-inflammatory cytokines include IL-4, IL-10, IL-11, IL-13, an TGF-β (Jeon and Kim, 2016). It must be noted that leukaemia inhibitory factor interferon alpha, IL-6 as well as TGF-β can be categorised as having either an anti-inflammatory property or a pro-inflammatory property under various circumstances (J. M. Zhang and An, 2007) .

1.2.4.2.1 Interleukin 4

IL-4 is an important anti-inflammatory cytokine that regulates brain homeostasis and support neurogenesis as well as oligodendrogenesis. The function of IL-4 is to regulate immunity and is an important player in leukocyte survival under pathological and physiological conditions. IL-4 starts signalling transduction by two different receptor complexes (type I receptor expressed on hematopoietic cells or a type II receptor expressed on nonhematopoietic cells. (Rossi et al., 2018). Figure 5 is a representation of the IL-4 signalling pathway (A. D. Keegan et al., 2021). Signalling transduction occurs through one of the IL-4 receptors which is either type 1 or type 2 (Junttila, 2018). Type 1 IL-4 receptor comprises of IL-4Rα and gamma chain/IL-2 R gamma subunits. Whereas type 11 receptors consist of IL-4 Rα and IL-13Ra1 which can become activated by either cytokine (IL-4 and IL-13). The IL-4 signalling pathway is vital toward differentiation of Th2 cells, regulation of B cells, immunoglobulin class switching, promoting mast cell survival and proliferation (Kelly-Welch et al., 2005; Daines et al., 2021; A. D. Keegan et al., 2021; Bio-techne, 2023b). Macrophage production of several pro-inflammatory cytokines including TNF-α, IL-1β and IL-6 can be inhibited by the anti-inflammatory IL-4 via transcriptional repression (Anovazzi et al., 2017).

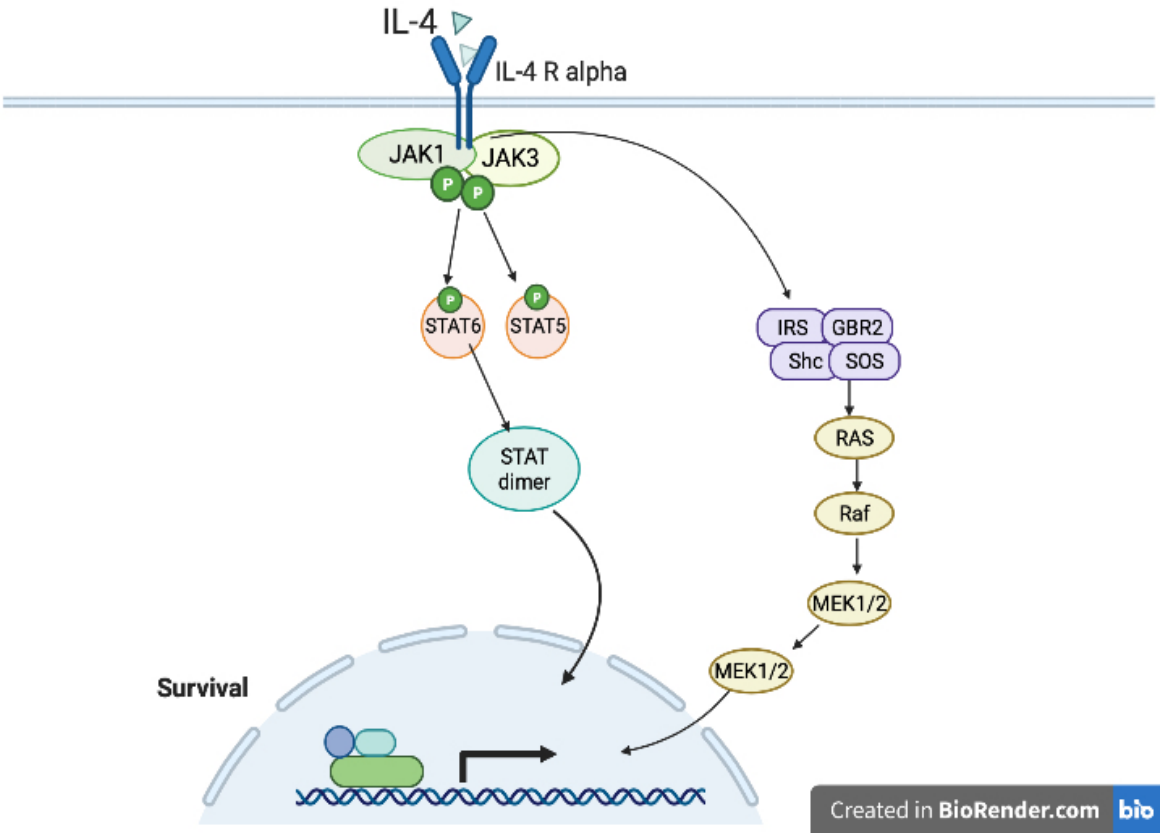

Figure 5 - IL-4 signalling pathway.

IL-4 binding to the IL-4Rα induces heterodimerization with a gamma chain to form the type II receptor in macrophages. Janus kinases (Jaks) becomes activated and type II receptors activate Jak1, Jak2, and Tyk2. Tyrosine residues in the cytoplasmic tail of the IL-4Rα become phosphorylated and act as docking sites for signalling molecules. Insulin receptor substrate family (IRS) and Shc also have ability to dock to this site and become phosphorylated. Phosphorylated STAT6 dimerizes, migrates to the nucleus, and binds to promoters of genes. STAT6 can act as a transcriptional activator or a transcriptional repressor, depending on the specific target gene and activation state of the cell. (Created with BioRender.com) and adapted from (Kelly-Welch et al., 2005; A. D. Keegan et al., 2021; Bio-techne, 2023b).

1.2.4.2.2 Interleukin 10

IL-10 is a significant anti-inflammatory cytokine that has inhibitory effects on a variety of immune cells. IL-10 was first identified in mouse Th2 cells, and was subsequently found to be secreted in astrocytes, neurons, B cells, monocytes/macrophages, keratinocytes, and human Th1 cells (Iyer and Cheng, 2012). IL-10 could inhibit the production of numerous different inflammatory cytokines, which include TNF-α, IL-1β and IL-6. IL-10 has the potential to reduce the function of the pro-inflammatory markers in ischemic stroke (Kes et al., 2008; Porro et al., 2020). The IL-10 gene has a molecular weight of 4.7 kb and is located on chromosome 1 on the long arm and contains five exons. The biological activated form of IL-10 is a 36 kDa homodimer which is 160 amino acids in length and has two non-covalently bonded monomers (Verma et al., 2016). IL-10, when bound to its receptors, causes phosphorylation of Janus kinase 1 (JAK1) and Tyrosine kinase 2 (Tyk2). These then become a docking site for signalling transducer and activator of transcription 3 (STAT3) which translocate to the nucleus and cause binding to the promoter of several IL-10 genes, which is presented in figure 6 (Porro et al., 2020)

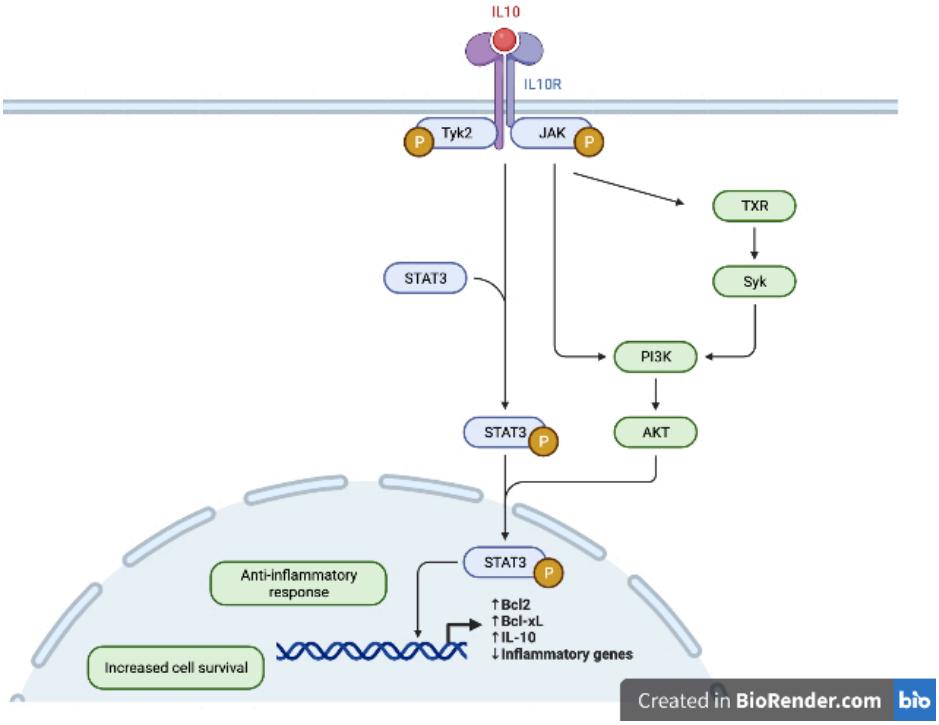

Figure 6 – Interleukin 10 signalling pathway

Jak1/Tyk2/signal transducer and activator of transcription 3 (STAT3) system are the most characterized pathway for IL10 (Porro et al., 2020) Created with BioRender.com

1.2.5 Chemokines

The CNS is regarded as immune privileged due to the BBB (Muldoon et al., 2013). Chemokines are an important protein with the CNS which can regulate and coordinated immune response within the human body (Ramesh et al., 2013). Chemokines belong to the family of chemoattractant cytokines. These cytokines play a vital role in cell migration and induction of cell movement in response to chemotaxis (Poeta et al., 2019). Chemokines can be broken into subclass which are CC, CXC, XC and CX3C and mammals are seen to have among 45 distinct types (Bonecchi and Graham, 2016). Chemokine function which is most studied in research is cell migration with a particular interest in leukocytes. Chemokine which are dysregulated are an important feature which is central to the development of neuroinflammation and neurodegeneration. This response can be seen to mediate cell death in several different cell types which include neuronal and glial cells. Subsequently. This can then lead to the production of pro-inflammatory chemokines and cytokines as previously mentioned (Ramesh et al., 2013). Macrophage inflammatory protein (MIP-1α/CCL3), MIP-1β, MCP-1, and RANTES are members of the C-C chemokine family. MIP-1α is produced by different cell types during inflammation. The biological function of MIP-1α is inducing the inflammatory response by neutrophil infiltration. Monocytes, T lymphocytes, B lymphocytes, neutrophils, dendritic cells, and natural killer cells are known to secrete MIP-1α/CCL3 (Keane et al., 1999). In normal conditions, MIP-1α/CCL3 presents at low levels. Upon stimulation with different factors like (lipopolysaccharide (LPS) or pro-inflammatory cytokines (IL-1β), cellular signalling events become activated leading to the increase in MIP-1α (Bhavsar et al., 2015).

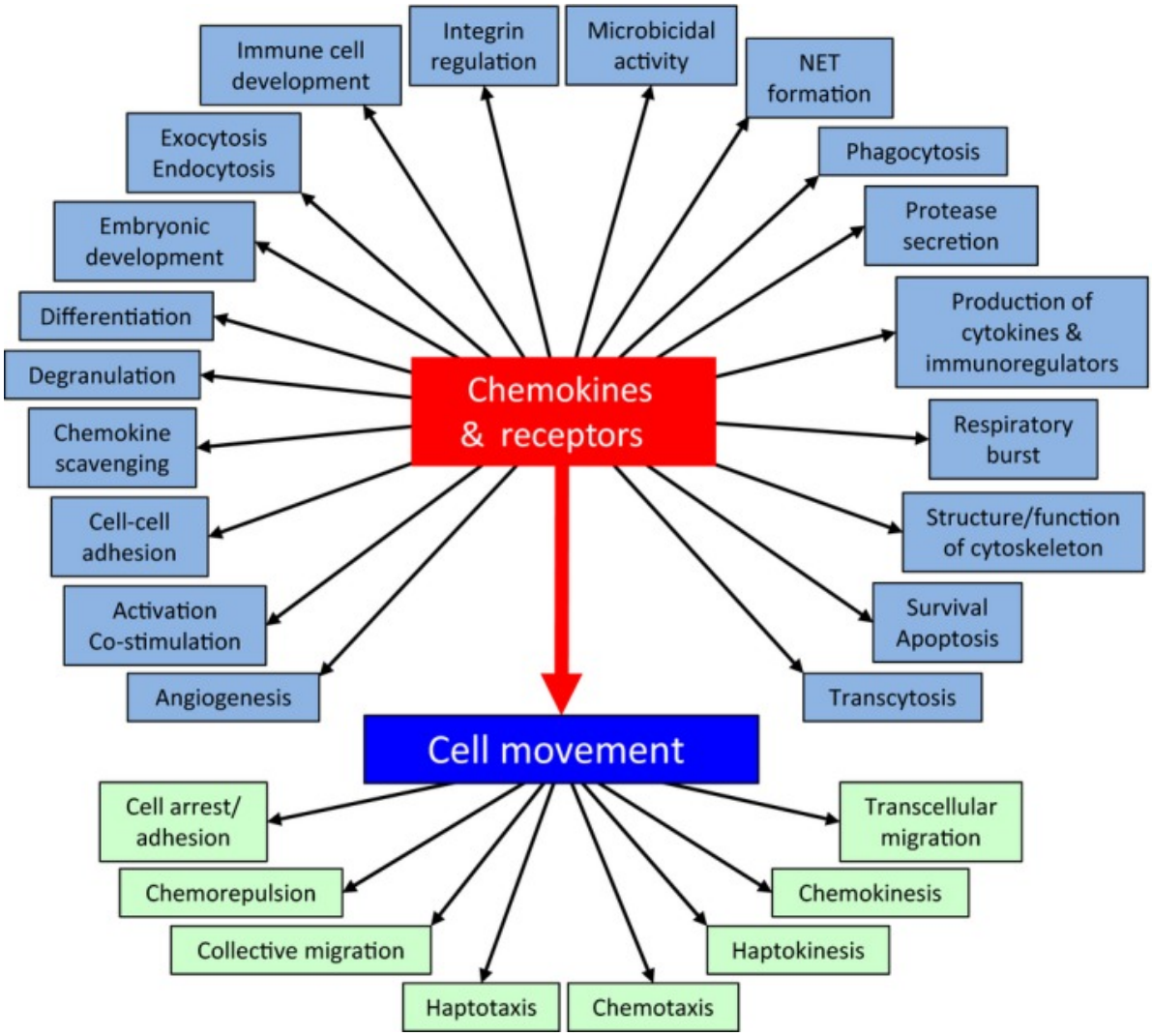

Figure 7 -Chemokine and receptor function.

Represented in blue, is the biological process which have been established to be regulated by chemokines and their receptors. Cell movement is central and presented as the main biological function with the migratory behaviour of the cell movement presented in the light green boxes (Hughes and Nibbs, 2018).

1.2.6 Inflammatory mediators

1.2.6.1 Introduction to C reactive protein

An important predictor of cardiovascular disease is C reactive protein (CRP) and has a significant role in damage to vessels and plays a role in vascular inflammation (Z. Zhang et al., 2012). CRP was discovered in 1930 by Tillet and Francis (Sproston and Ashworth, 2018). Normal CRP protein is circulating at reduced concentration in healthy people but in response to an inflection, injury, or inflammation the levels increase rapidly to over 1000-fold (Khreiss et al., 2004; Boncler et al., 2019). Levels of CRP in serum are some of the highest concentrations found. Interestingly, when there are no stimuli the levels decrease quickly over a 20-hour period. After tissue damage, trauma, cancer and infection, CRP levels within the plasma can increase from 1 µg/mL to 500 µg/mL over 24 to 72 hours. IL-6 pro-inflammatory cytokine has been seen to be the main inducer of gene expression of CRP and the effects are further enhanced by IL-1 (Sproston et al., 2018). CRP can be distinguished into two isoforms, but previous research has only studied this protein as CRP. However, with advancing techniques it is possible to distinguish between the isoforms through monoclonal antibodies (Rajab et al., 2020). However, only until recently have these been researched as separate distinct isoforms (nCRP and mCRP) (Slevin et al., 2018). This is due to advancing technology in developing specific monoclonal antibodies to each specific isoform (Slevin et al., 2018; Sproston and Ashworth, 2018). CRP is found either as native c reactive protein (nCRP) in circulation or as non-soluble monomeric c reactive protein (mCRP) in tissues (Badimon et al., 2018). CRP Is known to present in both native and monomeric conformation but the relationship and roles in inflammation is less understood with contradictory conclusions on the physiological function (Z. Yao et al., 2019).

1.2.6.2 Native C reactive protein production, structure, and function

nCRP which can also be named as pentameric c reactive protein (pCRP) is made up of 5 identical non-covalently bound subunits (figure 8). Each subunit is 206 amino acids long and has a molecular mass of 23 kDa (Sproston and Ashworth, 2018; Ngwa and Agrawal, 2019). Within the human body, liver hepatocytes are the main cells source which synthesize nCRP. In more recent

times, other cells have been seen to synthesize nCRP too. These cells include smooth muscles cells, macrophages, endothelial cells, lymphocytes, and adipocytes (Sproston and Ashworth, 2018). CRP is known as a pattern recognition molecule which can bind to specific molecular configurations during cell death or present on surface pathogens. Figure 8 is a representation of the chemical structure of nCRP. nCRP consists of beta folded sheets which are stabilized by intrachain disulphide bonds and opposite to this includes two calcium ions which are vital to the integrity and stability of this structure (Slevin et al., 2010; De La Torre et al., 2013; Caprio et al., 2018; Slevin et al., 2018; Sproston et al., 2018).

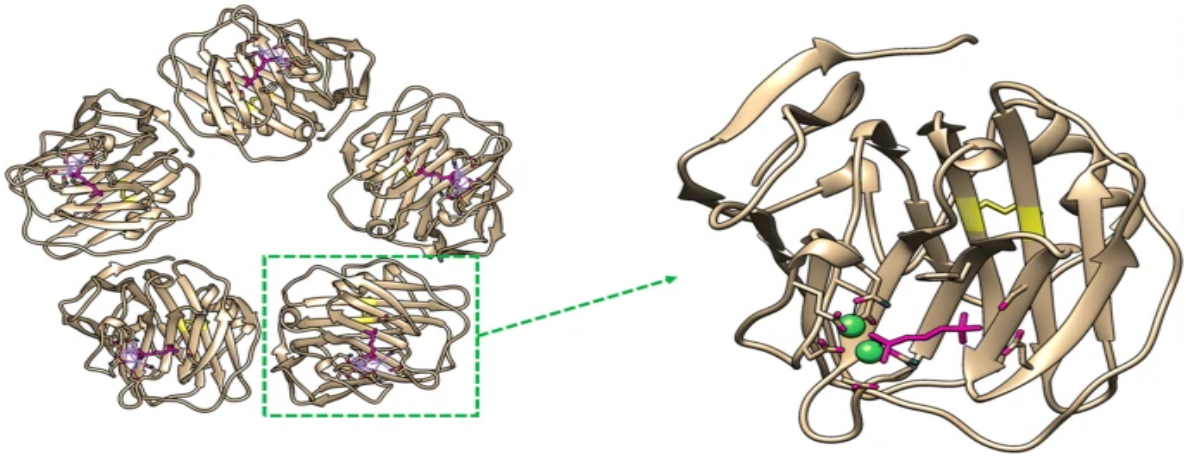

Figure 8 - Chemical structure of nCRP

nCRP is presented as 5 identical subunits which contains hydrophobic core stabilized by intrachain disulphide bond (Yellow). The other side of the subunits (Green) the subunit can bind to the two calcium ions which participate in the binding of phosphocholine (Z. Yao et al., 2019)

1.2.6.3 Monomeric c reactive protein structure and function

nCRP has anti-inflammatory properties and mCRP has pro-inflammatory. This highlights the importance of researching these proteins in their individual forms (Sproston and Ashworth, 2018). A naturally occurring isoform of CRP is mCRP. nCRP can dissociate into mCRP through the incubation of 8 mol/L of urea which contains 10 mM/l of EDTA. Another method of dissociation is through heating nCRP to 63^{o}C for around 5 minutes. The dissociation occurs due to loss of the secondary structure and alteration within the tertiary structure which leads to mCRP epitope expression (Sproston and Ashworth, 2018; Sproston et al., 2018; Z. Y. Yao et al., 2019). nCRP can be dissociated to mCRP through cell membranes, liposomes, and static activated platelets through the binding onto the phosphocholine group (Slevin et al., 2018). As

well as nCRP, monomeric forms of CRP can be localized in fibrous tissues of normal blood vessel intima (De La Torre et al., 2013). Further to this, mCRP has been seen to also accumulate within atherosclerotic lesion in which colocalization occurs with resident macrophages (De La Torre et al., 2013; Badimon et al., 2018). mCRP is prothrombotic and is important between the interface of thrombosis, innate, adaptive immunity and atherogenesis (Filep, 2009; De La Torre et al., 2013). (De La Torre et al.) found that mCRP but not nCRP increased activation of platelets, adhesion, and thrombus growth under arterial flow conditions. mCRP is present in atherosclerotic plaques. The mechanical and or spontaneous plaque rupture of lesions rich in mCRP may result in increased platelet aggregation and thrombus formation (Khreiss et al., 2004; Filep, 2009; De La Torre et al., 2013). There has also been detection of mCRP expression in the intimal and adventitia neo-vessels in unstable carotid plaques. Pro-angiogenic effect was observed *in vivo* and *in vitro* with the increase expression of mCRP via the signalling pathway ERK/MAPK with further increase in Notch 3 gene expression (Boras et al., 2014). mCRP is known to have a key role in modulating inflammation and associated with atherosclerotic plaques progression and instability. Within the brain parenchyma there is a build-up of the mCRP protein which causes vascular damage and presentation of neurodegenerative pathophysiology (Al-Baradie et al., 2021).

1.3 Therapeutics targets for the inflammatory response after ischemic stroke

The inflammatory response is a big part of the pathophysiology of a stroke, and the ability to block this response is an ever-increasing research issue. Several potential compounds were selected for their potential therapeutic effect and anti-inflammatory properties.

1.3.1 Existing anti-inflammatory compounds

Liver X receptors (LXR) belong to the nuclear receptor superfamily and upon activation will stimulate gene transcription (Wouters et al., 2019). LXR can be split into either LXRα or β (Morales et al., 2008). The human LXRα gene is located on chromosome 11p11.2, while the LXRβ gene is located on chromosome 19q13.3. The expression patterns for LXRα and LXRβ mRNA vary significantly from tissue to tissue (Im and Osborne, 2011; Michael et al., 2012). LXRα is found and expressed in the adipose tissue, liver, kidneys intestines and tissue macrophages. Whereas LXRβ is ubiquitous (Ramon-Vazquez et al., 2019). There are several questions which remain when looking into the role that LXR plays within the CNS and inflammation. There is still uncertainty if LXR can modulate the course of the CNS inflammation. In current literature there is still a question to answer regarding whether it is beneficial to target LXR to determine if it has the potential to protect the CNS inflammation. Moreover, LXRs have been shown to mediate specific anti-inflammatory activities and modulate the immune response. In turn, leading the expression of several distinct factors which play a significant role in the control of inflammatory disorders. Figure 9 represents several different LXR activators and how they activate gene regulation and by which pathway (Bilotta et al., 2020). As an example, LXR activation induces anti-inflammatory response in macrophages by antagonizing NF-κB signalling pathway (Wouters et al., 2019). GW3965 hydrochloride, LXR agonist has anti-inflammatory properties and has potential as a threptic target for inflammation in macrophages and other immune cells. GW3965 has also been seen to regulate the expression of several different pro-inflammatory genes (examples include COX2, *IL-6* and *iNOS*) in several different cell types which include macrophages, astrocytes, T cells, myeloid and smooth muscle cells. GW3965 has much research conducted and activation of LXR can promote neuroprotection and reduces brain inflammation in an experimental stroke model (Morales et al., 2008; Spyridon et al., 2011; McVoy et al., 2015). GW3965 has been shown to attenuate LPS induced posttranscriptional

TNF-α in Kupffer rat cells in a dose dependent manner but interestingly mRNA levels did not alter. This does showcase the anti-inflammatory properties GW3965 present with (L. Zhao et al., 2021). Therapeutic GW3965 has been shown to reduce stability and size of thrombi and can reduce its formation. This shows that GW3965 can be a therapeutic target for preventing thrombus formation (Nunomura et al., 2015).

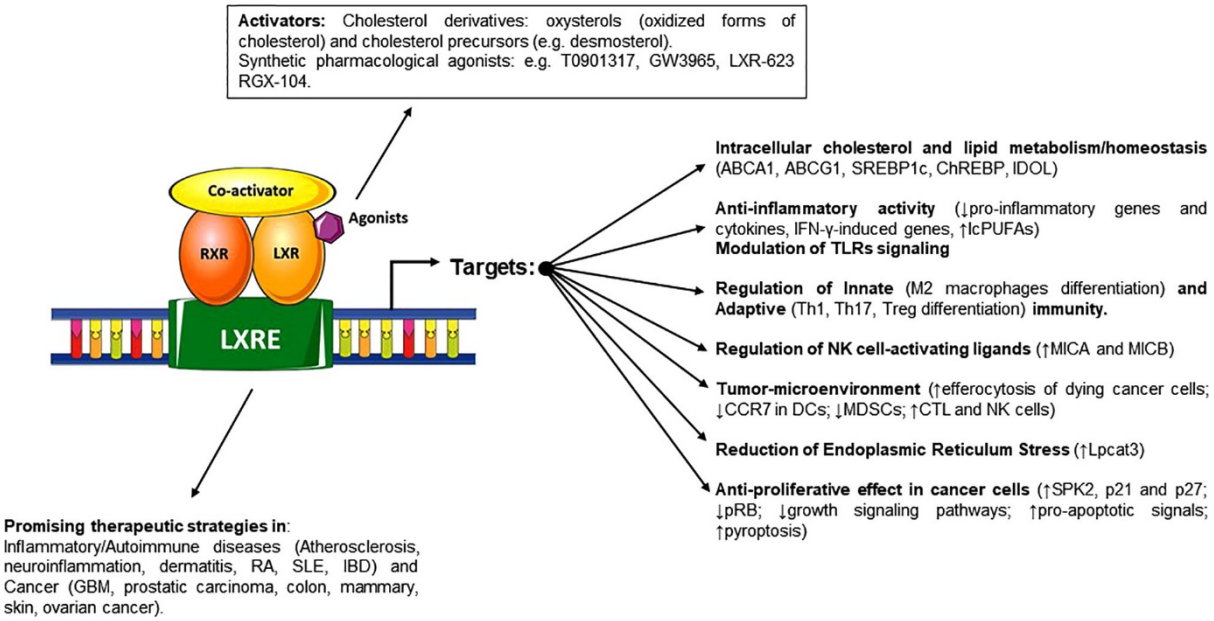

Figure 9 - LXR activators and effects on gene regulation and pathways

LXR can be activated by several factors and can regulate different genes and signalling pathways in several different ways as presented in schematic above (Bilotta et al., 2020).

Circadian rhythms have a role to play in inflammation. In a study, looking at LPS induced microglia activation, a suppression by REV-ERBα both in vitro and in vivo was shown. GSK4112 is a small molecule which targets the REV-ERBα, a dominant transcriptional silencer which represses the expression of several genes linked to inflammation, metabolism, and circadian rhythm (D. K. Guo et al., 2019). Circadian rhythm protein REV-ERBα can regulate neuroinflammation. It has been shown that REV-ERBα, which is a nuclear receptor and circadian clock component can mediate activation of microglial as well as neuroinflammation. BMAL1 is a potential pathway which could regulate neuroinflammation via the transcriptional regulation of REV-ERBα (Griffin et al., 2019).

1.4 Overview of stem cells

There has been promising research over the last several years on stem cell therapy. Stem cells are unspecialized and can differentiate into more than 200 different cell types and due to their nature they are ideal for potential therapeutic repair and regeneration (Zakrzewski et al., 2019). The division of stem cells is highly regulated and can differentiate into three different germ lines which are ectoderm, mesoderm, and endoderm (Biehl and Russell, 2009). Figure 10 is a summary of adult and embryonic stem cells and their differentiation potential (Dayem et al., 2016). There are several different regions in which adult stems cells can be obtained from, which include the brain, skin, bone, and organs which allows the differentiation into specific cell lineages (Pittenger et al., 2019). Embryonic stem cells (ESC) come from the inner cell mass of a growing blastocyst, and they hold pluripotent properties and give rise to the ectoderm, mesoderm, and endoderm which is shown below in figure 10. There are still many disadvantages in using ESC which include moral and ethical issues as well as immune reactions which could arise after transplanted ESC. There is much research focused on ESC due to the potential they hold in regenerative medicine and the engineering of tissue. ESCs are known for their pluripotent differentiation capabilities; however, this also can cause issues with long-term culture, reliability, and reproducibility. Another crucial factor to note is that it studies have shown that ESC can differentiate spontaneously into tumour cells (Zakrzewski et al., 2019). However, ESCs and induced pluripotent stem cells (iPSCs) are similar in pluripotency, gene expression pattern, morphology, and epigenetic status. The technology of iPSC overcomes the issue faced with moral and ethical related issue of human ESC and the potential immune rejection. In comparison adult stem cells do not present with the limitation above within in vivo models. There is much interest in using adult stem cells in regenerative medicine. However, due to the nature of adult stem cells they are limited in their differentiation potential (Moradi et al., 2019).

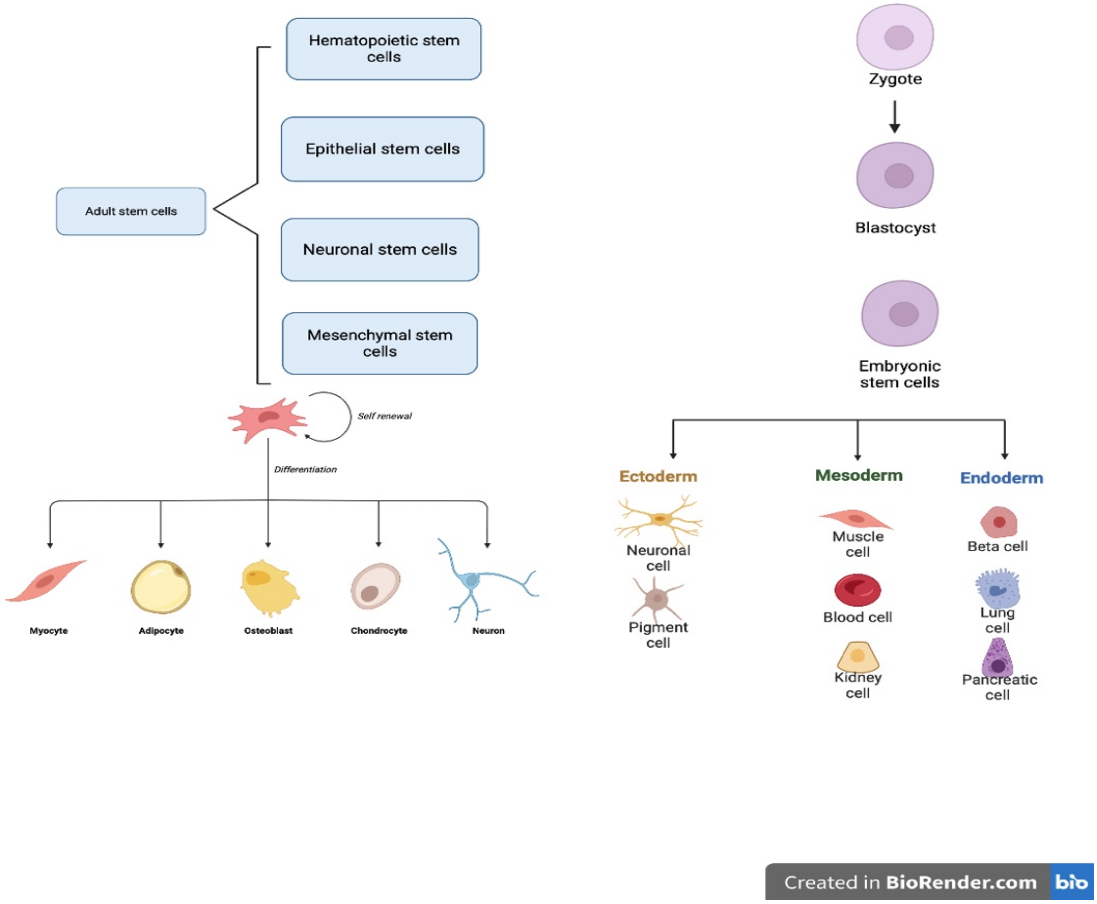

Figure 10 - Differentiation on potential of both adult and embryonic stem cells

Differentiation pathway of either adults stem cells or embryonic stem cells presenting the different germ lineages. Image rendered in Bio-Render.com.

1.4.1 Mesenchymal stem cells

1.4.1.1 Mesenchymal Stem Cells and their potential in neurological regenerative medicine.

Developing new regenerative therapies to repair the brain after ischaemic stroke is vitally important and one promising candidate is mesenchymal stem cells (MSCs) which are widely investigated as a cell therapy for ischemic stroke (Zheng et al., 2018). MSCs have anti-inflammatory potential and are immune regulatory with immunosuppressive capabilities (Y. Han et al., 2019). MSCs express several different key surface markers which include CD73, CD90, CD105 as positive and negative marker for CD14, CD34, CD45 and HLA-DR (Camilleri et al., 2016). MSCs are multipotent stem cells and can be known under different names which include but not limited to mesenchymal stem cells, mesenchymal stromal cells, and

mesenchymal progenitor cells (Pittenger et al., 2019). MSCs can differentiate into all end stage lineages (figure 11) (Musial-Wysocka et al., 2019). Table 2 is a representation of some of the most researched MSCs with common characteristics and specific cell surface markers. There are great advantages of using MSCs over other stem cells, however their clinical applications are hindered by research barriers. One example is being able to obtains adequate cell numbers without losing potency during subculture and at high passage numbers (Ullah et al., 2015). There have been several studies and clinical trials which have conducted safety tests on mesenchymal stem cell-based therapies (Galderisi et al., 2022). Clinical trials have been conducted and show that MSC therapy for the potential treatment in ischemic stroke is feasible and safe (H. Chen and Zhou, 2022).

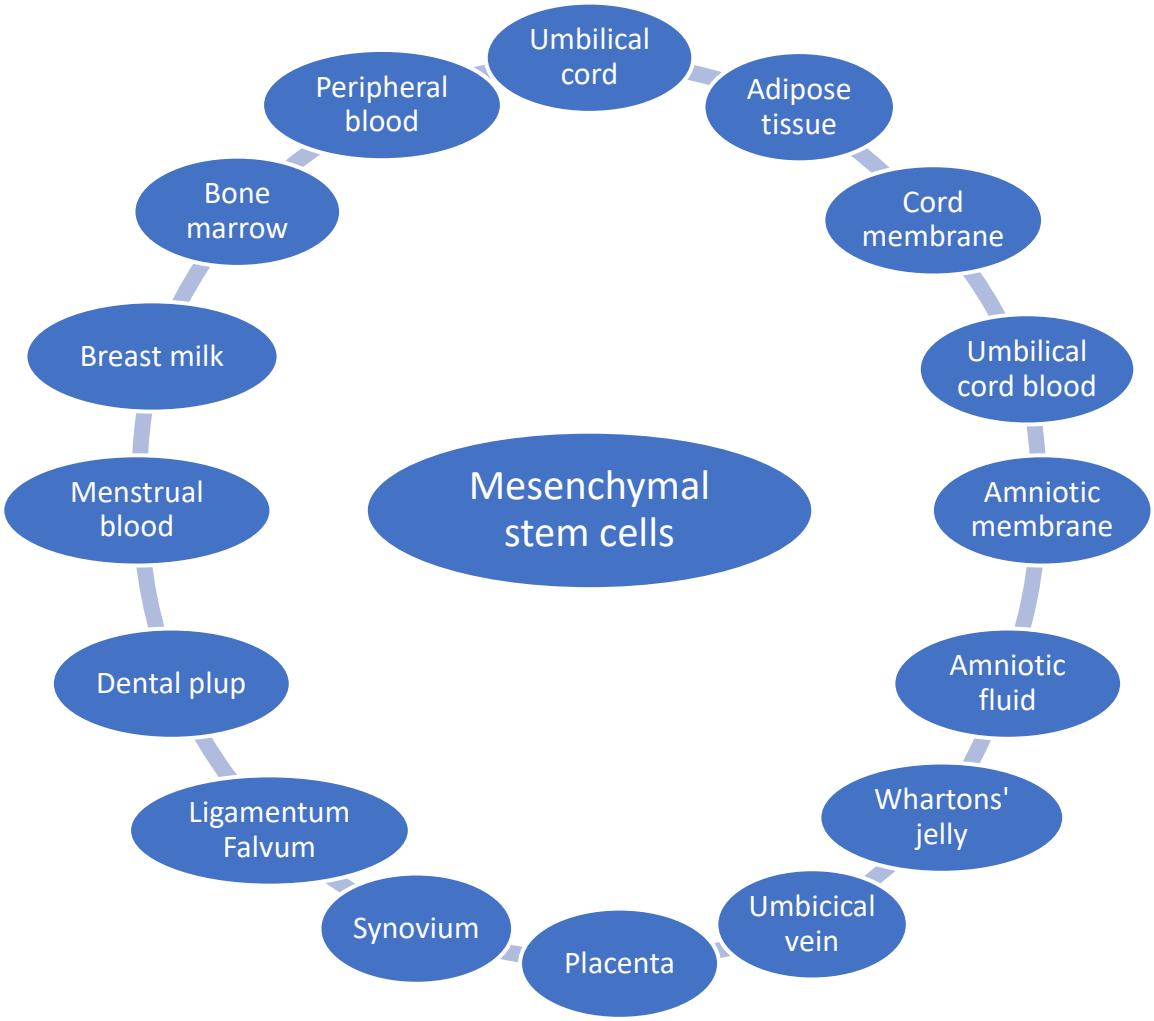

Figure 11 - Location MSC can be harvested.

MSC can be harvested from several different areas within the human body.

Table 2 – Extraction and culture of MSCs derived from various tissues.

MSC Type	Source	Marker	Reference
Adipose derived Stem cells	Human: subcutaneous adipose in abdomen, buttocks, and abdominal zone	$CD29^{+}$ $CD44^{+}$, $CD73^{+}$, $CD90^{+}$, $CD105^{+}$, $CD146^{+}$, $CD166^{+}$, MHC-I^{+}, $CD31^{-}$, $CD45^{-}$, and HLA-DR^{-}	(Zuk et al., 2002; Smadja et al., 2012; B. Q. Guo et al., 2021)
Bone marrow stem cells	Human: tubular bones, iliac crest, and bone marrow	$CD29^{+}$, $CD44^{+}$, $CD73^{+}$, $CD90^{+}$, $CD105^{+}$, Sca-1^{+}, $CD14^{-}$, $CD34^{-}$, $CD45^{-}$, $CD19^{-}$, $CD11b^{-}$, $CD31^{-}$, $CD86^{-}$, Ia^{-}, and HLA-DR^{-}	(Zhu et al., 2010; El-Ansary et al., 2012; Mao et al., 2013)

1.4.1.2 Micro-fragmented Adipose tissue as a source of mesenchymal stem cells

Adipose tissue is the most abundant in humans and there are two forms which are white adipose tissue (WAT) and brown adipose tissue (BAT) (A. Park et al., 2014). WAT is the focus of research, and this tissue is located throughout the body (abdomen, buttocks, and thighs) (Gesta et al., 2007). At the cellular level, WAT has high volume of mature adipocytes, MSC, pericytes and smooth muscle cells. These MSCs are of particular interest in the WAT due to the capacity of further proliferation and expansion. A further benefit of adipose tissue is the extreme high metabolic rate with the continuous remodelling (Christiaens and Lijnen, 2010). The use of adipose derived mesenchymal stems cells (adMSC) over recent years has gained tremendous support and have been isolated from fat tissue through liposuction. The advantages to these stem cells and procedures are that there is little or none apparent side effects (Nava et al., 2019). Enzymatic digestion or mechanical force are two ways to obtain adipose tissue. Firstly, enzymatic digestion technique uses enzymes (Collagenase, Trypsin and dispases) to breakdown the adipose tissue to form a stromal vascular fraction. This fraction can then be cultured or long-term storage through cryopreserved methods. There are several negatives with this method including how expensive the method is, the prolonged isolation time, external compounds added (enzymes) and can be too aggressive and potentially destroy exosomes during processing. In turn, damaging the cells and affecting cell function and viability. On the other hand, this method is efficient and yields a higher cell count (Tiryaki et al., 2020). Mechanical isolation of adipose tissue is a minimal invasive procedure which uses liposuction and fat tissue is normally taken from the abdomen. There are several positives including the procedure is minimally invasive. FDA approval has already been granted and the treatment is quick and is enzyme free. However, the negative is that this method is particularly expensive. Further to this, adMSC is presented in copious quantities in most patients compared to the lesser amounts of BM-MSC (0.001 – 0.01 % of total bone marrow nucleated cells). AdMSC would be a clinical advantage through these reasons alone, especially if an elderly patient would need this as BM-MSC is increasingly challenging to get from elderly patients (Strioga, 2012; Tremolada et al., 2016). There are numerous patented devices but one of particular interest is Lipogems. The process uses micro-fragmented adipose tissues (MFAT) which preservers the structural niche of the tissue. This preservation allows pericytes to turn into MSCs that initiates

the regenerative process and releases anti-inflammatory factors. Therefore, Lipogems is often described as a 'time-release' medium (Randelli et al., 2016; Tremolada et al., 2016; B. Guo et al., 2021).

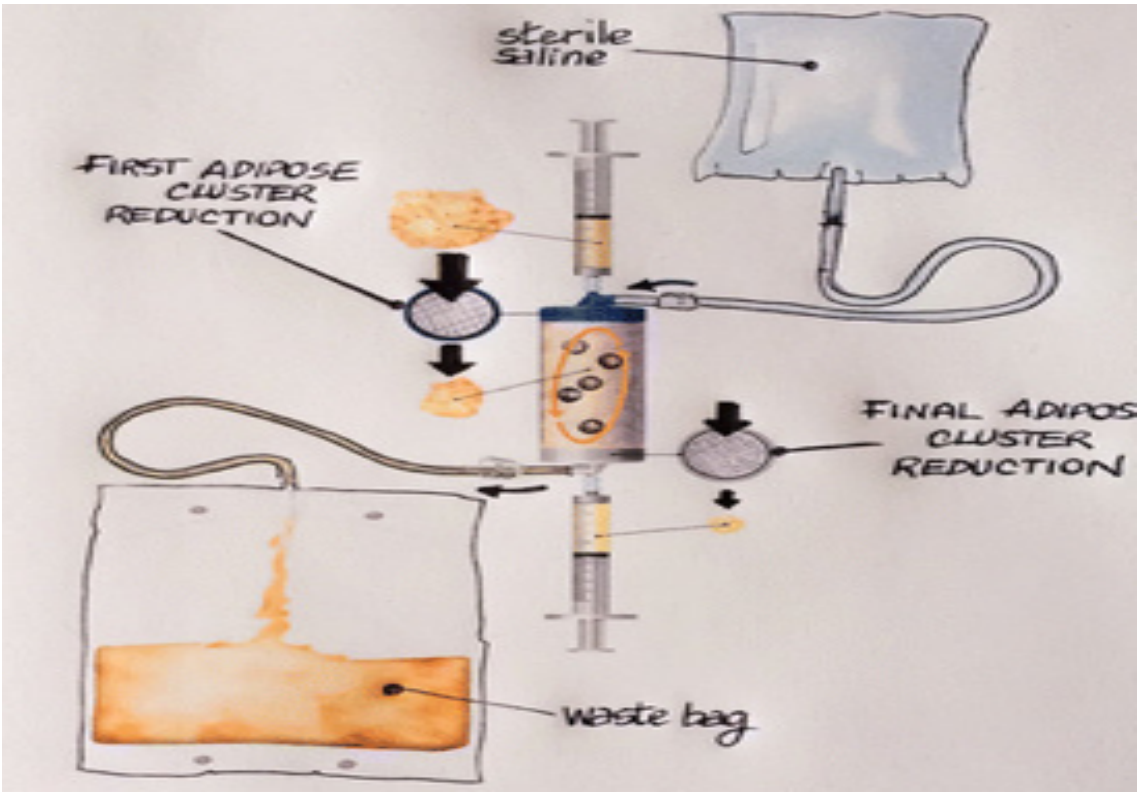

Figure 12 – Mechanism of lipogems device for adipose tissue processing

Drawing from (Tremolada et al., 2016) showing the adipose tissue processing through the lipogems device. This system is closed and is a low pressure cylindric to harvest a product containing pericytes and MSCs.

1.4.1.3 Current stroke and inflammatory models available in vitro and in vivo

Stroke is an extraordinarily complex disease, and many factors are included, currently stroke research is conducted using either in vitro and in vivo models (Holloway and Gavins, 2016). Animal models have been indispensable as a tool to model complex pathophysiology of ischemic stroke (Fluri et al., 2015). The development of animal models was developed with the aim to elucidate the mechanism that underline cerebral ischemia and develop new therapeutic agents for treatment (Ma et al., 2020). There is ongoing research into establishing in vitro cell based models to study the complexity of an ischemic stroke. Brain sections can be used in neurological research; however, tissue is limited and during processing tissue can become damaged leading to abnormal function. On the other hand, the physiological relevance is high and there is application to stroke research through oxygen glucose depletion, chemical ischemia, and excitotoxicity (Nogueira et al., 2022). Primary cells are another source to study ischemic stroke, in which they are physiological relevant and can be used in OGD, chemical ischemia, excitotoxicity and BBB modelling. One disadvantage is that they are limited in availability and passage number once in culture (Holloway and Gavins, 2016). The main cellular platform used for in vitro stroke research consists of monocultures of human and rodent cell lines or primary cells. In general, the use of monocultures is preferred when studying cell-specific responses to OGD and/or to evaluate the action of neuroprotective compounds on specific cell types (Holloway and Gavins, 2016; Van Breedam and Ponsaerts, 2022). The current basic in vitro model systems have disadvantages in studying ischemic stroke due to the lack of intact blood vessel and flow (Wevers et al., 2021; Van Breedam and Ponsaerts, 2022). Microfluidic modelling using 3D printed designs or commercially available chips are bridging the gaps in research. Microfluidic devices are a promising way for to allow researchers to generate complex environments (oxygen glucose depletion) which can be treated under many different conditions (Holloway and Gavins, 2016).

1.5 Aims and objectives.

Investigating the effects of inflammatory mediators on the neuroinflammatory response

The principal aims of the work presented in this thesis were to:

1. Characterise morphological changes in monocytes and macrophages caused by mCRP.
2. Characterise mCRP as pro-inflammatory mediator.
3. Investigate potential novel anti-inflammatory therapeutic targets using an inflammatory in vitro model set up.
4. Characterise micro-fragmented adipose tissue and its ability as an anti – inflammatory target using an inflammatory in vitro model set up.

Chapter 2 – Materials and methods

2.1 Materials

Table 3 - Materials

Reagents and chemicals	*Company*
U937	ATCC® CRL-1593.2
HMC-3	ATCC CRL-3304
Roswell Park Memorial Institute Medium (RPMI)	Lonza, UK
Dulbecco's phosphate buffered saline	Lonza, UK
Dulbecco's modified eagle medium	Sigma Aldrich
Foetal bovine Serum (FBS)	Sigma Aldrich
Phorbol myristate acetate (PMA)	Sigma Aldrich
GSK4112	Sigma Aldrich
GW3965	Sigma Aldrich
Human IL-8 ELSIA	Sigma Aldrich
Human MCP-1	Sigma Aldrich
Human TGF beta 1	Sigma Aldrich
Lipopolysaccharides (LPS)	Sigma Aldrich
Minimum Essential Medium alpha	Sigma Aldrich
Tris base	Fisher Scientific, UK
Tween-20	Fisher Scientific, UK
Bovine serum albumin (BSA)	Fisher Scientific, UK
Ethylenediaminetetraacetic acid (EDTA)	Fisher Scientific, UK
Bicinchoninic acid assay (BCA)	Fisher Scientific, UK
Dimethyyl sulfoxide (DMSO)	Fisher Scientific, UK
IgG 568 goat anti mouse	Fisher Scientific, UK
Pierce™ Chromogenic Endotoxin Quant Kit	Fisher Scientific, UK
Alexafluro 488 goat anti-rabbit IgG	Fisher Scientific, UK
Quantikine multiplex system 32 self-designed	R&D Systems, bio-techbrand®
DuoSet ELSIA (IL-1 beta, IL-6, IL-10, TNF alpha)	R&D Systems, bio-techbrand®
Human TNF-α DuoSet ELISA	R&D Systems, bio-techbrand®
Human IL-1β/IL-1F2 DuoSet ELISA	R&D Systems, bio-techbrand®
Human IL-6 DuoSet ELISA	R&D Systems, bio-techbrand®

Human IL-10 DuoSet ELISA	R&D Systems, bio-techbrand®
Human TGF beta 3 DuoSet ELISA	R&D Systems, bio-techbrand®
DuoSet ELISA Ancillary Reagent Kit 2	R&D Systems, bio-techbrand®
IL-6 anti-mouse (1/50)	R&D Systems, bio-techbrand®
RNAeasy mini kit	Norgen
QuantiTect Reverse Transcription Kit	Qiagen
QuantiNova Syber green qPCR	Qiagen
Bio-Rad 27-plex human cytokine kit	Biorad
Endotoxin Removal Kit - (Rapid)	ABCAM
Native C reactive protein	My BioSource
FITC Annexin V Apoptosis Detection Kit 1	BD (Becton, Dickinson) Bioscience
Trypan Blu solution	Corning
Urea	Promega
Trypsin EDTA	Lonza, Belgium
Anti-NF-kB p65 (phospho S 536) antibody (1/100).	Cell signalling
Depc-Treatted Water, DNase/RNase fre	Bioline
Ethanol	Fisher chemicals
Invitrogen™ UltraPure™ Urea	Invitrogen

Table 4 -Equipment and software

0.2 um filter pores	Merck
24 well ibidi	ibidi
12 well plate	Star labs
2k Slide A – lyzer dialysis cassette	Thermofisher UK
-80 freezer UltraFlow Freezer	Nuarie
Countless II (cell counter)	Life technologies
Centrifuge 3-16KL	Sigma Aldrich
FLUOstar Omega plate reader	BMG-Labtech FluOstar Omega
Graph Pad version 9	Graph pad
IR direct heat CO 2 incubator	Autoflow
LAS-X	Leica
Luminex	Biorad
MACSQuant 16 flow cytometer	Miltenyi
Mr. Frosty™ Freezing Container	Fisher
NanoDrop™ One/OneC Microvolume UV-Vis Spectrophotometer	Thermofisher UK
Pipette	Gibson
qPCR CFX system	Biorad
Safe Fast premium tissue culture hood	Safe fast
Thunder imaging system and microscope	Leica
T25 and T75 tissue culture flask	Star labs
Microsoft 365 app suite	Microsoft
Water bath	Grant JB Nova

2.2 Methods

2.2.1 Tissue culture

2.2.1.1 Complete media preparations

Table 5 - U937 cell line complete media recipe

RPMI	500 ml
Foetal bovine serum	100 ml (20%)
Penicillin – streptomycin	100 I.U./ml

Table 6 - HMC-3 microglia complete cell media recipe

Component	Volume
EMEM	500 ml
Foetal bovine serum	100 ml (20%)
Penicillin – streptomycin	100 I.U./ml

Table 7 - Adipose derived mesenchymal stem cells complete media recipe

DMEM	500 ml
Foetal bovine serum	100 ml (20%)
Penicillin – streptomycin	100 I.U./ml

2.2.1.2 Human promonocytic leukaemia U937 cells (ATCC® CRL-1593.2)

Human promonocytic leukaemia U937 cells (ATCC® CRL-1593.2) were thawed rapidly in a 37°C water bath until 80% defrosted and decontaminate by spraying with 70% ethanol and placed in a class 2 cell culture hood. The defrosted cells were transferred to a 15 ml falcon tube containing 9.0 ml of RPMI-1640 complete culture medium (Table 5). The flacon tube was placed in a centrifuge and spun at 125 x g for 7 minutes. The supernatant was removed without disturbing the pellet and resuspended with the recommended complete medium and dispensed into a T-25 cm^2 flask. The flask was placed into a tissue culture incubator set to 37^oC with 5% CO^2. The media was changed every 2/3 days until subculture was needed.

2.2.1.3 Subculturing human promonocytic leukaemia U937 cells

U937 cells were cultured under aseptic conditions using RPMI-1640 complete medium (table 5). Firstly, the U937 cell suspension was centrifuged at 125 x *g* for 7 minutes before the supernatant was discarded and pellet resuspended in 9.0 ml of complete medium. The cells were counted using sterile filtered 0.4 % trypan blue dye in a 1:1 ratio and counted using a TC-10 automated cell counter (Bio-Rad, USA). For all experiments unless stated otherwise the cells were set to $1x10^6$/0.5 ml in 12 well plates. Cell viability maintained above 90% for all experiments. U937 cells were routinely checked for good health (figure 13). Cells appear round and floating in a tightly pack manner indicating confluence. Image was taken using an Axiovert inverted phase contrast microscope at 10x magnification.

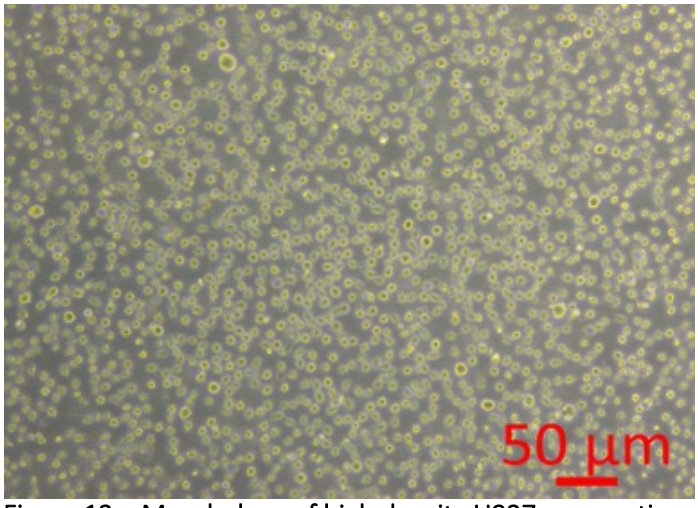

Figure 13 – Morphology of high density U937 monocytic cells. Images were taken using an Axiovert 10x inverted phase contrast microscope.

2.2.1.4 Freezing process for suspension cells

U937 monocyte cells were placed in a 15 ml or 50 ml flacon depending on the volume with 20 µl of supernatant taken to measure cell count. From the cell suspension, 20 µl is taken and mixed equally (1:1) with trypan blue and counted using the TC-10 automated cell counter (Thermofisher). Cells were set to $1x10^6$/ml in freezing media (90 % FBS and 10% DMSO v/v) and transferred to 1 ml cryogenic vials. The cryogenic vials were placed in a Mr frosty which allowed gradual freezing of the cells over 24-hour period and placed in liquid nitrogen for long term storage.

2.2.1.5 PMA differentiation of U937 monocytes to M0 macrophages

U937 monocytes were taken from the T-75 flask and placed in a new 15 ml falcon tube. Phorbol 12-myristate 13-acetate (PMA) (Sigma Aldrich) cultured medium was prepared to a concentration of 50 ng/ml. Cells were set to 1 x 10^6 cells/0.5 ml and resuspended in PMA cultured media. In a 12 well plate, 500 µl of PMA treated monocytes were added to each well and placed in a cell culture incubator. Media containing PMA was changed the following day to fresh complete media and incubated for a further 48-hours in incubator set to 37°C and 5% CO_2.

2.2.1.6 Defrosting HMC-3 microglia cells

Vial of HMC-3 microglia cells was thawed by gentle agitation in a 37°C water bath. The content of the vial was transferred into a 15 ml falcon tube and centrifuged at 125 x g for 7 minutes. The cell pellet was resuspended in fresh complete medium (Table 6) and placed in a new T-25 flask and incubated at 37°C and supplemented with 5% CO_2. Media was changed every 2/3 days until 80% confluence was reached and the cells were sub-cultured. Viability was maintained at 90%.

2.2.1.7 Sub-culturing adherent cells

Firstly, the old media is removed, and cell layer rinsed with PBS to wash any remaining media away. Trypsin-EDTA solution (3.0 ml) was added and then the flask was placed into the cell culture incubator at 37°C with 5% CO^2 for 5 minutes. The flask was checked under the microscope for detachment and 3 ml of complete growth medium was added to the flask to stop the reaction. Cultures were maintained between 1.0 x 10^4 and 2.0 x 10^5 cell/$cm^{2,}$ with the media changed every 2/3 days. Cell health was checked via cell viability assay using trypan blue and visually inspecting cells (Figure 14). Viability was maintained above 90%.

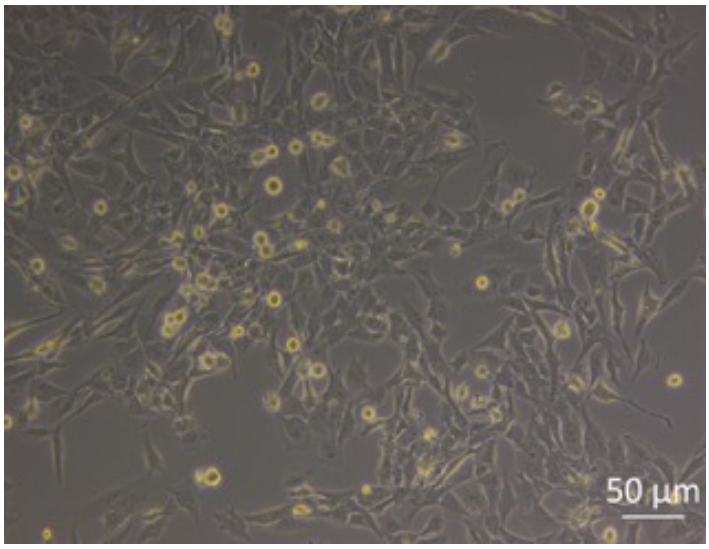

Figure 14 - Morphology of confluent HMC-3 microglia cells. Images were taken using an Axiovert 10x inverted phase contrast microscope.

2.2.1.8 Cryopreservation HMC-3 cells

Cells which are around 80-90% confluent were prepared for freezing. The media was removed from the flask and the cell remained attached. The cells are firstly washed with DPBS (2X) to remove any old media. Trypsin (5 ml) was added to the T-75 flask and placed in cell culture incubator with 5% CO^2 and 37°C humidity for 5 minutes. Cells were checked under the microscope for detachment. The media was collected with the detached cells and pipetted into a new 15 ml flacon tube and centrifuged at 125 x g for 7 minutes. The supernatant was removed and 1 ml of freezing media (10% DMSO and 90% FBS) was added to the cell pellet and then place into cryovials and then into Mr Frosty to allow slow freezing.

2.2.1.9 Preparation of MFAT conditioned media

Micro-fragment adipose tissue (MFAT) was obtained from 10 healthy volunteers according to the policies of Manchester Metropolitan University with ethical approval granted (Ethos; project ID 24407). MFAT obtained from the clinic within 8 hrs, after washing twice with DPBS by centrifuging for 10 minutes at 300 x g. One unit (0.25mL) of MFAT was added into a 6 well plate. After 24 hrs and 5 days, the supernatant was harvested and filtered through a 0.22 μm protein low binding filter. MFAT conditioned media was stored at -20 ^{o}C.

2.2.1.10 Isolation, Expansion and Characterisation of Adipose-Derived (AD)-MSCs

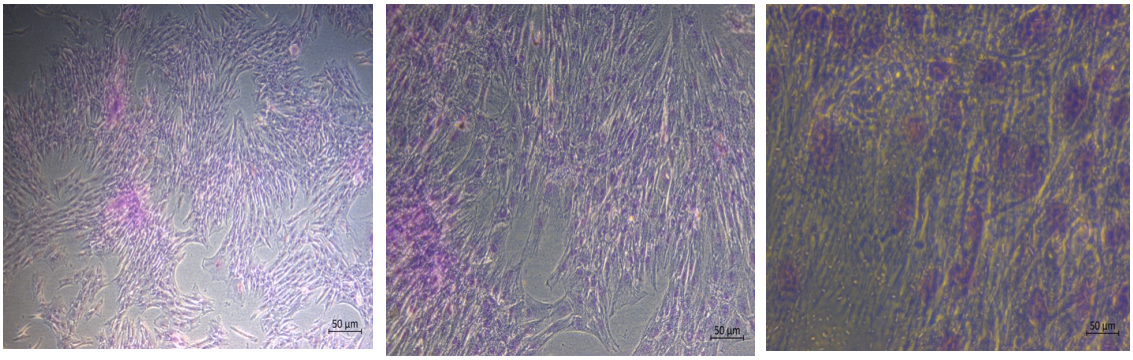

Figure 15 - MFAT sample 10 - Geimsa stain to determine colony count.

A) 4x10 magnification, B) 10x10 magnification, C) 10x40 magnification. Images were taken using an Axiovert 10x inverted phase contrast microscope.

From each MFAT sample, 2 ml were processed for mesenchymal stem cell isolation. Firstly, each of the samples of MFAT were washed with PBS and centrifuged at 250 × g for 3 minutes to remove blood residual. After discarding of the supernatant, MFAT were digested in collagenase type I (1 mg/ml) (ThermoFisher Scientific, Altrincham, UK) with gentle agitation for 1 hour at 37°C. After 1-hour samples were neutralised MEMα which contained 20 % foetal calf serum and centrifuged at 800 x g for 5 minutes to separate the stromal cell fraction pellet from the adipocytes. Red blood cell lysis buffer (160 mM) of NH_4Cl was added to each sample for 10 minutes whilst kept on ice and centrifuged at 800 x g for another 5 minutes. The supernatant was discarded, with the pellet re-suspended in MEMα containing 20% FBS. The samples were then passed through 100 μm nylon strainer and then placed in a separate T-25 flask to allow for stem cell growth. Non-adherent cells were observed and removed from the flask the next day by washing with PBS to remove such non adherent cells. Fresh MEMα medium containing

20% FBS. The change of medium was done every two to three days. Cells were tested by the Slevin research group previously for adipose stem cell phenotype and results were presented in (B. Guo et al., 2021).

2.2.2 Preparation of C reactive protein isoforms

2.2.2.1 nCRP preparation and dialysis

In a sterile tissue culture hood, nCRP solution (Bio-source) was added to a 50,000 Da 2k Slide A – lyzer dialysis cassette. This was then placed in a cylinder with 2 mM $CaCl_2$ buffer for 24 hours with 3x changes of buffer. After 24 hrs, nCRP was extracted from the cassette and a bicinchoninic acid (BCA) analysis was performed to determine the new concentration (2.2.6.2).

2.2.2.2 Dissociation of nCRP to mCRP

Dialysed nCRP was dissociated to mCRP using the urea/chelation method. In a 1:1 ratio, 1.5 ml of nCRP was chelated with stripping buffer (10 mM EDTA and 8M urea/100 mL ddH_20). The solution was incubated at 37°C for 2 hours prior to the dialysis stage and endotoxin removal.

2.2.2.3 Dialysis of CRP isoforms (nCRP and mCRP) through 2k lyzer caseate

In a 5-litre cylinder with autoclaved PBS buffer, the 2k Slide A – lyzer dialysis cassette was hydrated for 2 minutes. Once the cassette was hydrated then mCRP was injected into the cassette using a needle and a syringe, being careful not to puncher the membrane. The air was removed out of the cassette with the syringe ensuring that all the solution remained. The cassette was then placed in fresh autoclaved buffer and incubated for 24 hours, and the buffer changed 3x during that time. The cassette was removed from the cylinder and air was placed in the cassette and then the samples was withdrawn using a needle and a syringe. This was conducted in a class II hood to ensure sterile conditions. The concentration of mCRP protein was checked for purity and quantified using BCA analysis.

2.2.2.4 Endotoxin removal

The columns were firstly prepared by placing them in endotoxin free collection tubes and 500 µl of endotoxin removal equilibration buffer was placed in the column and centrifuged at (15,000 x g for 5-10 seconds). The flow through was discarded at this point. The column was then regenerated by adding 0.5ml rapid endotoxin removal regeneration buffer and centrifuged with flow through discarded. This process was repeated for a total of 3x. After this was completed then the column was washed 3x using rapid removal wash buffer and centrifuged to discard the flow through. The next step was to equilibrate agarose by adding 0.5 ml endotoxin removal equilibration buffer and a quick spin to remove the solution. This step was repeated for a total of 2x. The column was placed in a new collection tube and 0.5 ml of nCRP or mCRP was added to the column. The column was incubated for 1 hour at room temperature and the sample pass through 3x before centrifuged to collect samples. This entire process was completed 2x to remove endotoxins to an acceptable level for experiments. BCA is performed on nCRP and mCRP to determine the final protein concentration after purification.

2.2.2.5 Pierce Chromogenic endotoxin quantitation kit

Firstly, endotoxin standard stock solution is prepared following the guidance from ThermoFisher scientific. Each standard vial contains a range of 10-50 EU of lyophilized endotoxin which was reconstitute with room temperature Endotoxin-Free Water with the volume indicated on each standard vial.

Table 8 - Dilution table of standard

Vial	Vol of endotoxin standard solution (ml)	Volume of standard 1 (ml)	Endotoxin free water (ml)	Final endotoxin concentration (EU/ml)	Vortex time (Min)
Standard 1	0.20	-	1.80	1.00	2
Standard 2	-	1.00	1.00	0.50	1
Standard 3	-	0.5	1.50	0.25	1
Standard 4	-	0.20	1.80	0.10	1
Blank	-	-	0.50	0	-

mCRP pH was tested to insure it was in the range of 6-8 to allow analysis with the endotoxin kit. The endotoxin plate was placed on a heat block at 37°C to pre heat the plate before 50 µl of endotoxin standards, blank and samples were added. The plate remained on the heat block when solution was added and then 50 µl of reconstituted amoebocytes lysate reagent added to each well. The plate was removed from the heat block and samples were mixed by gently tapping the plate 10x and then placed back. The plate was then incubated for 10 minutes. The chromogenic substrate was reconstituted and prewarmed for 5 minutes before 100 µl of this solution was added to each well and incubated for 6 minutes at 37°C After the 6-minute timer was up, stop solution (25% acetic acid) was added to each well at 50 µl each. The plate was read on a plate reader at 405nm.

2.2.3 Microscopy

2.2.3.1 Inverted microscope

To observe the morphology of U937 monocytes after treatment with mCRP the cells were set in a 12 well plate at 1 x 10^6 / mL and serum starved for 24 hours. The monocytes were treated with mCRP protein (100 µg/ml), nCRP (100 µg /ml), LPS at 10 ng/ml and negative control serum free media (RPMI). Observation took place using the Anxio invert microscope at 10x magnification at two different time points which were 3, 6 and 24 hours.

2.2.3.2 Viability assays trypan blue

U937 monocyte cells were set to 3 X 10^5/ml total 1 ml in 12 well plate and treated with LPS 10 ng/mL, mCRP 100 µg/ml and nCRP 100 µg/ml for 24 hours with readings taken at 3, 6 and 24 hours to measure cell viability after treatment. Cells were counted using the Bio-Rad TC-10 automated cell counter and the average was taken from 3 reading per a condition at each time point.

2.2.3.3 Holomointor live cell tracking of adherent cells.

HMC-3 microglia cells were seeded at 5% confluence in a 24 well ibidi plate (10,000 cells) in complete media and left for 24 hours to adhere to the plate surface. The Holomointor is set up in a humified chamber with 5 % CO^2 at 37°C. The cells were treated with complete media, LPS 10 ng/ml, mCRP 100 µg/ml and nCRP 100 µg/ml. The plate is sealed with sterilized HoloLids designed for live cell microscope. Holographic imaging was set up according to manufacturer's manual, and a minimum of three fields of view per well was selected with image taken every hour for 24 hours. Parameters that will be measured include cell tracking, cell morphology and cytotoxicity analysis.

2.2.3.4 Immunofluorescence

HMC-3 microglia cells were grown on a glass slide inserted into 24 well plate with a seeding density set to 1000 cells per slide. The cells were left for 24 hours to allow the cells to attach. The old media was aspirated off and the cells were washed with DPBS to remove any unbound cells. Each condition was added to the corresponding wells and incubated for 6 hours. (Control, LPS 10 ng/ml, mCRP 100 µg/ml, nCRP 100 µg/ml, GW3965 2.5 µm, GW3965 2.5 µM and LPS 10 ng/ml and finally, GW3965 2.5 µm and mCRP 100 µg/ml). After the treatment period, media was aspirated, and the glass cover slips were washed with DPBS. The slides were then blocked for 30 minutes with 4% goat serum in DPBS with 80 µl added to each slide. Primary antibodies were prepared in blocking solution which included anti human IL-6 anti-mouse (1/50) and Anti-NF-kB p65 (phospho S 536) antibody (1/100). On to each slide, 80 µl were added and then incubated in the dark at 4^{o}C overnight. The slides were rinsed 2x in DPBS for 5 minutes at a time. The secondary antibodies included were IgG 568 goat anti mouse to detect IL-6 (red) and Alexafluro 488 goat anti-rabbit IgG to detect Phoso NfKb P65 (green) at 1/200 dilution with blocking solution for 1 hour. The slides were washed 2x with DPBS for 5 minutes at a time to remove unbound secondary. Finally, the glass slides were mounted onto cover slip with vector shield (h-1200 with DAPI). To fix the glass slides to the coverslips enamel paint was used. The samples were view on the thunder microscope system and at analysis with computational clear was also performed using the integrated analysis software. The samples were view at 10x63 oil magnification at 3 different points (n3). No primary control was added to the analysis.

2.2.3.5 Scanning electron microscope

2.2.3.5.1 Scanning electron microscope on adherent cells

HMC-3 cells were set to 500 cells in 50 µl and pipetted in 24 well plate containing silicon wavier slides (1 cm in diameter) and left to adhere for 24 hrs in incubator at 37°C with 5% CO_2. Cells were treated with LPS 10 ng/ml, mCRP 100 µg/ml and nCRP 100 µg/ml for 6 hours. Media was removed after 6 hours, and slides washed with DPBS to remove any media. Cells were fixed with 2 % glutaraldehyde for 24 hours. The cells were dehydrated using an ethanol gradient (30%, 50%, 70% and 100%) and then left to dry before being coated with gold. The waivers were mounted on stubbiest ready for viewing on the scanning electron microscope.

2.2.3.5.2 Scanning electron microscope on suspension cells

U937 cells were set to 500 cells in 50 µl and pipetted in 96 well plate. Cells were treated with LPS 10 ng/ml, mCRP 100 µg/ml and nCRP 100 µg/ml and DMSO (20%) for 6 hours. After treatment cells were pipetted onto silicon wavier slides 1 cm in diameter and allowed to settle onto to the slides and media dry out. Cells were fixed with 2 % glutaraldehyde for 24 hours. After 24 hours the cells were dehydrated using an ethanol gradient (30%, 50%, 70% and 100%). The waivers were left to dry before being coated with gold and mounted on stubbiest ready for viewing on the scanning electron microscope.

2.2.4 Flow cytometry

2.2.4.1 Phenotyping analysis of differentiated U937 macrophages by flow cytometry.

U937 cells differentiated macrophages and undifferentiated monocytes were washed 3x with DPBS. A total of 500 µl of Trypsin-EDTA solution per well was added and incubated for 7 minutes in tissue culture incubator. Another 500 µl of complete media (table 5) was added to the 12 well plate. The cells were transferred to 6 separate centrifuge tubes and centrifuged for 7 minutes, at a speed of 180 x g with the supernatant discarded. The cells were washed twice in DPBS and centrifuged at 180 x g for 7 minutes. Following the last washing procedure, 40 µg/ml of anti-human CD11c antibody (Thermo-fisher Anti–Hu CD11c LOT2008210) was diluted in a washing buffer containing 10 % FBS and DPBS and incubated in the dark for 15 minutes. The unbound antibody was washed with 200 µl of washing buffer and centrifuged at 180 x g for 7 minutes. The supernatant was removed, and cell pellet was resuspended in FACS buffer and run on the Miltyni flow cytometry instrument and analysed using flowlogic.

2.2.4.2 FITC Annexin V Apoptosis Detection by flow cytometry

U937 monocytes were observed for apoptosis by flow cytometry using the Annexin-V Fluorescein isothiocyanate (FITC) apoptosis detection kit. U937 cells were set in a 12 well plate at 1 x 10^6 / 500 µl. The monocytes were treated with mCRP (100 µg/ml), nCRP (100 µg/ml), LPS at 10 mg/ml, negative control (RPMI) and positive control (20% DMSO). After treatment, U937 cell suspension was removed and placed in new eppendorf tubes. Cells were washed via centrifuging (180 x g for 7 minutes) and washed with DPBS 1X. DPBS was removed, and the cell pellets were resuspended in 1x binding buffer at a concentration of 1 x 10^6 cells/ml with 100 µl of the solution (1 x 10^5 cells) transferred to the falcon tube for flow cytometry. To the falcon tubes 10 µl of FITC Annexin V and 10 µl PI was added and vortexed for 10 seconds and incubated for 20 minutes, at room temperature in the dark. 15 minutes later, 400 µl of 1x binding buffer was added to each tube and sample run though the Miltyni flow cytometry instrument and analysis using flowlogic (n=3).

2.2.5 RNA analysis

2.2.5.1 Primer design

Primers for qPCR were designed using the primer design tool located on the NCBI website. Each new set of primer were tested and optimised before use to determine the best annealing temperature as seen in figure 16 and 17. After optimisation on primers, it was deemed that 61 ^{o}C was the optimal annealing temperature for syber green qPCR with 2 µl of cDNA loaded at 500 ng.

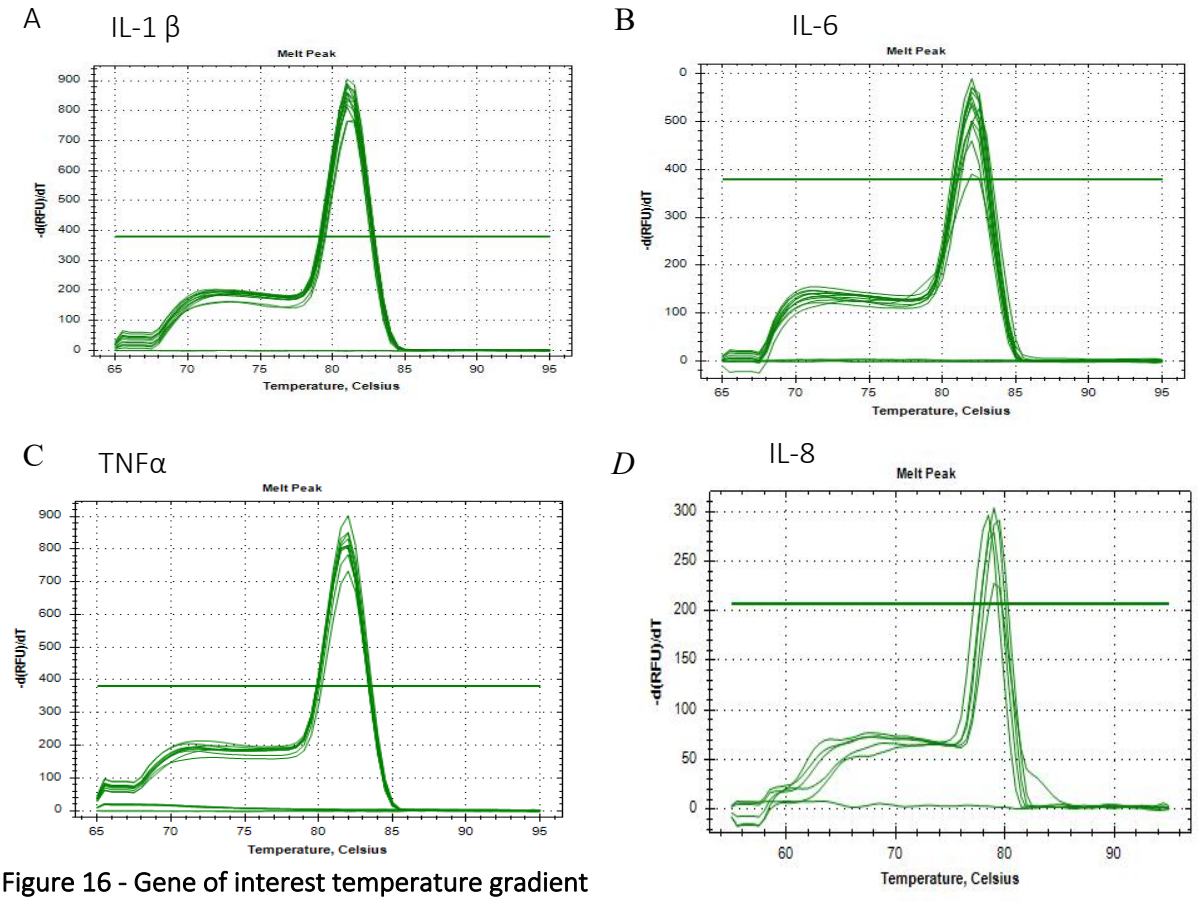

Figure 16 - Gene of interest temperature gradient

Temperature gradient melt peak analysis. Range in annealing temperatures (58 – 65 ^{o}C) A) IL-1β melt peak, B) IL-6 melt peak, C) TNFα melt peak and D) IL-8 melt peak. Bio-Rad integrated CFX analysis software

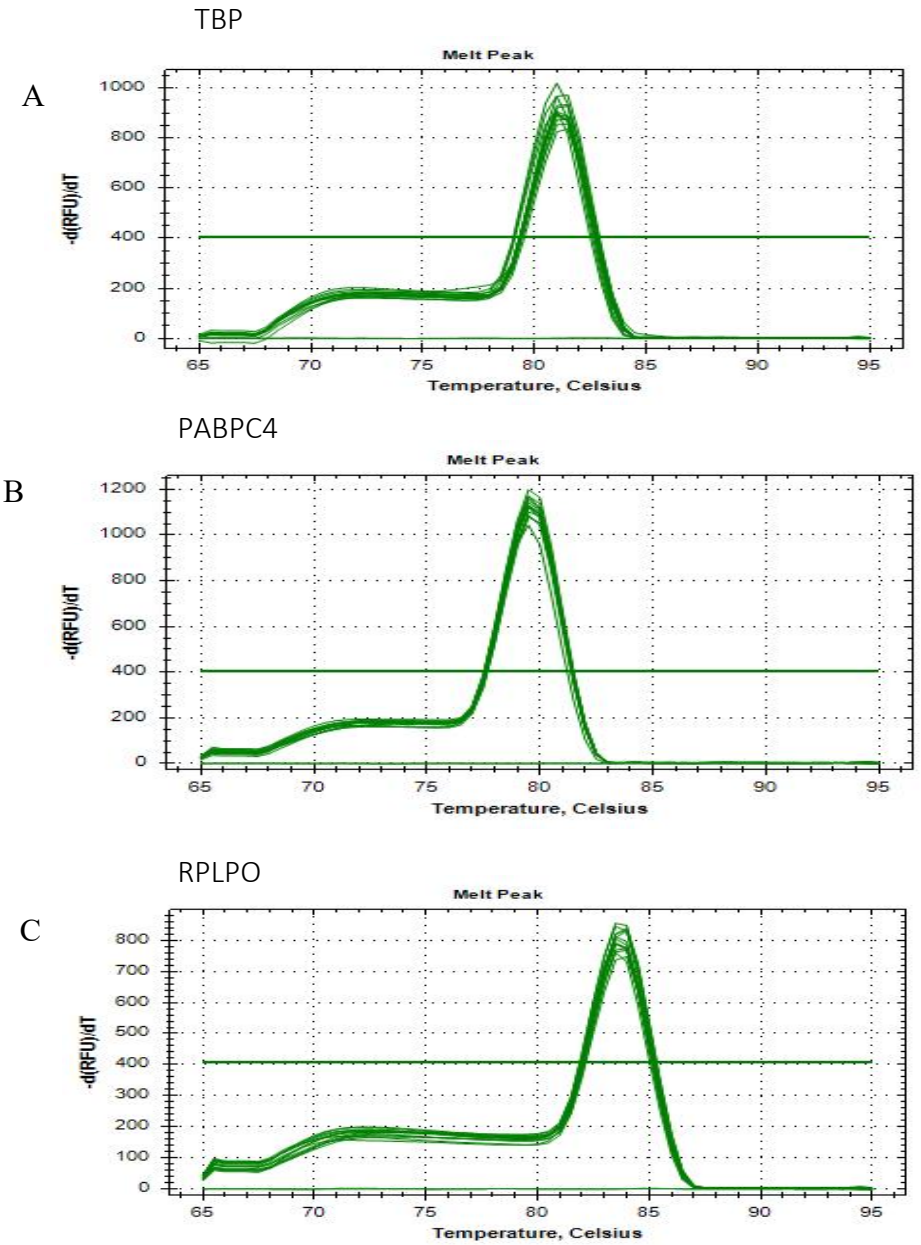

Figure 17 - Housekeeping genes temperature gradient

Temperature gradient. Temperature gradient melt peak analysis. Range in annealing temperatures (58 – 65 °C) A) TBP, B) PABPC4 and C) RPLPO, Bio-Rad integrated CFX analysis software

Table 9 - Forward and reverse primers

Primer	Forward sequence	Reverse sequence
IL-6	GTGTTGCCTGCTGCCTTCC	TCTGCCAGTGCCTCTTTGCT
IL-8	GATTTCTGCAGCTCTGTGTAA	AGACAGAGCTCTCTTCCATCA
IL-10	AGGGCACCCAGTCTGAGAAC	AGGCTTGGCAACCCAGGTAA
TNFα	CTGCACTTTGGAGTGATCGGC	CTTGTCACTCGGGGTTCGAGA
IL-1β	TTCGAGGCACAAGGCACAAC	TTCACTGGCGAGCTCAGGTA
PABPC4	AAGCCAATCCGCATCATGTG	CTCTTGGGTCTCGAAGTGGAC
TBP	CCACGCCAGCTTCGGAGAGT	TCAGTGCCGTGGTTCGTGGC
RPLPO	GCAGCAGATCCGCATGTCCC	TCCCCCGGATATGAGGCAGCA

2.2.5.2 RNA extraction

Total RNA was extracted using the Norgen total RNA purification kit, according to manufacturer's instructions: Cells were washed with DPBS prior to lysis with RL buffer, the lysate was then added to microcentrifuge tube with 200 µl of 100 % ethanol. Next the lysate was centrifuged at ≥ 3,500 x g (~6,000 RPM) for 1 minute to allow the RNA to bind to a spin column. The bound RNA was then washed before being eluted from the spin column into a collection tube. The purified RNA sample was then stored at -80^{o}C.

2.2.5.3 Reverse transcription PCR

Total RNA was converted into complementary DNA (cDNA) using the tetro cDNA synthesis kit (Bioline, UK). All samples were set to 500 ng before being added to the cDNA master mix (equates 50ng) to Master mix includes Oligo (dT)18 (1 µl), 10mM dNTP mix (1 µl), 5x RT Buffer (4 µl), RiboSafe RNase Inhibitor (1 µl), Tetro Reverse Transcriptase (200 u/µl) (1 µl). The reaction was prepared on ice and once ready was placed in a thermocycler and ran for 45^{o}C for 30 minutes, 85^{o}C for 5 minutes. cDNA was further diluted 1/10 with RNAase free water (5 ng) and stored at -20^{o}C.

2.2.5.4 Quantitative PCR

The master mix contain 2 µl cDNA (equates to 0.5 ng/ml per rection), 5.2 µl of RNAse free water, 10 µl of syber green master mix, 1.4 µl of forward primer (0.7 µM) and 1.4 µl of reverse primer (0.7 µM). The solutions were placed in the thermocycler and ran for step one 95 ^{o}C for 2 minutes, Step two 95^{o}C for 5 seconds and 61^{o}C annealing and extension for 5 seconds. Step two was repeats for 35 cycles.

2.2.6 Protein analysis

2.2.6.1 Protein determination - Bicinchoninic acid (BCA assay)

BCA protein concentration was used to observe the final concentration mCRP and nCRP after endotoxin and dialysis purification steps.

The kit contains:

- 2 mg/ml Albumin Standard
- BCA Protein Assay Reagent A
- BCA Protein Assay Reagent B

The unknown protein concentrations were determined using a bicinchoninic acid (BCA) assay kit (Pierce, Thermofisher). Standards were made from bovine serum albumin (2 mg/ml) diluted in lysis buffer. 25 ml of all samples and standards were added to individual wells on a 96 well plate, run in triplicate. 200 ml of master mix (50 parts buffer A to 1-part buffer B) was added to both samples and standards, mixed well. Plate was incubated at 37°C for 30 minutes before being read at 562 nm on a Synergy HTX Multi-mode reader (BioTek) (540-590 suitable if another wavelength not available.

2.2.6.2 DuoSet Enzyme linked immunosorbent assay (IL-1β, IL-6, TGFβ 3 TNFα)

Supernatant was harvested and placed in 1.5 ml eppendorf's and spun at 1000 x g and placed in new clean eppendorf's and stored at -80 degree. ELISA were conducted following the R&D system duo kit ELSIA manufactories instructions. Capture antibody was prepared using PBS included in ELISA kit and 100 µL plated into 96 well plate, sealed and left overnight at room temperature. Following day, the plate is washed with 3 x with wash buffer 300 µL and then plated blocked with 300 µL of reagent diluted for 1 hour. The standard was prepared using a serial dilution following the instruction provided. After blocking, the plate was washed a further 3 x time using an automated multichannel pipette and added 300 µL per a well and gentle tapped on clean tissue paper to remove liquid. The prepared standard and blank were added at 100 µL per well which was then followed by 100 µL of samples added to the remaining empty wells. The plate was sealed using plate seals provided by Biotechne and incubated at room temperature for 2 hours. After 2 hours the plate was washed 3x time and a total of 100 µL of detection antibody (detection antibody included in the DuoSet ELISA Ancillary Reagent Kit 2) was added to each well and plate was sealed and incubated at room temperature for a further 2 hours. Plate was washed 3 more times and 100 µL of Streptavidin-HRP, was added to each well and covered and incubated at room temperature for a total of 20 minutes. After which, the plate was washed three more times and 100 µL of substrate solution was added to each well this time incubated in the dark at room temperature for a totally of 20 minutes. Stop solution was then added at 50 µl per well to stop the reaction and then plate was read on plate reader using wavelength 450 and 570 nm for background correction. Analysis was performed using graph and 4-point standard curve was used to determine unknown concentrations. All sample were represented in biological and technical repeats (n=3).

2.2.6.3 Sigma Enzyme linked immunosorbent assay (MCP-1, TGFβ1 and IL-8)

Firstly, the kit was brought up to room temperature before any experiment was started using the sigma ELISA kits. Once, components had reached room temperature, wash buffer and sample diluted buffers were made to the working stock concentration as stated in the protocol from sigma. Samples were taken from the -20 storage and allowed to defrost slowly while the standards were prepared according to the protocol provided. This is an example taken from IL-8 ELISA kit, but concentration of solutions does differ from kit to kit. Briefly the stock concentration of standard was briefly spun and 800 µl of 1 x assay dilutant was added and vortexed to mix. From this working stock a serial dilution was performed to achieve 7 standards with known concentrations. As seen in table 10 presented below.

Table 10 - Serial dilution example preparation taken from IL-8 sigma ELISA kit used during this work.

	1	2	3	4	5	6	7
	10	200	200	200	200	200	200
Diluent vol	Stock solution 800 µl	823.3	400	400	400	400	400
Conc.	50 ng/mL	600 pg/mL	200 pg/mL	66.7 pg/mL	22.2 pg/mL	7.4 pg/mL	2.5 pg/mL

The 7 standards and blank were added to the pre coated capture antibody ELISA plate and samples were added to the remain wells. The plate was sealed and placed on a plate shaker set to 50RPM and incubated at room temperature for 2.5 hours. After the incubation period, the solution was removed, and the plate was washed 4 times with wash buffer using an automated multi-channel pipette to dispense 300 µl. After which, the plate was gently tapped on clean tissue to remove liquid. To each of the wells, 100 µl of detection antibody is pipette and the plate is resealed and incubated at room temperature on a plate shaker set to 50 RPM for 1 hour. The wash steps were repeated as previously described and then 100 µl of streptavidin solution was pipetted into each

well and the plate covered and incubated with gentle shaking for 45 minutes. After a final plate washing TMB one stop substrate was added to each well at a total of 100 µl per well and incubated for 30 minutes in the dark. Finally, after 30 minutes the stop solution was added to stop the reaction and the plate was read using plate reader to measure the absorbance at 450 nm.

2.2.6.4 Inflammatory response multiplex analysis

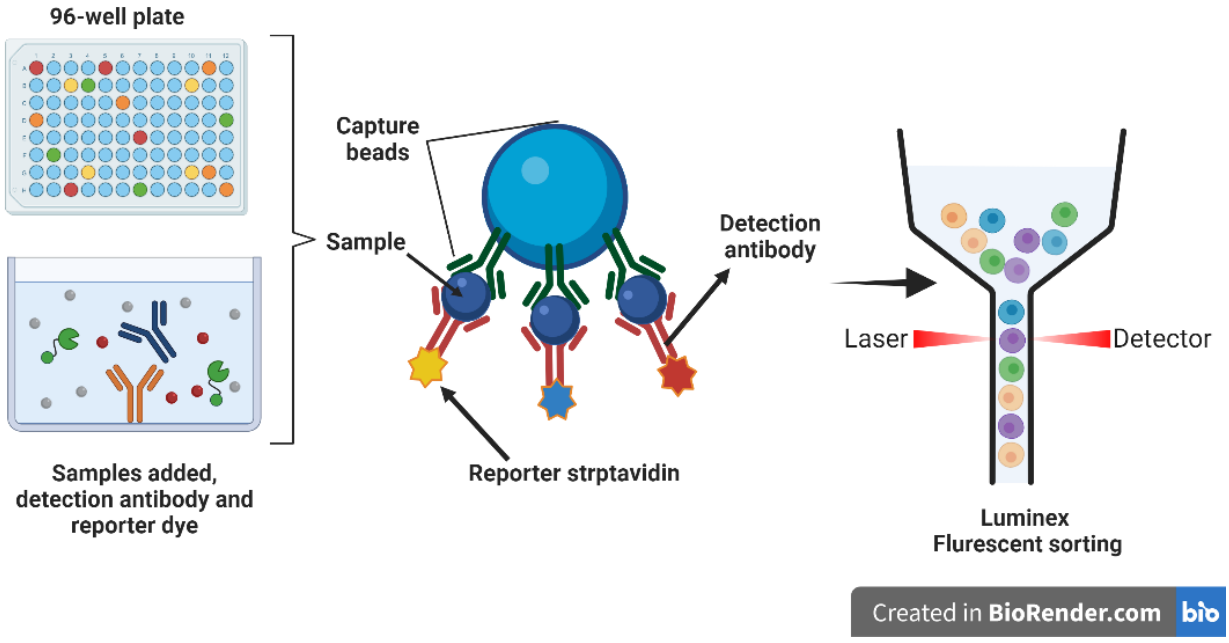

Figure 18 - Diagram of the mechanism of multiplex analysis

Supernatant harvested from 12 well plate, from the experiment observing inflammatory effect of mCRP and LPS treated with and without GW3965 (2.5 µM) were used for inflammatory response multiplex analysis. Firstly, the cell supernatant was centrifuged for 15 minutes at 1000 x g and placed in new Eppendorf collection tubes. The all in one 27 cytokine bioplex standard (table 11) was prepared by adding 250 µl of HB standard dilutant and vortex for 10 seconds and placed on ice for 30 minutes prior to use. A serial dilution was performed in accordance with the protocol to achieve 8 known standards of varying concentration which are depicted within the software. To each well 50 µl of bead solution was pipetted into each well. The plate was placed on a plate washer with a magnetic strip to avoid bead lose during washing stages. 100 µl of wash solution was automated by the washer into each well and aspirated and this was repeated 2x. After the washing

step, standards, samples, and blank controls were added to wells and incubated at room temperature for 30 minutes whilst shaking at 850 RPM. The plate was removed from the shaker and the seal removed before the plate was wash 3x using the plated washer as described above. After this stage, the detection antibody was added to each well at 25 µl and the plate was covered and placed on a shaker for 30 minutes. The plate was washed another 3x and 50 µl of streptavidin – PE was added and incubated for a further 10 minutes. The final wash step was performed and 125 µl of assay buffer was added to each well to prepare for reading. The plate was read using the bio-plex luminex and prepared in the bio-plex manager software.

Table 11 - Inflammatory cytokines and chemokines observed. (Bio-Rad 27-plex human cytokine kit)

FGF basic	IL-2	VEGF	IL-8	PDGF-BB	IL-12 (p70)
Eotaxin	IL-4	MIP-1α	IL-9	TNF-α	IL-13
G-CSF	IL-5	MIP-1β	IP-10	RANTES	
GM-CSF	IL-6	IFN-γ	IL-17A	IL-10	
IL-1β	IL-1ra	IL-7	MCP-1 (MCAF)	IL-15	

2.2.6.5 Measurement of MFAT Critical Cytokine Expression

(R&D Systems Inc, Oxford, UK) 32 self-designed multiplex kit was prepared for analysis of MFAT. Firstly 50 µl of a conditioned culture medium (from MFAT samples of 10 volunteers cultured in T-25 cm flasks) or control medium obtained after 24 hours, and 5 days of culture were plated onto the multiplex analysis plate. Serial dilution of standards was performed and added to plate with a microplate cocktail added to each well at 50 µl and incubated for 2 hours. The plate was washed using the magnetic plate washer and 100 µl of wash buffer was added per well and this was performed once. After the washing procedure was completed then prepared biotin antibody cocktail 50 µl was added to each well with and incubated for 1 hour with the plate sealed. The wash step was repeated and 50 µl of streptavidin – PE was added and incubated for 30 minutes at room temperature. The final wash step was completed, and the microplate was resuspended is wash buffer to prepared for reading on the Luminex. This assay was performed by a fellow researcher within the Selvin group and data was generated for analysis for this work and the paper which is indicated in chapter 5 (B. Guo et al., 2021).

Table 12 - Inflammatory cytokines and chemokines observed (Quantikine multiplex system (R&D Systems Inc, Oxford, UK)

MIG	MIP-1b	IL-6	IFN-g	IL-1Ra
IL-12(p40)	IL-5	GM-CSF	MIF	TNF-a
RANTES	IL-2	IL-1B	Eotaxin	Basic FGF
VEGF	PDGF-BB	IP-10	IL-13	IL-4
MCP-1	IL-8	MIP-1a	IL-10	G-CSF
GRO-a	HGF	IL-3	IL-15	IL-7
IL-12(p70)	IL-17	IL-9		

2.2.7 Statistical analysis

The statistical significance of all data was determined using graph pad version 9 (GraphPad, USA). qPCR analysis to determine delta delta CT values was determined using the biorad qPCR software and values were transferred to graph pad. The normality of data was determined using the Shapiro-wilk test and was conducted using graph pad. Test which was employed during this project included One way analysis of variance and two-way ANOVA with post hoc analysis using either Bonferroni or Tukey analysis. All data presented as mean and standard error mean unless stated other wise and significant was deemed another below $p = 0.05$.

Chapter 3 – The impact mCRP plays on the morphology and physiology of monocytes.

\

3.1 Introduction

3.1.1 The Role of mCRP in the vascular pathology and atherothrombosis

Atherothrombosis is a complex pathological inflammatory process important to research. Atherothrombosis can have detrimental impacts on human health due to forming of atheromatous plaques that become unstable and rupture leading to the formation of thrombus and accumulation of platelets and coagulation protein (Asada et al., 2020). The occlusive thrombi formed could break and induce an ischemic event. Platelets are important between innate and adaptive immunity (Ali et al., 2015). The inflammatory pathway is triggered by platelets and contributes to atherosclerotic lesion formation and atherothrombosis (Huilcaman et al., 2022). nCRP is not detectable in healthy or atherosclerotic vessels. Interestingly, mCRP is not detectable in healthy tissue but detected within vessel walls of all stages of atherogenesis and begins to accumulate during the progression of atherosclerosis (Badimon et al., 2018). The classical complement system becomes activated when nCRP is exposed to ligands and microbial through interaction with the C1q. It is understood that nCRP can be dissociated into mCRP. For example, when the endothelium is damaged, platelets become activated and spread. On the surface of the activated platelets, nCRP becomes stuck and leads to the dissociation of nCRP to mCRP which causes a pro-inflammatory effect by activating blood cells. This intern causes the activation of an inflammatory response that can lead to the deposit in atherosclerotic lesions (Boncler et al., 2019). mCRP which has dissociated has been classed as a critical molecule which perpetuates inflammation in many different serious diseases such as Alzheimer's disease and ischemic stroke to name a few. mCRP has been shown to have adhesive-like properties, which cause aggregation of blood cells and platelets which in turn stick to arterial tissue. This process can lead to further complications including thrombosis in turn leads to atherosclerosis and then acute coronary event (Slevin et al., 2010; Badimon et al., 2018; Slevin et al., 2018; Sproston et al., 2018; Garcia-Lara et al., 2021; Zeinolabediny et al., 2021).

3.1.2 Effects of mCRP on monocytes.

The largest leukocytes are monocytes, and they are found in vertebrates and produced in the bone marrow before being released into circulation. In normal human conditions, monocytes make up between 3-8% of the cell circulating population. Circulating levels of monocytes change based on infection or inflammatory response (Chiu and Bharat, 2016). Monocytes have a short life span and some but not all undergo apoptosis within a 24-hour period. The monocytes which have not undergone apoptosis migrate into tissues or to the sites of damage or infection where they later mature into macrophages (Kratofil et al., 2017). There has been ongoing research into the role of platelets, CRP and inflammation have upon each other. The role of CRP as a modulator of inflammation and thrombosis stays elusive. As it has both pro and anti-inflammatory actions. mCRP stimulates enhanced local production of pro-inflammatory cytokines including IL-8, MCP-1, TNF-α IL-6, and associated transcription factors such as Nf-κB (Khreiss et al., 2004). CRP can be dissociated into mCRP in several ways but particular of interest is how dissociation occurs through activated tissue and cells (including circulating monocytes and platelets) when at sites of inflammation or infection. Important properties have been seen in mCRP including adhesive like properties. It is understood that mCRP causes aggregation of blood cells and platelets within arterial tissue. This then can contribute to further complications including thrombosis, linking it potentially to atherosclerosis and subsequent ischemic events (Filep, 2009; Slevin et al., 2018; Zeinolabediny et al., 2021).

3.2 Aims and objectives.

This chapter aimed to determine, prepare, and test whether CRP isoforms have a morphological effect on U937 monocytes.

1) Observe morphological and physiological changes in U937 monocytes after stimulation with mCRP or nCRP.

2) Determine apoptosis/necrosis effects of CRP isoforms on U937 monocytes.

3) Elucidate the mechanism in which morphological changes are occurring after CRP isoform stimulation.

3.3 Results

3.3.1 mCRP causes morphological changes in U937 monocytes.

U937 monocytes were set in a 12 well plate to $1x10^6$/mL treated with control (complete media), LPS 10 ng/ml, mCRP 100 µg/mL and nCRP 100 µg/mL for 24 hr period with images taken at 3 hrs, 6 hrs and 24 hrs respectively (2.2.3.1). Dissociated isoform of CRP (mCRP) caused monocytes to aggregate as seen in figure 19 (C1-C3) over 24 hr period compared to the control (A1-3). Figure 18E, mCRP 100 µg/ml shows significant aggregation formation at 3-, 6- and 24-hour mark compared to control CI 95% 3 hrs (-111.0 -48.53) p= <0.0001, CI 95% 6 hrs (-102.2 to -39.74) p=<0.0001 and CI 95% 24 hrs (-131.7 to -69.22) p = <0.0001. Further to this mCRP is significantly different from CRP isoform nCRP at CI 95% 3 hrs (48.53 – 111.0), CI 95% 6 hrs (39.74 to 102.2) p=<0.0001 and CI 95% 24 hrs (69.22 to – 131.7) p = <0.0001.

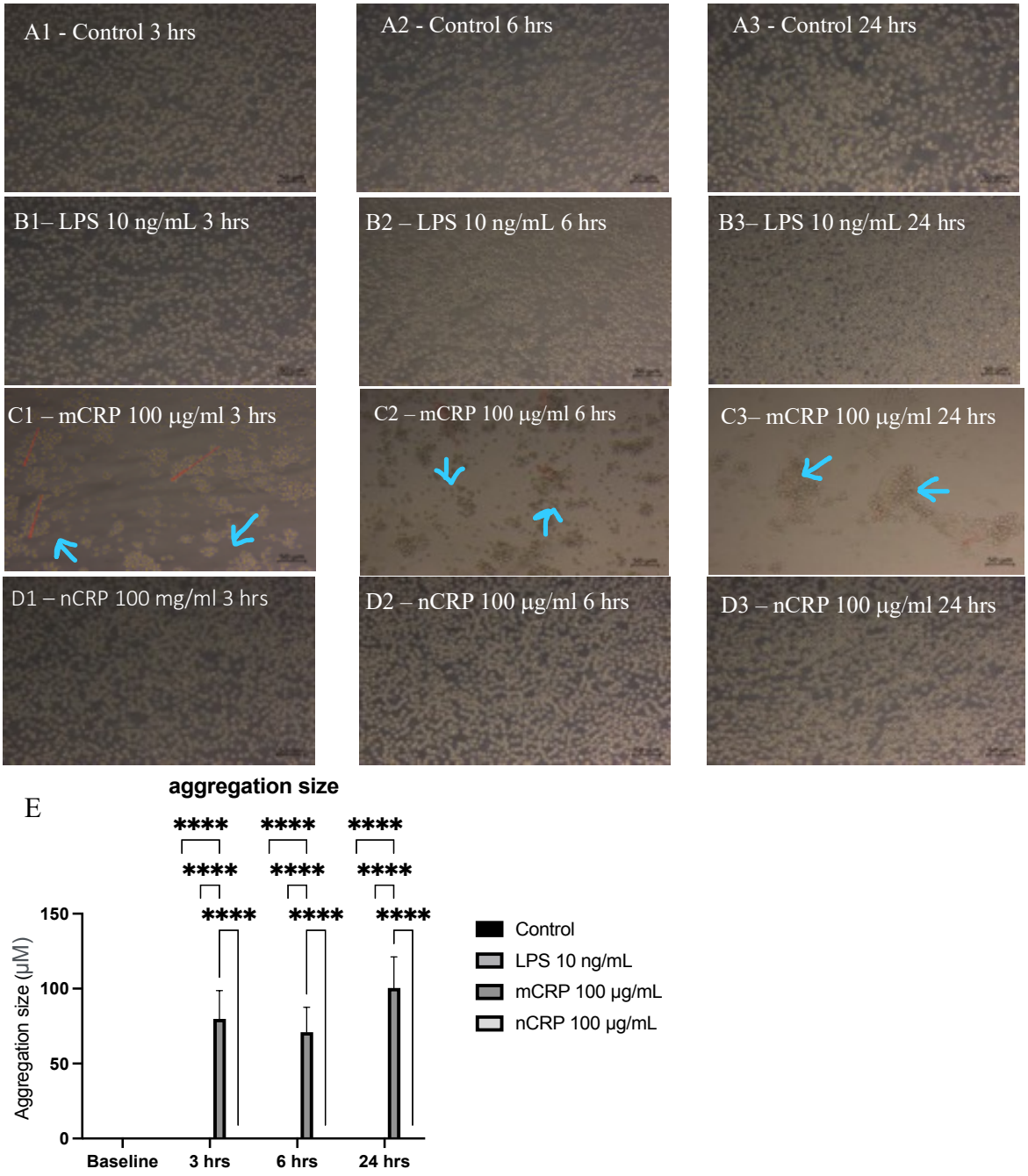

Figure 19 – Cell aggregation induced by CRP isoform (mCRP 100 µg/mL)

*U937 monocytes were stimulated with either (-VE) control, (+VE) LPS 10 ng/ml, mCRP µg/mL or nCRP µg/mL for 3,6 - and 24-hour. A1-3 Control, B1-3 LPS 10 ng/ml, C1-3 mCRP 100 µg/mL and D1-3 nCRP 100 µg/mL. E) mCRP caused significant aggregation formation in U937 monocytes. The size of aggregation was measure from point to point in cells which created a clear cluster. Images taken at 10 x magnification at two fields of view per time point on Zeiss axio microscope. Data represented as Mean± SEM, Two-way anova (Post hoc turkey) (p**** <0.0001) n3)*

3.3.2 mCRP affects the cell viability of U937 monocytes.

Figure 20A, treatment with mCRP 100 mg/ml (2.426 ± 0.1178) caused a significant decrease in cell viability of monocytes at the 3 hrs point, which was significantly lower compared to negative healthy control cells (3.684 ± 0.3263) with CI 95% (0.3061 to 2.210), p = 0.0080. Figure 20B, treatment with mCRP 100 μg/mL (2.086 ± 0.0618) caused a significant decrease in cell viability of monocytes at the 6 hrs point, which was significantly lower compared to negative healthy control cells (3.338 ± 0.3762) with CI 95% (0.3516 to 2.152), p = 0.0054. Figure 20C, treatment with mCRP 100 μg/mL (0.500 ± 0.03313) caused a significant decrease in cell viability of monocytes at the 24 hrs point, which was significantly lower compared to negative healthy control cells (1.059 ± 0.07440) with CI 95% (0.3405 to 0.7771), p = <0.0001.

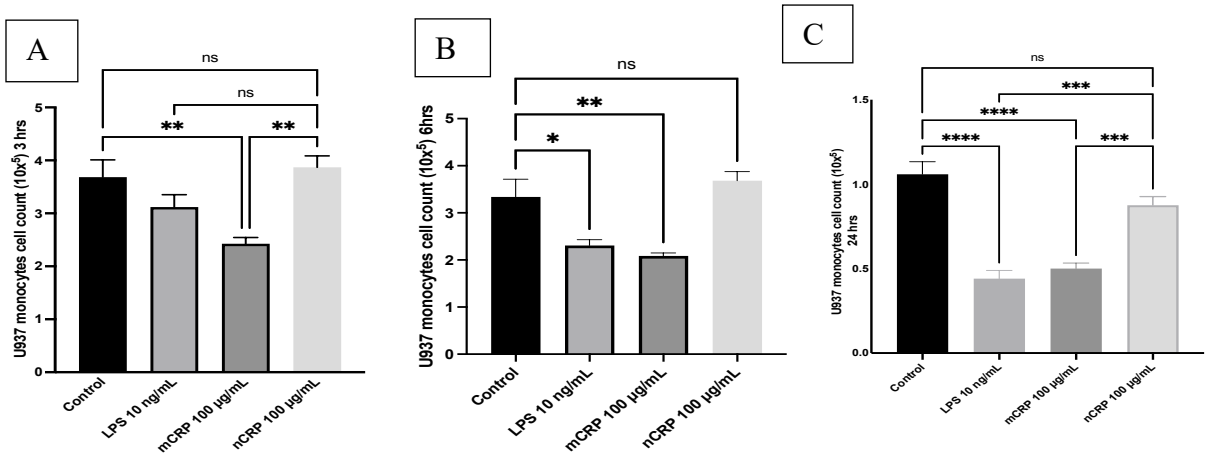

Figure 20 – The effects of mCRP stimulation on U937 monocytes were examined.

Cells were treated with either control (-), LPS 10 ng/ml (+), mCRP 100 µg/mL or nCRP 100 µg/mL for 24-hour period. Cell counts were taken at 3 time points (3,6, and 24 hours) to observe viability. A) mCRP significantly reduces cell count over 3 hours period. B) mCRP significantly reduces cell count over 6 hours period. C) mCRP significantly reduces cell count over 24 hours measurement. Data presented as Mean ± SEM, One-way anova (Post Hoc turkey) (p =< 0.05 p ** = <0.01, p*** = < 0.001, p**** <0.0001. (n=3)*

3.3.3 mCRP promotes U937 monocytes necrosis.

3.3.1 – 3-hour measurement of potential apoptosis and necrosis caused by mCRP.

U937 monocytes were treated with either complete medium (-), DMSO 20% (+), mCRP 100 µg/mL, nCRP 100 µg/mL. Figure 21A is a display of the negative control which has been gated for necrosis, apoptosis, dead and live cells. The positive percentage representation is outline as necrosis 0.78 %, Dead 10.72%, Apoptosis 1.83% and live 86.89%. Showing that U937 monocytes were mostly alive. LPS 10 ng/mL, in figure 21B showed comparable results to the negative control (necrosis 0.71%, Dead 12.30%, Apoptosis 1.65 % and 85.33%). Figure 21C, mCRP 100 µg/mL, showed no significant cell death at the 3-hour mark (necrosis 2.4 %, Dead 15 %, Apoptosis 2.06 % and 80.54%). Figure 21D, nCRP 100 µg/mL stimulated monocytes remained mostly alive (necrosis 1.17%, Dead 14.93 %, and Apoptosis 1.9 9 % and 81.70 %). Figure 21E, the positive control (DMSO 20%) is showing cell death as expected (necrosis 11.31 %, Dead 55.87 %, Apoptosis 1.27 % and 31.70 %). Figure 21F represents statical analysis performed on the flow cytometry analysis of U937 monocytes treated with mCRP 100 µg/mL and nCRP 100 µg/mL. At the 3-hour mark, DMSO treated cells caused necrosis positive cells and this was significantly different from the negative control which was expected CI 95% -13.86 to -7.600 ($p<0.0001$). mCRP CI 95% -4.954 to 1.307) and nCRP CI 95% -3.727 to 2.534) did not cause the cells to become necrotic when comparing to the control. Interesting, when looking at the dead cells, mCRP CI 95% (-7.417 to -1.156), nCRP (-7.347 to -1.086) and DSMO +ve CI 95% (-48.29 to -42.03) were all significantly different from negative control. Apoptosis positive cells in all treated groups showed no significance difference compared to the control. mCRP CI 95% -3.364 to 2.897, nCRP CI 95% -3.294 to 2.967 and DMSO CI 95% -2.430 to 3.830. Finally, when observing the live cells, there was significant difference between the negative control and mCRP CI 95% (3.213 to 9.474) $p<0.0001$, nCRP CI 95% (1.850 to 8.110) $p<0.001$ and DMSO (20%) CI 95% (1.850 to 8.110) $p<0.0001$). However, this reduction was not in the same line at the positive control of DMSO treated cells.

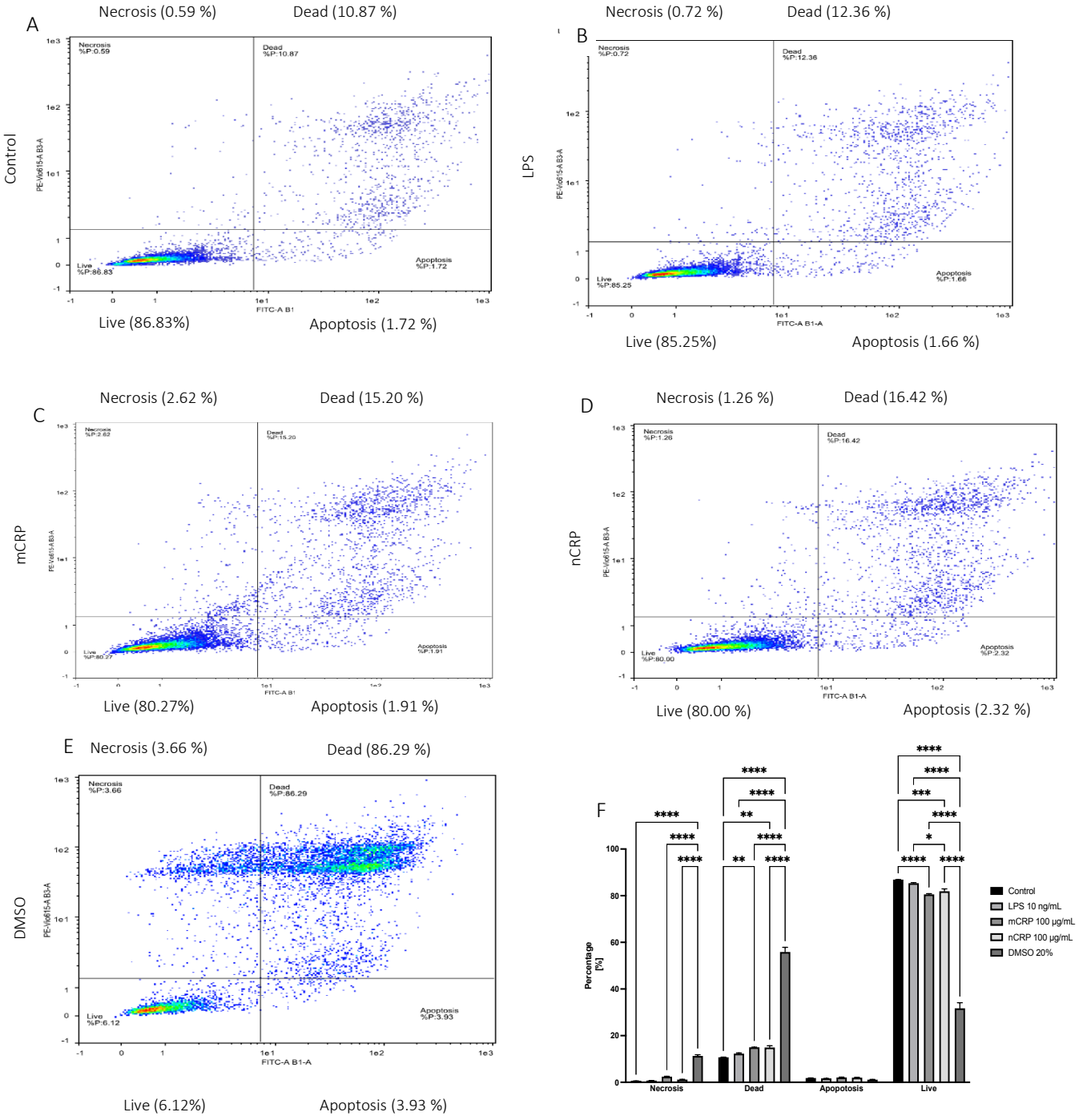

Figure 21 – Flow cytometric analysis of apoptosis and necrosis in 3-hour mCRP treated U937 monocytes. Cells were pre-treated with either complete medium (-ve), LPS 10 ng/mL, mCRP µg/mL and nCRP µg/mL and DMSO (20%) +ve for 3 hours. FITC (Annexin V) and PE (PI) double staining was used to separate viable cells into live, necrotic, apoptotic, and dead cells. A) Complete media (-VE), B, LPS 10 ng/mL, C) mCRP 100 µg /mL, D) nCRP 100 µg /mL and E) DMSO 20% (+VE). F) Statistical analysis of flow cytometry data for 3 hours. Representative scatter plots PI Y axis vs FITC x axis. Data represents Mean± SEM (Two-way anova (Post Hoc Turkey) (p* = < 0.05 p **= <0.01, p*** = < 0.001, p**** <0.0001. (n=3)

3.3.2 – 6-hour measurement of potential apoptosis and necrosis due to mCRP

U937 monocytes were treated with either complete medium (-), DMSO 20% (+), mCRP 100 µg/mL, nCRP 100 µg/mL. The negative control presented in figure 22A shows the cells are alive and do not present as either necrotic or apoptotic based on control treatment (necrosis 2.10%, Dead 8.91%, apoptosis 1.09% and 87.91%). U937 monocytes were treated with LPS 10 ng/mL for 6-hour period and scatter plot presented in figure 22B showed a similar result to the negative control in which cells presented as alive (necrosis 1.26%, Dead 15.80%, apoptosis 1.95% and live 81%). U937 monocytes were treated with mCRP 100 µg/mL for 6-hour period and figure 22C, showed significant cell death at the 6-hour mark after treatment (necrosis 6.73 %, Dead 76.48%, apoptosis 0.78 % and live 16.02%). nCRP 100 µg/mL showed no significant cell death (necrosis 1.35%, dead 14.21 %, apoptosis 2.06 % and live 82.37 %) figure 22D. The positive control (DMSO) is showing death of cells as inspected in figure 22E (Necrosis 15.64 %, dead 73.28 %, apoptosis 2.68 % and live 8.39%). Figure 22F represents statistical analysis performed on the flow cytometry analysis of U937 monocytes treated with mCRP 100 µg /mL and nCRP 100 µg/mL. At the 6-hour mark, DMSO treated cells caused necrosis positive cells and this was significantly different from the negative control which was expected CI 95% (-22.78 to -4.311) p = 0.0013. mCRP CI 95% (-13.87 to 4.602) p = 0.6107 and nCRP CI 95% (-8.492 to 9.979) p = 0.9994 did not cause a significant difference to the control when looking if cells became necrotic. Interesting, when looking at the dead cells, mCRP CI 95% (-76.81 to -58.34) p = <0.0001 and DSMO +ve CI 95% (-73.61 to -55.14) p = < 0.0001 were all significantly different from negative control. Apoptosis positive cells in all treated cells showed no significant difference to the control. mCRP CI 95% (-8.925 to 9.545) p = >0.9999, nCRP CI 95% (-10.21 to 8.262) p = 0.9981, DMSO (20% CI 95% (-10.82 to 7.649) p = 0.9878. mCRP treated cells were significantly different from the control when looking at the live population, CI 95% (62.65 to 81.13) p = <0.0001 and this was the case for the positive control DMSO (20%), CI 95% (70.28 to 88.75) p = <0.0001.

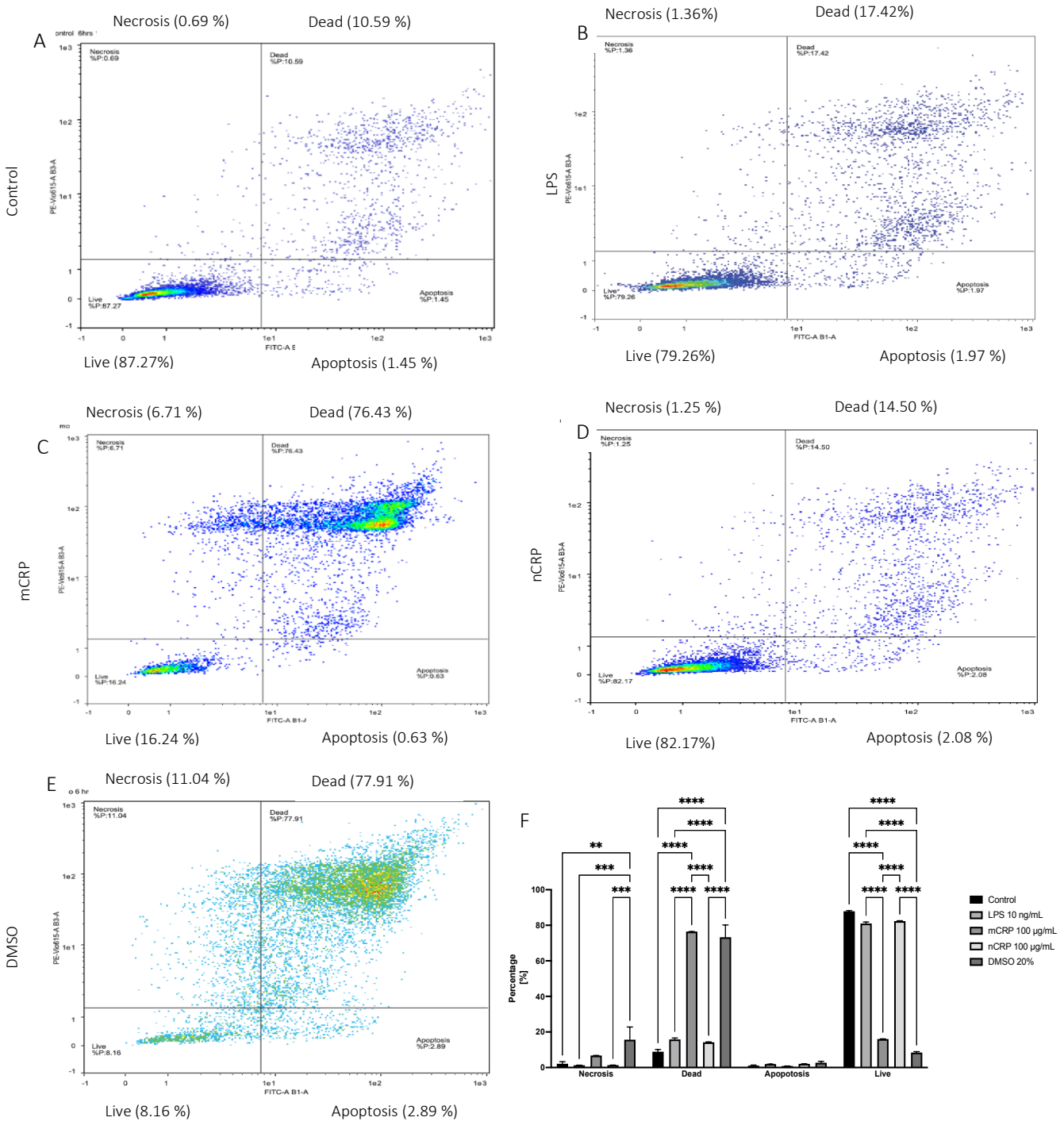

Figure 22 - Flow cytometric analysis of apoptosis and necrosis in 6-hour mCRP treated U937 monocytes.

Cells were pre-treated with either complete medium (-ve), LPS 10 ng/mL, mCRP µg/mL and nCRP µg/mL and DMSO (20%) +ve for 6 hours. FITC (Annexin V) and PE (PI) double staining was used to separate viable cells into live, necrotic, apoptotic, and dead cells. A) Control, B, LPS 10 ng/mL, C) mCRP 100 µg /mL, D) nCRP 100 µg /mL and E) DMSO 20%. F) Statistical analysis of flow cytometry data for 6 hours. Representative scatter plots PI Y axis vs FITC x axis. Data represents Mean ± SEM (Two-way anova (Post Hoc Turkey) (p* = < 0.05 p **= <0.01, p*** = < 0.001, p**** <0.0001. (n=3)

3.3.3 - 24-hour measurement of potential apoptosis and necrosis due to mCRP

The negative control, figure 23A on the scatter plot showed cells were alive and did not present with significant apoptosis or necrosis (Necrosis 2.68 %, Dead 16.48%, Apoptosis 1.53 % and 79.30 %) LPS 10 ng/mL, in figure 23B showed comparable results to the negative control (Necrosis 12.72 %, Dead 15.54 %, Apoptosis 1.99 % and 79.76 %). Figure 23C, mCRP 100 µg/ml, showed significant cell death at the 24-hour mark (Necrosis 32.12 %, Dead 56.57 %, Apoptosis 0.91 % and 10.40 %). Figure 23D, nCRP 100 ug/ml showed no significant cell death (Necrosis 0.71%, Dead 9.01 %, Apoptosis 1.70 % and 88.60 %). The positive control (DMSO) is showing the death of cells as inspected in figure 23E (Necrosis 2.97 %, Dead 86.98%, Apoptosis 4.11 % and 5.94 %). Figure 23F represents a statical analysis of U937 monocytes treated under several conditions (mCRP 100 µg /mL and nCRP 100 µg/mL). At the 24-hour mark, DMSO-treated cells had comparable results to the positive control in which no significant necrotic cells compared to the control CI 95% (-3.410 to – 2.830) p = 0.9989. Interestingly, when comparing mCRP-treated cells to the positive control it showed that mCRP caused cells to become necrotic CI 95% (-32.56 to –26.32) p = <0.0001. At the 24-hour mark, DMSO-treated cells caused significant cell death which was expected compared to the positive control CI 95% (-73.62 to -67.38) p = <0.0001. At the 24-hour mark, mCRP-treated cells caused significant cell death compared to the positive control. CI 95% (-43.21 to -36.97) p = <0.0001. U937 cells which were treated did not present any statistical difference from the control which observed apoptotic cells. Finally, when observing the live cells, mCRP and DSMO caused a notable change in the negative control group.

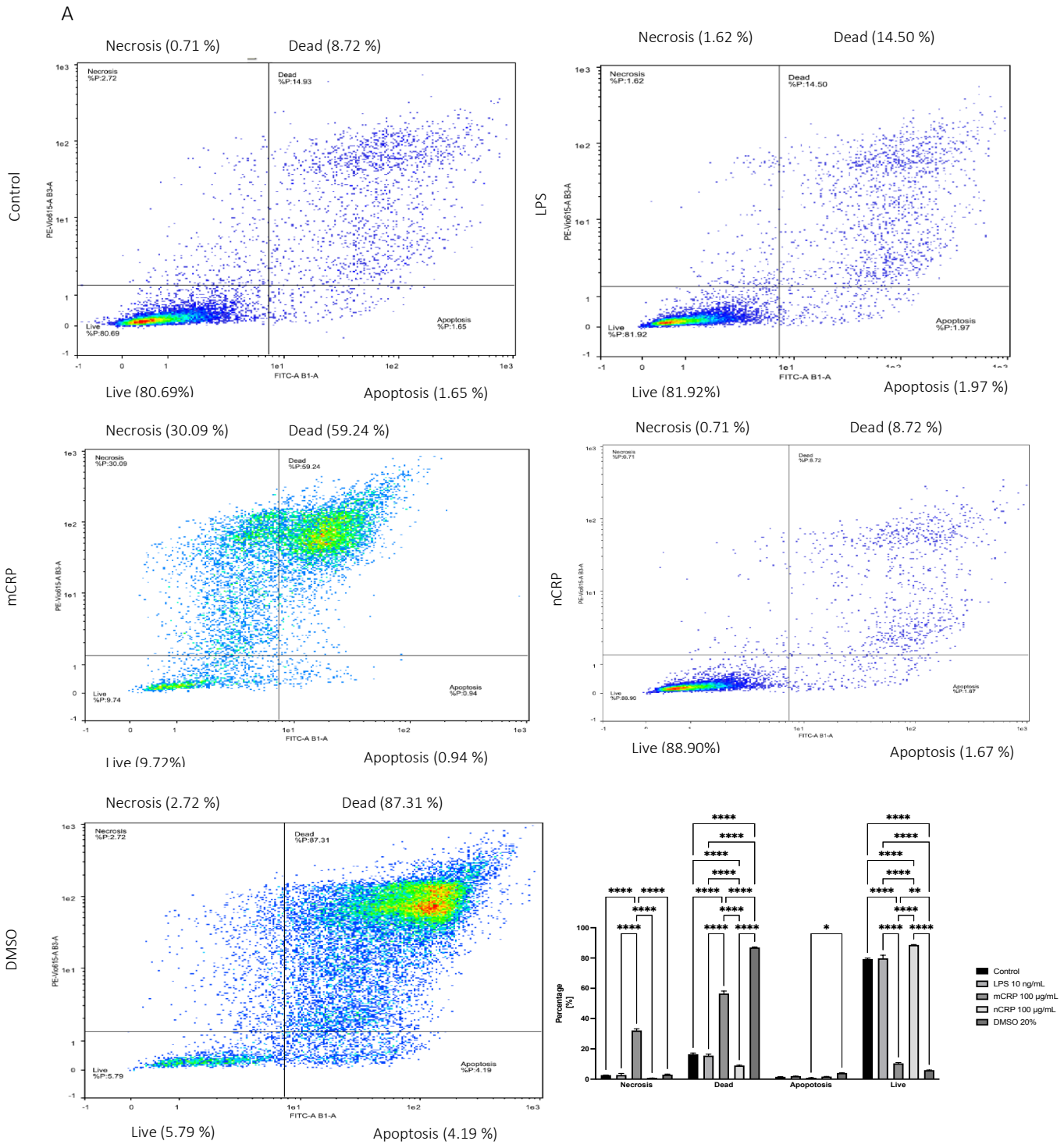

Figure 23 - Flow cytometric analysis of apoptosis and necrosis in 24-hour mCRP treated U937 monocytes.

Cells were pre-treated with either complete medium (-), LPS 10 ng/mL, mCRP µg/mL and nCRP µg/mL and DMSO (20%) (+) for 24 hours. FITC (Annexin V) and PE (PI) double staining was used to separate viable cells into live, necrotic, apoptotic, and dead cells. A) Control, B, LPS 10 ng/mL, C) mCRP 100 µg /mL, D) nCRP 100 µg /mL and E) DMSO 20%. F) Statistical analysis of flow cytometry data for 24 hours. Representative scatter plots PI Y axis vs FITC x axis. Data represents Mean ± SEM (Two-way anova (Post Hoc Turkey) (p* = < 0.05 p **= <0.01, p*** = < 0.001, p**** <0.0001. (n=3)

3.3.4 mCRP treated monocytes cells exhibit apoptosis and necrosis characteristic under scanning electron microscope.

All morphological features of apoptotic processes, include change in membrane, integrity, losing microvilli, budding, swelling, formation of apoptotic body, and total cell rupture, were presented. To visualise and compare detailed features of U937 monocytes treated with different pro-inflammatory mediators (mCRP and LPS), samples were visualised using a supra 40VP electron microscope. Positive and negative controls were used as reference images to determine a healthy cell and a dead cell which are in panels Figure 24 - A1-2 DMSO (20%) positive cell death control and B1-2 – normal healthy cell control. mCRP but not nCRP caused a surprising morphological change in the appearance of U937 monocytes. Representation of the morphological changes are presented in panels D1-3 of varying magnifications. Presenting in the lowest magnification panel, the treatments of the cells with mCRP appear to cause the cells to lay down an extracellular matrix-like substance which is indicated by a red arrow and a clustering of monocytes which are circled in red in D1. Further to this, there is a clear change in membrane morphology with the integrity of the cells lost through, losing microvilli, budding, swelling, formation of apoptotic body, and total cell rupture were present.

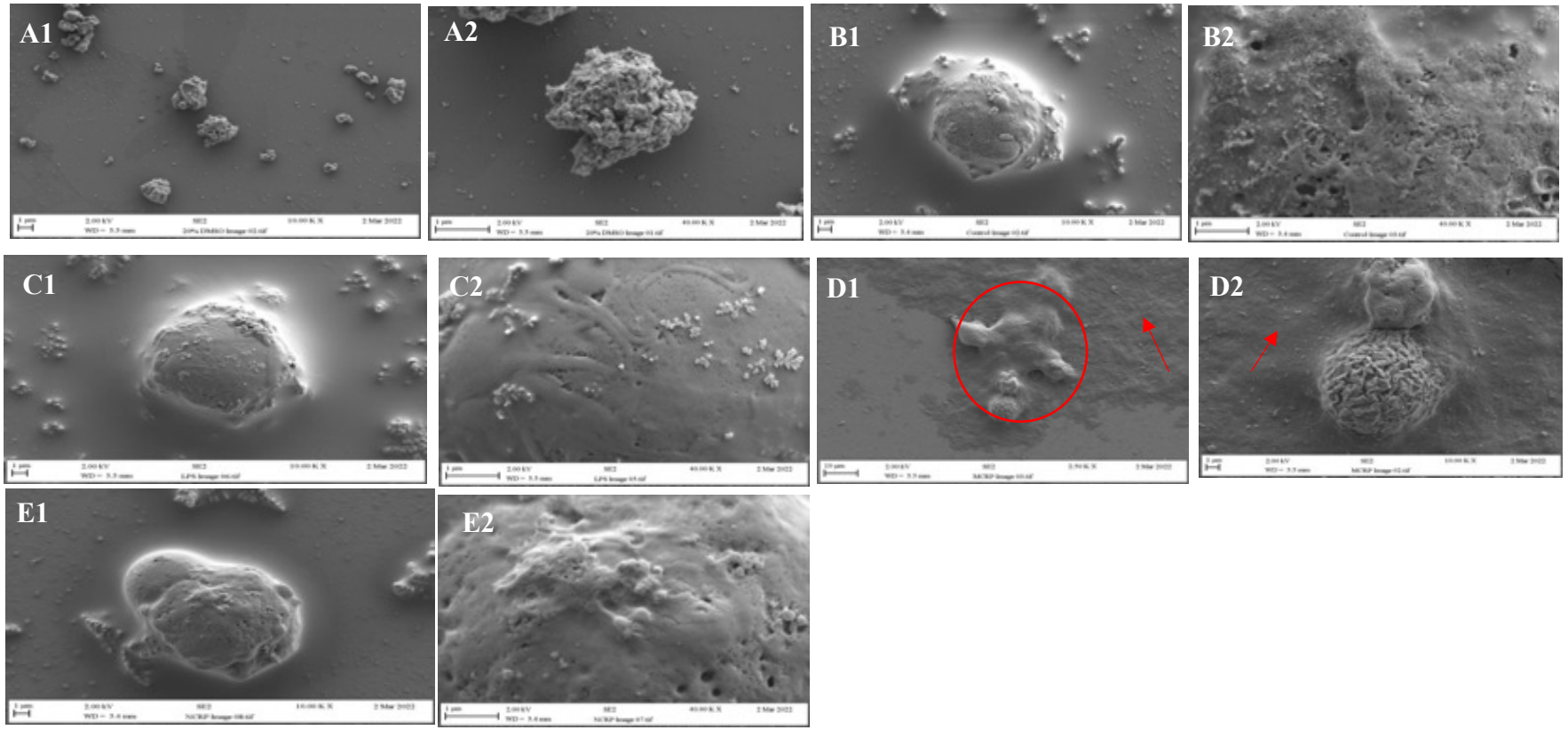

Figure 24 - Scanning electron microscopic observation on the effects of mCRP on cellular and nuclear morphology in U937 Cells.

U937 cells grown in 35 mm dishes (500 cells/dish) were treated with (+) control DMSO (20%) – A1-2, Control B1-2, LPS 10 ng/mL C1-2, 100 µg/mL of mCRP D1-3, nCRP E1-2. Image where takes with a range of magnification (10,000 kk – 40,000 kk and mCRP had 3 magnification point (2500 kk, 10,000 kk and 40,000 kk to insect changes closer. n=3

2.3.5 mCRP induced expression of MCP-1 and IL-8 by U937 monocytes in vitro over time.

Housekeeping gene stability was observed as seen in figure 25. TATA-box binding protein (TBP) and Polyadenylate-binding protein 4 (PABPC4) was deemed ideal for the use in gene expression analysis.

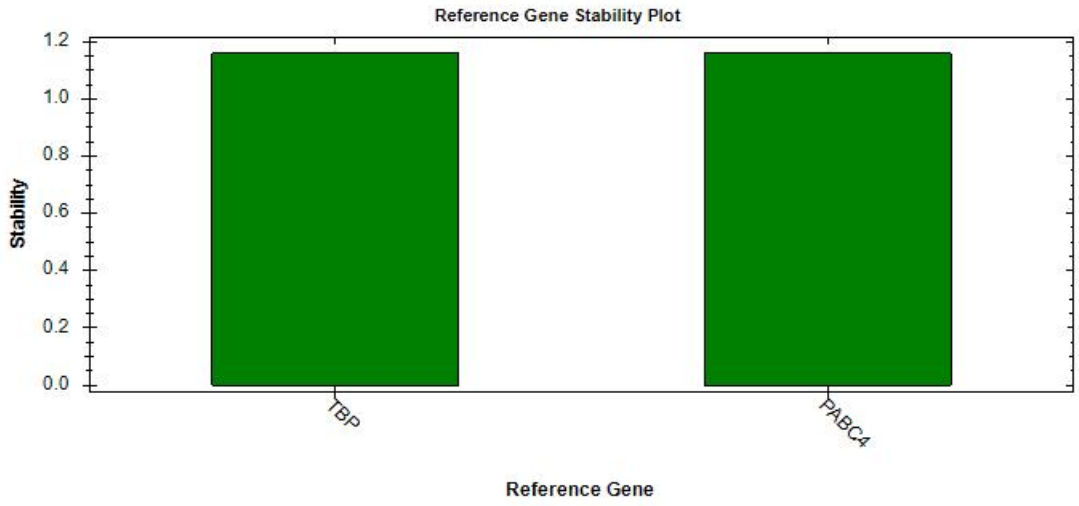

Figure 25 – Housekeeping reference gene (TBP + PABC4) stability plot.

TBP and PABC4 were used as housekeeping genes and reference gene stability plot was generated using CFX software based on all samples control (complete media negative -), LPS 10 ng/mL (positive +), mCRP 100 µg/mL, nCRP 100 µg/mL to determine the stability of housekeeping primers (Green – ideal), n=3

Table 13 displays the regulation of IL-8 gene expression based on treatment with Figure 26 representing the statistical analysis of IL-8 gene expression levels presented as relative gene expression. U937 monocytes were treated with complete media (-), LPS 10 ng/ml (+), mCRP 100 µg/ml and nCRP µg/ml for 3, 6 and 24 hours. At the 3-hour mark, LPS caused IL-8 gene expression levels to significantly increase compared to the control ($p = <0.0001$). Interestingly even though mCRP caused an up-regulation in IL-8 gene expression levels this was not deemed significant compared to the negative control and this was the case for nCRP in which up-regulation occurred but was not significant. Comparing positive inflammatory mediator LPS to mCRP and nCRP. LPS induced IL-8 expression levels ($p = <0.0001$ and $p = <0.0001$) compared. Samples taken from the 6 hours mark were measured for the expression of IL-8 expression levels. LPS-treated U937 monocytes caused a significant increase ($p = 0.0326$) when compared to the control. Interestingly, mCRP and nCRP caused a downregulation in IL-8 gene expression levels compared to the control baseline. Further to this, when mCRP and nCRP were treated, samples were compared to LPS treatment levels were deemed to be significantly different $p = 0.0087$ and $p = 0.0087$. Samples taken from the 24-hour mark were measured for the expression of IL-8 expression levels. LPS-treated U937 monocytes caused a significant increase ($p = 0.0005$) when compared to the control. Interestingly, mCRP-treated monocytes caused IL-8 expression levels to be upregulated however this level of increase was not deemed significant when compared to the control $p = 0.1250$. nCRP showed the opposite effect in which levels were downregulated but this was not a significant decrease when compared to the control levels $p = 0.9469$. However, this downregulation was not significant when compared to the control. Further to this, when mCRP and nCRP were treated, samples were compared to LPS treatment levels were deemed to be significantly different $p= 0.0087$ and $p = 0.0087$.

Table 13 - IL-8 gene expression analysis of LPS /mCRP treated U937 monocytes.

3 hrs	IL-8	Control VS LPS	-1.853 to -1.674	<0.0001
		Control VS mCRP	-0.1027 to 0.07603	0.9759
		Control vs nCRP	-0.09774 to 0.08102	0.9938
		mCRP vs nCRP	-0.08439 to 0.09437	0.9987
6 hrs	IL-8	Control VS LPS	-0.1851 to -0.006362	0.0326
		Control VS mCRP	-0.07073 to 0.1080	0.9384
		Control vs nCRP	-0.07073 to 0.1080	0.9384
		mCRP vs nCRP	-0.08938 to 0.08938	>0.9999
24 hrs	IL-8	Control VS LPS	-0.2413 to -0.06258	0.0005
		Control VS mCRP	-0.1641 to 0.01470	0.1250
		Control vs nCRP	-0.07171 to 0.1070	0.9469
		mCRP vs nCRP	0.002972 to 0.1817	0.0410

N: B yellow highlights (Significant)

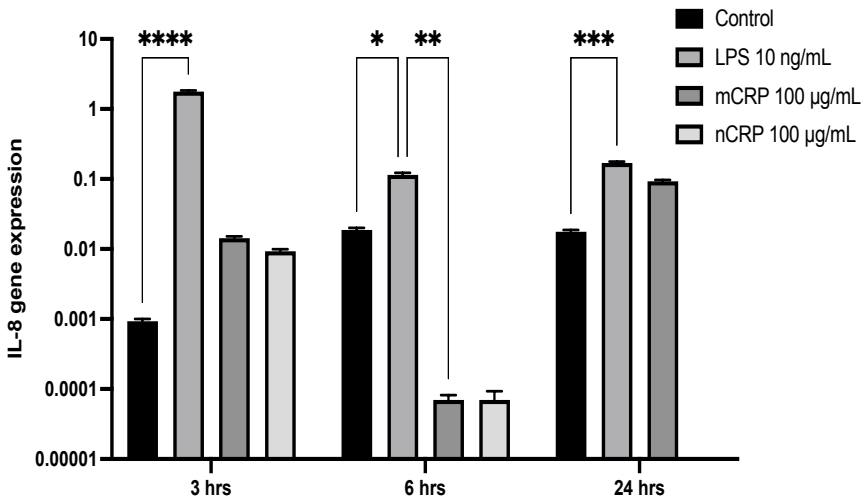

Figure 26 - IL-8 gene expression from U937 monocytes over 24-hour period

U937 monocytes expressed altered IL-8 gene expression after treatment with pro-inflammatory mediators (LPS and- mCRP) or nCRP. U937 monocytes were treated with either control, LPS, mCRP or nCRP before cells were lysed and prepared for gene expression analysis. A) Pro-inflammatory mediators mCRP and LPS significantly alter IL-8 gene expression levels over 24 hours. Delta delta CT method was used for analysis with TBP and PABC4 used as housekeepers' genes. Samples were run in 3 technical repeats and 3 biological repeats. Data represents as Mean ± SEM (Two-way ANOVA (Post Hoc Turkey) (p = < 0.05 p **= <0.01, p*** = < 0.001, p**** <0.0001. (n=3)*

Table 14 displays the regulation of MCP-1 gene expression based on treatment with figure 27 representing the statistical analysis of MCP-1 gene expression levels presented as relative gene expression. Figure 27 shows the results from the qPCR analysis of MCP-1 gene expression levels from the samples observed for aggregation LPS-treated U937 monocytes at the 3-hour mark causing the upregulation of MCP-1 which was deemed a significantly increased compared to the control p = <0.0001. mCRP caused downregulation of MCP-1 gene expression levels however this was not deemed a significant decrease compared to the control. A further note is that nCRP-treated monocytes caused an upregulation in MCP-1 expression but again this was not deemed a significant increase when compared to the bassline control levels. Levels of MCP-1 gene expression were significantly downregulated compared to the control when U937 monocytes were treated with LPS, mCRP and nCRP for 6 hours. These were all deemed to be significant decreases p = <0.0001, p=<0.0001 and p=<0.0001. MCP-1 gene expression levels were significantly upregulated after treatment with both LPS and mCRP for a 24-hour period P = <0.0001 and p = 0.0224).

Table 14 - MCP1 gene expression analysis of mCRP treated U937 monocytes.

3 hrs	MCP 1	Control VS LPS	-1.562 to -1.250	<0.0001
		Control VS mCRP	-0.1341 to 0.1779	0.9799
		Control vs nCRP	-0.2448 to 0.06721	0.4138
		mCRP vs nCRP	-0.2666 to 0.04534	0.2321
6 hrs	MCP 1	Control VS LPS	0.1538 to 0.4658	<0.0001
		Control VS mCRP	0.2088 to 0.5208	<0.0001
		Control vs nCRP	0.2075 to 0.5194	<0.0001
		mCRP vs nCRP	-0.1573 to 0.1546	>0.9999
24 hrs	MCP 1	Control VS LPS	-1.592 to -1.280	<0.0001
		Control VS mCRP	-0.3325 to -0.02058	0.0224
		Control vs nCRP	-0.1115 to 0.2004	0.8601
		mCRP vs nCRP	0.06502 to 0.3770	0.0035

Table present 95.00% CI of diff and p value - N: B yellow highlights (Significant)

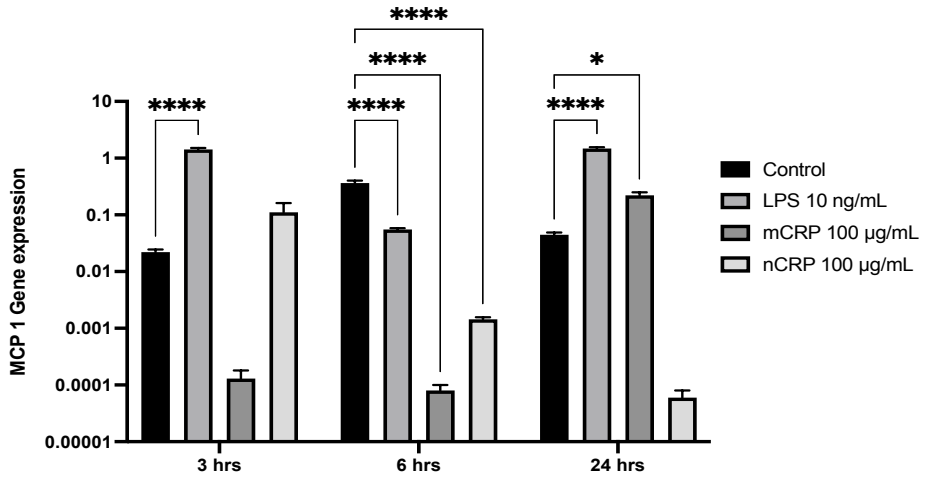

Figure 27 – LPS and mCRP alter MCP1 gene expression in U973 monocytes.

U937 monocytes altered IL-8 gene expression after treatment with pro-inflammatory mediators (LPS and- mCRP) or nCRP. U937 monocytes were treated with either control, LPS, mCRP or nCRP before cells were lysed and prepared for gene expression analysis. A) mCRP significantly alter MCP-1 gene expression levels. Delta delta CT method was used for analysis with TBP and PABC4 used as housekeeper genes. Samples were run in 3 technical repeats and 3 biological repeats. Data represents as Mean± SEM (Two-way ANOVA (Post Hoc Turkey) (p* = < 0.05 p **= <0.01, p*** = < 0.001, p**** <0.0001. (n=3)

3.4 Discussion

It is only recently in the last years that research has been conducted on individual isoforms of CRP but until then research was conducted on CRP with conflicting results. This could have been due to CRP isoform not being specified in the research and results could have been due to nCRP dissociation into mCRP or lipopolysaccharide contamination (Sproston and Ashworth, 2018). Therefore, it is vital in research to focus not as a whole but on the specific isoforms of CRP.

3.4.1 Monomeric c reactive induces U937 monocyte physiological and morphological changes.

Firstly, this study demonstrates that mCRP can cause monocytes to form aggregates which increase in size over time which was demonstrated and observed under the microscope. Cell aggregation is a process of two parts in combination which include cell-to-cell recognition and cell adhesion (Youssef, 2016). mCRP has recently been observed to have adhesive-like properties which in turn leads to the aggregation of blood cells and platelets (Zeinolabediny et al., 2021). mCRP has the potential to contribute to thromboinflammation which is a complex interactions of blood coagulations and inflammation (Melnikov et al., 2023). Previous studies showed that mCRP induced endothelial cell monocyte adhesion and in the presence of nicotine and acetylcholine, this was inhibited (Slevin et al., 2018). This current research into aggregation and previous research is vital due to the links of mCRP stickiness to inflammation. Potential mechanism of action could be though mCRP platelet glycoprotein (GP) IIb/IIIa which is activated by mCRP and causes platelet adhesion via activation of GP IIb/IIIa receptors(Melnikov et al., 2023). It is understood that mCRP infiltration encourages monocyte attachment to the vascular cell wall specifically in the preliminary stages of atherosclerosis. This can lead to a thrombosis formation through platelet aggregation leading to a potential ischemic event (Molins et al., 2011; Slevin et al., 2018). In previous studies, CRP has been shown to promote platelet adhesion to endothelial cells and monocytes (Z. Zhang et al., 2012). Platelet aggregation analysis in previous studies showed that 100 ug/mL of mCRP induced aggregation of platelets but also found that in the presence of 8C10 and 3H12 monoclonal antibody (mAb), aggregation

formation was blocked. Interestingly, during this work mAb could not block monocyte cell aggregation (Slevin et al., 2018). mCRP protein has played a role in causing aggregation in several different cell types including monocytes as seen in the current study (Khreiss et al., 2004; De La Torre et al., 2013).

3.4.2 Monomeric c reactive protein promotes cell death and necrosis.

Further, there has been little research into individual CRP isoforms and their interaction with apoptosis. It has been established that mCRP is causing morphological changes in U937 monocytes and the cells are appearing to undergo necrosis and cell death. This was presented through flow cytometry analysis over several time points. Scanning electron microscopy was performed to observe the morphological changes occurring due to the treatment of mCRP at higher magnification. This analysis further enhanced the flow cytometry data and the previous aggregation results in which the cells were undergoing necrosis and leading to cell death over 24 hours. In previous work, mCRP but not nCRP was shown to cause apoptosis in human coronary artery endothelial cells (HCAECs) through the P38 mitogen signaling pathway. mCRP was also seen to cause a significant decrease in cell proliferation, increase cell injury and cause apoptosis. However, the effect of pCRP pre-treated HCAECs had no significant effects on atherosclerosis-related factors and cell damage. These data suggest that pCRP and mCRP exhibit distinct functions, and the CRP activity is expressed only when the circulatory pentameric structure of CRP is lost to form mCRP in disease (Y. Zhang and Cao, 2020). Interestingly, another study which observed neutrophils showed that mCRP inhibited apoptotic morphology development. This indicated that mCRP has different mechanistic roles depending on the cell type and conditions they present under. In forcing the importance of observing the effects mCRP has on the different cell types concerning inflammation (Khreiss et al., 2002; Khreiss et al., 2004). nCRP can make apoptotic cells more susceptible to induced phagocytosis. For example, nCRP-bound to apoptotic monocytes and macrophages may be removed via the FcγR-mediated phagocytosis (Gershov et al., 2000; Khreiss et al., 2002; Kim et al., 2014). During this body of work, it was not found that mCRP nor nCRP treated monocyte underwent apoptosis which is different to the observation found in the studies outlined above. However, it must be noted that each study used different cell types and different mechanisms were observed

potentially leading to different results. It was found in this research that mCRP but not nCRP caused necrosis and death of monocytes which fell in line with the positive control used (DMSO). As noted, not only did mCRP cause cell aggregation, but there was also the presence of necrosis and cell death after the treatment from the 6-hour mark onwards. A study looking at HCAECs and the impact of CRP isoforms showed that mCRP caused suppression of proliferation, increased damage to the cells and lead to apoptosis. These factors were reversed through p38 MAPK inhibitors. This result is presented in a comparable way to the research presented above. mCRP was seen to cause cell damage to the U937 cell and inhibited proliferation. In the literature, it stated that mCRP can cause a delay in apoptosis, whereas nCRP can cause apoptosis through the activation of the complement system. Again, this is contradictory to research in this work and by (Y. Zhang and Cao, 2020). However, in a study looking at neutrophil apoptosis, mCRP was seen to cause a delay in the onset but not inhibit the process altogether (Khreiss et al., 2002; Khreiss et al., 2004).

3.4.3 MCP-1 and IL-8 gene expression levels are altered after treatment of monomeric c reactive protein.

MCP-1 and IL-8 gene expression was analysed after U937 monocytes were treated with several conditions including mCRP which was shown to cause monocyte cell-cell adhesion and aggregation formation. IL-8 gene expression levels were seen to be upregulated at both the 3 hours and 24-hour mark compared to the control but not deemed significant after treatment with mCRP. Interesting, expression levels decreased at the 6-hour mark. In terms of pro-inflammatory cytokine production, mCRP increases IL-8 and nCRP has no detectable effect on their levels. MCP-1 gene expression levels were measured in this study after U937 monocytes treated with mCRP. MCP-1 expression at 3 hrs and 6 hrs time points showed decreased levels after treatment with mCRP compared to the control but were unregulated at the 24 hrs time mark. MCP-1 is a downstream mediator of CRP activity (Sproston and Ashworth, 2018; Sproston et al., 2018). Furthermore, CRP has been shown to increase the expression levels of MCP-1, IL-6, IL-8, and VCAM-1. With the upregulation of these key markers and pathways, CRP potentially could cause increased inflammation in a vascular setting leading to atherosclerosis becoming accelerated and intern increase the risk of ischemic stroke (Zhong et al., 2006). On the other hand, it is important to note that CRP has two isoforms, and it is also vital to distinguish which

isoforms are causing the upregulation in these key inflammatory markers. In this body of work outlined above, levels of both IL-8 and MCP-1 showed a marked increase in gene expression levels at different time points after the stimulation of mCRP. More interestingly, nCRP showed a marked increase as well. Another study, focusing on vascular-damaged CRP stimulation in endothelial vascular cells caused a marked increase in the expression of several different markers which include MCP-1, ICAM-1 and VCAM-1 which was also seen in the previous study discussed. This study found that after 24-hour stimulation with CRP, there was a two-fold change in 11 genes which were up-regulated and 6 which showed down–regulation. Most interestingly, IL-8 was found to be the most upregulated chemokine (Wang et al., 2005). It is important to understand the mechanism by which mCRP is causing this significant increase as MCP-1 and IL-8 have roles in the inflammatory acute phase of ischemic stroke (Kostulas et al., 1998; Losy and Zaremba, 2001; Zhu et al., 2022).

Chapter 4 – Targeting LXR pathway with a Liver X receptor agonist (GW3965) as a potential anti-inflammatory therapeutic target for neuroinflammation.

4.1 Introduction

4.1.1 Clinical problems of neuroinflammation

Neuroinflammation is a pathological feature of a wide range of CNS diseases and is evident by the loss of structure and function. Inflammation is mediated by the production of several different cytokines, chemokines, ROS, and secondary messengers as seen in figure 29. These mediators are produced by resident CNS glia (microglia and astrocytes), endothelial cells and peripherally derived immune cells. Microglia cells are one of the main drivers in neuroinflammation. These cells perform surveillance and macrophage-like activities of the CNS, including production of cytokines and chemokines. The neuroinflammatory response is mediated by IL-1β, IL-6, and TNFα, CCL2, CCL5, CXCL1, NO, prostaglandins and ROS (Orihuela et al., 2016; S. C. Zhao et al., 2017; S. X. Zhang, 2019; Yu et al., 2020). Many of these mediators are produced by activated resident CNS cells including microglia and astrocytes (Dong et al., 2021). Neuroinflammation is known to have several different effects and can present as both positive but also negative, as seen in figure 28. On the left-hand side of the schematic presented, it shows the positives of neuroinflammation such as injury induced remodelling by an increase in IL-4 which drives repolarization of macrophages toward M2 which is anti-inflammatory. On the right, negative aspects of neuroinflammation are outlined. Chronic, uncontrolled inflammation is characterized by increased production of cytokines (IL-1 and TNF), ROS, and other inflammatory mediators (iNOS). These markers are accompanied by significant recruitment and trafficking of peripheral macrophages and neutrophils. Additionally, a low-level and chronic inflammatory response driven by IL-1 and IL-6 is caused by aging, follows the acute phase of CNS trauma, and leads to reduced neuronal plasticity and cognitive impairments. More chronic inflammation is damaging to the nervous system and is characteristic of neurodegenerative diseases (DiSabato et al., 2016).

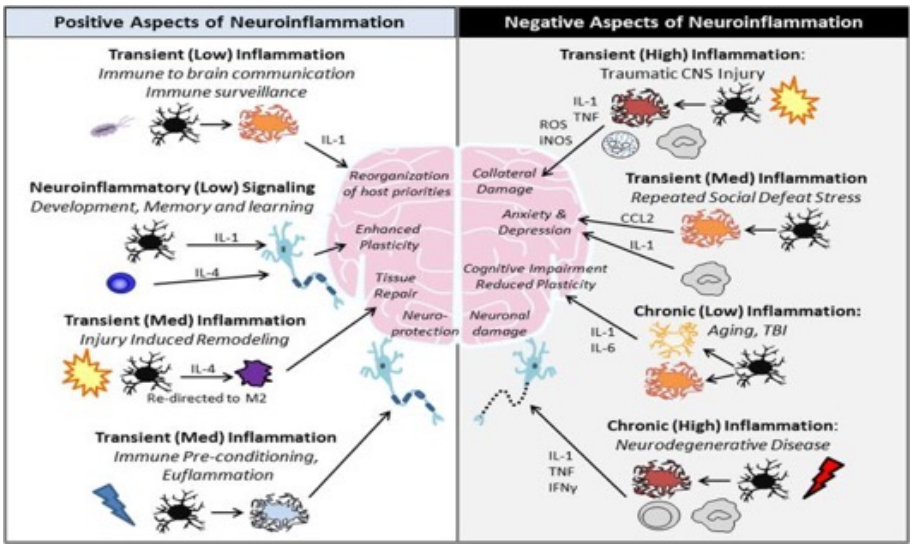

Figure 28 – Overview of the positive and negative aspects of neuroinflammation

4.1.2 The role of mCRP in neuroinflammation

CRP has two isoforms which are nCRP and mCRP. It is known that at different sites of inflammation or infection, CRP can increase up to 1000-fold (Sproston and Ashworth, 2018). CRP is a biomarker which is used in the clinical setting to measure inflammation or infection. In recent times, it was thought that nCRP was a direct mediator of inflammation. In turn, causing several different cell processes including endothelial cell adhesion, phagocytosis, and distribution of signalling inflammatory proteins. Interestingly, more recent research in and around both CRP isoforms has shown that it is the dissociation to mCRP that is the main inflammatory event (Caprio et al., 2018). mCRP is a key modulator of inflammation and has links to atherosclerotic arterial plaque progression, instability and neuroinflammation after stroke. mCRP is known to build up in the parenchyma and seems to connect to vascular damage, and neurodegenerative pathophysiology and there are potential links to Alzheimer's disease and dementia (Al-Baradie et al., 2021; Garcia-Lara et al., 2021).

4.1.3 Agonist compound GW965 as potential treatment for inflammation

Several questions remain when considering the role the liver x receptor (LXR) plays in the CNS and inflammation (Spyridon et al., 2011; L. Zhao et al., 2021). In the current literature, there is still a question to answer as to the targeting of the LXR pathway in response to an inflammatory event (Spyridon et al., 2011). In cells of the myeloid lineage, LXR has been shown to inhibit the inflammatory response through the transcriptional repression of several genes including Nos2, Cox2 and IL-6 (Morales et al., 2008; Nunomura et al., 2015). Thus, LXR is one among several biological signal pathways that link lipid metabolism and inflammation. Previous studies have shown that activation of LXR by oxysterols inhibits pro-inflammatory responses in cultures of microglia and astrocytes, suggesting that the LXR pathway might serve as a compensatory anti-inflammatory function in response to oxidative stress (McVoy et al., 2015). LXR agonist (GW3965 hydrochloride) has anti-inflammatory properties and has potential as a therapeutic target for inflammation in macrophages and other immune cells. The chemical structure of GW3965 can be seen in figure 29. GW3965 has also been seen to regulate the expression of several different pro-inflammatory genes (examples include *IL-6* and *iNOS*) in several different cell types which include macrophages, astrocytes, T cells and smooth muscle cells. GW3965 has much research conducted and activation of LXR can promote neuroprotection and reduces brain inflammation in an experimental stroke model. (Morales et al., 2008; Spyridon et al., 2011). GW3965 therapeutic has been shown to reduce the stability and size of thrombi and has the potential to reduce the formation of thrombi. This indicates that GW3965 has the potential to be a therapeutic target for the treatment to prevent thrombus formation (Nunomura et al., 2015).

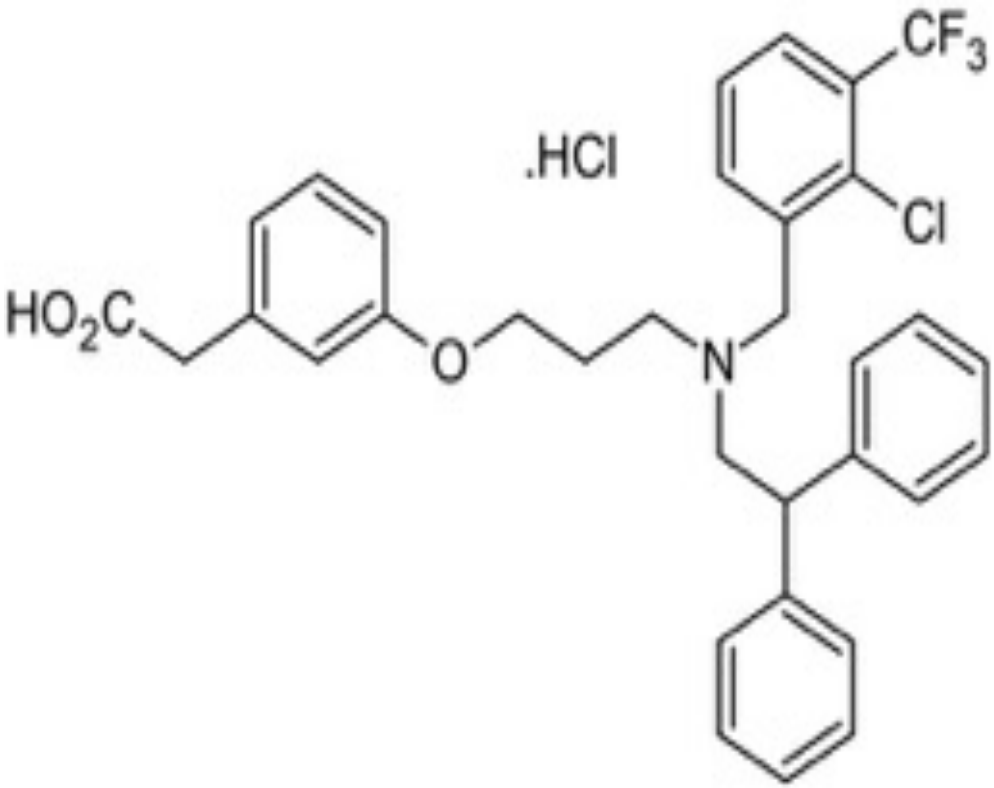

Figure 29 - GW3965 chemical structure

GW3965 hydrochloride is a selective agonist for the liver X receptor (LXR). It is a cell-based reporter and GW3965 targets LXRα and LXRβ.. This compound presents with a molecular weight of 618.51 KDa.

4.2 Aims and objectives.

The principal aims of the work presented in this chapter were to:

1) Observe morphological changes in HMC-3 microglia cells after stimulation LPS and CRP isoforms (mCRP and nCRP) (Motility um, motility speed u/h, migration, and migration vs directness, cell count, confluence, and cell volume

2) Observe cytotoxicity of potential therapeutic targets GW3965 and GSK4112

3) Characterise the inflammatory response of mCRP in treated microglia HMC-3 cells.

4) Elucidate the role of GW3965 as a potential therapeutic to reduce inflammatory response.

4.3 Results

4.3.1 mCRP causes morphological changes to HMC-3 microglia cells.

First, it was important to establish whether CRP isoforms could cause the HMC-3 cell line (Microglia) to undergo morphological changes which were observed through live cell imaging. Cells were grown 1) Control, 2) LPS 10 ng/mL positive control, 3) mCRP and 4) nCRP as described in chapter 2 section 2.2.3.3. The morphology of HMC-3 cells was checked at 3 different time points which were 3,6 and 24 hours as seen in figure 30. In the control cells presented in A1-3 over several different time points, normal morphological features were observed. HMC-3 cells were stimulated with LPS 10 ng/ml as a positive control for inflammation activation and to observe enhanced microglial proliferation. B1-3 represent LPS-stimulated microglia cells. The morphology of the cells does not appear to be changed and presents as healthy, however the number of cells within the frame appears more compared to the negative control which presents like the literature in which LPS has a proliferative effect on HMC-3 cells. C1-3 represents mCRP 100 µg/ml treated microglial cells. At different time points there has been a morphological change within the cells. These cells are round and do not have the characteristic of microglia cells. Further to this, a matrix-like grainy structure is shown in and around the microglial cells. Finally, D1-3 represent nCRP 100 µg/ml treated microglial cells at the three different time points. Again, the images show no morphological changes have occurred with nCRP 100 µg/ml.

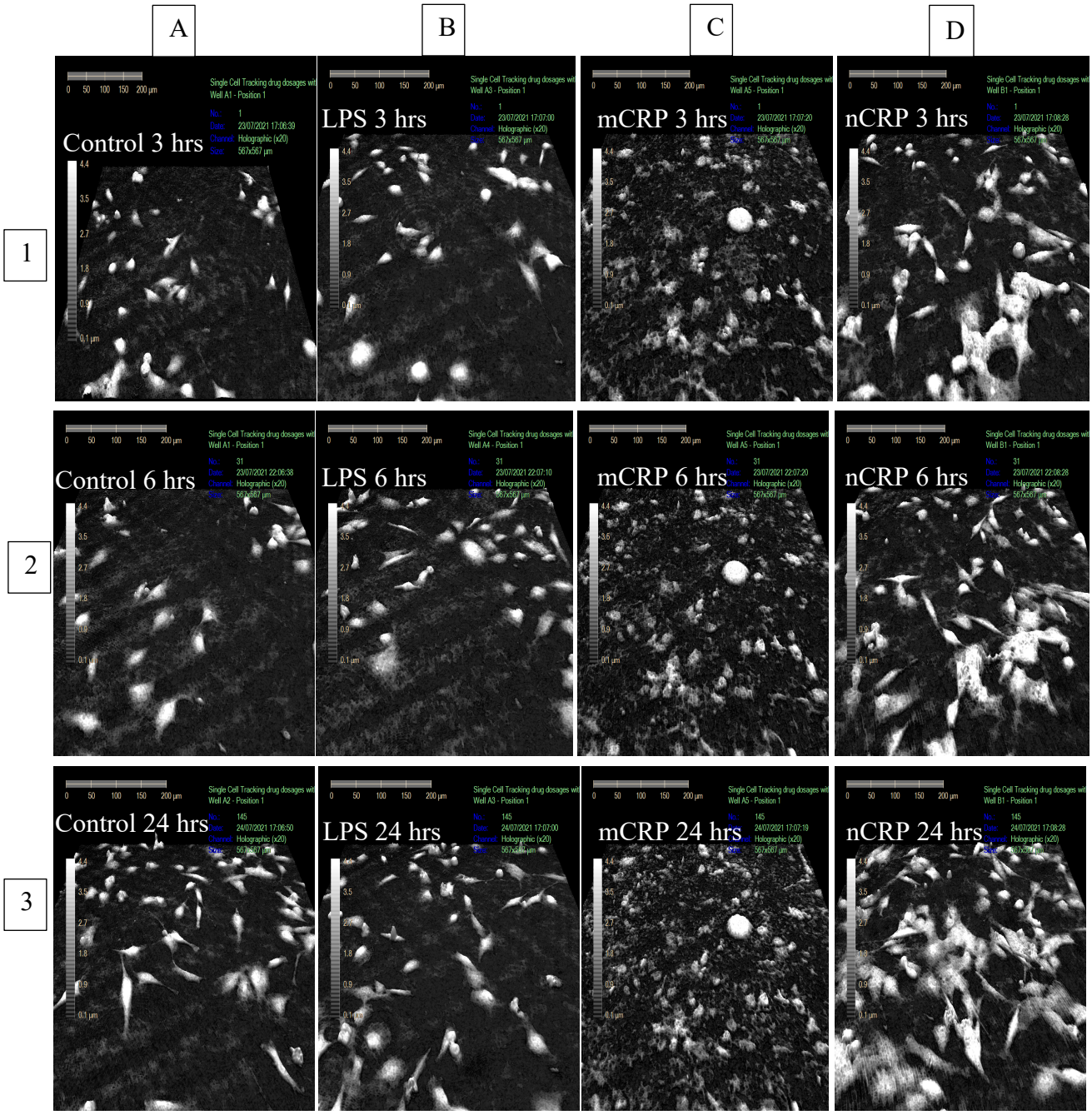

Figure 30 - Observing HMC-3 morphological changes caused by mCRP.

The effects of mCRP (100 µg/ml) on HMC – 3 cells were investigated. 4 treatments were investigated in total 1) Control (complete media), 2) LPS 10 ng/mL positive control, 3) mCRP and 4 nCRP. 1A-C - Control (3,6 and 24 hrs), B1-3 represents LPS 10 ng/ml. C1-3 represents mCRP 100 µg/ml. D1-3 represent nCRP 100 µg/ml. Images taken on live cell holographic imager at 20x with 3 fields of view per condition and repeated n=3.

As demonstrated in the figure above, mCRP is causing a morphological change in HMC-3 cells. The morphological effects were observed in more detail, and scanning electron microscopy was used to obtain higher magnification images of the cell surface. Cells were grown and treated with 1) Control, 2) LPS 10 ng/mL positive control, 3) mCRP 100 μg/ml and 4 nCRP μg/ml as described in chapter 2 (2.2.3.5.1). The qualitative analysis of scanning electron microscope images showed good viability in the control group and HMC3 cells presented with normal morphology. When HMC-3 microglial cells were treated with mCRP, a morphological change was observed. All morphological features of intensive apoptotic processes, including changing membrane morphology and integrity, losing microvilli, budding, swelling, formation of apoptotic body, and total cell rupture. In the images representing treatment with mCRP (figure 31E and F), there is clear disruption on the cell surface. When observing the cells under more intense magnification, HMC-3 cells presented with budding, cell rupture and a change in membrane morphology and integrity. Interestingly, when observing nCRP-treated microglia cells, there were no adverse morphological changes and presented visually in a similar way to the control.

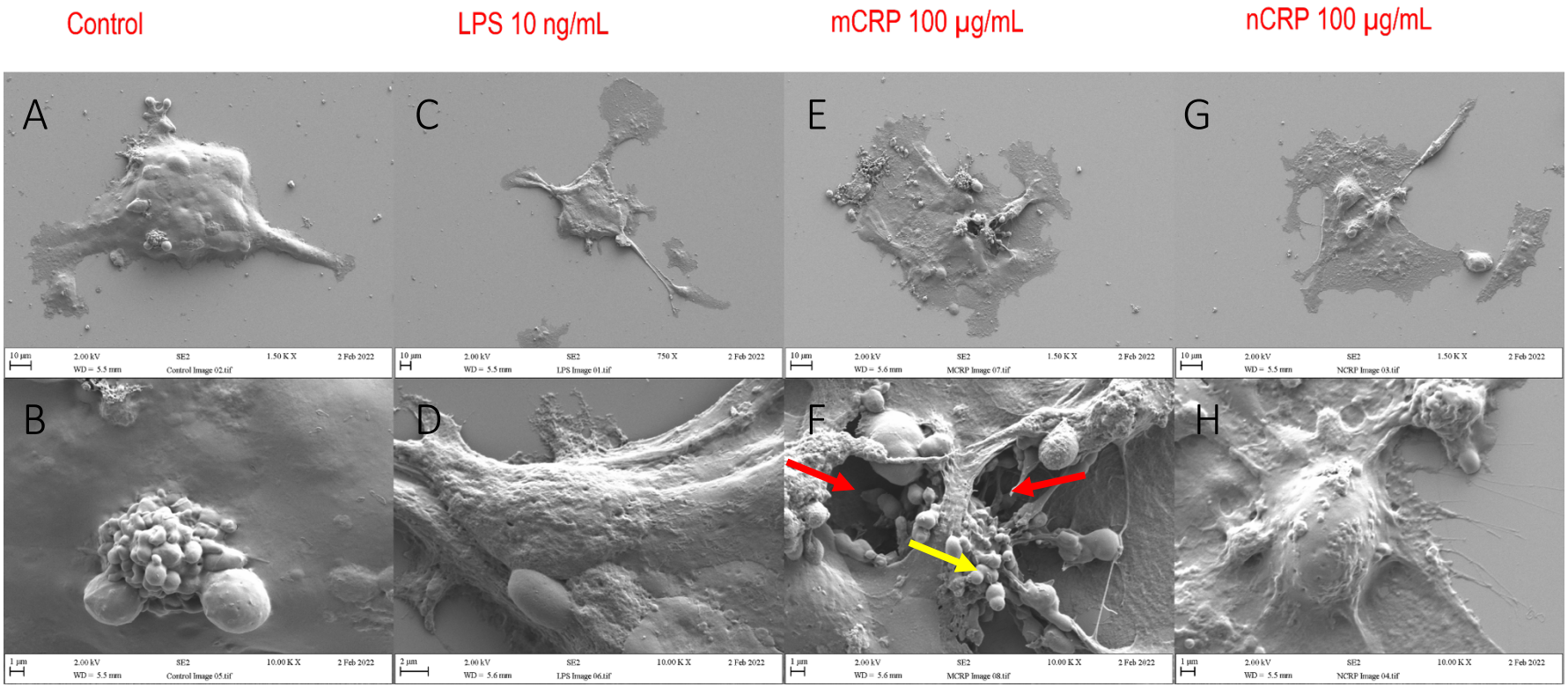

Figure 31 – mCRP causes morphological chances to HMC-3 microglia cells.

HMC-3 microglia cells - control (A and B) tends to adopt a more rounded morphology with flat protrusions. Further to this the surface appears smooth and no loss of membrane integrity. LPS 10 ng/ml (C and D) and nCRP 100 µg/ml (G-H) presents in similar way to the control in which membrane appears intact but the surface of the membrane appears not a smooth. mCRP 100 µg/ml (E and F) treated microglia cells appears to have cell surface structural changes with increase surface debris and under higher magnification appear to have membrane damaged as indicted with red arrows. mCRP causes these nodule formations on the cell surface (yellow arrow). Images were taken at 750 x and 10.00 KX, 3 images taken per field of view.

4.3.2 Holographic quantifiable cell morphological and proliferative features after treatment with CRP isoforms

The effects of mCRP on microglia cells (HMC-3) were analysed using the phase shift holographic live cell imager. This microscope and the integrated analysis software allowed several different types of analyses to be completed. Figure 32A-D represents rose plots produced by the integrated analysis software to observe the migration of cells. Visually looking at the rose plots, mCRP treatment is affecting the migration ability of HMC-3 microglia cells. 32E represents the migration of HMC-3 microglia cells which have been treated with several conditions. Interestingly, treatment with mCRP protein for 24 hours significantly reduced the migration of cells compared to the control (CI 95% 3.440 to 6.567) p = <0.0001. Further to this, when comparing the two isoforms mCRP vs nCRP migration is only altered by mCRP (CI 95% -17.78 to -14.65) p = <0.0001. Figure 32 F, HMC-3 migration directness (migration vs motility) was significantly affected over 24 hours after treatment with mCRP (CI 95% -0.08869 to 0.1270) p = <0.0001. mCRP compared to nCRP caused a significant effect in migration directness (CI 95% -0.1112 to 0.07287) P = <0.0001. Figure 32G, HMC-3 Motility (µm) was significantly affected over 24 hours after treatment with mCRP (CI 95% 35.15 to 44.80) P = <0.0001. mCRP caused a significant difference in the cells compared to nCRP (CI 95% -41.31 to -31.66) P = <0.0001. Indicating Motility (µm) is affected after treatment with mCRP. Figure 32H, Motility speed (µm/h) was significantly affected over 24 hours after the treatment of mCRP (CI 95% 5.317 to 6.186) P= <0.0001. mCRP caused a significant difference in speed compared to nCRP CI 95% -5.949 to -5.080) P = <0.0001. Indicating speed is affected after treatment with mCRP.

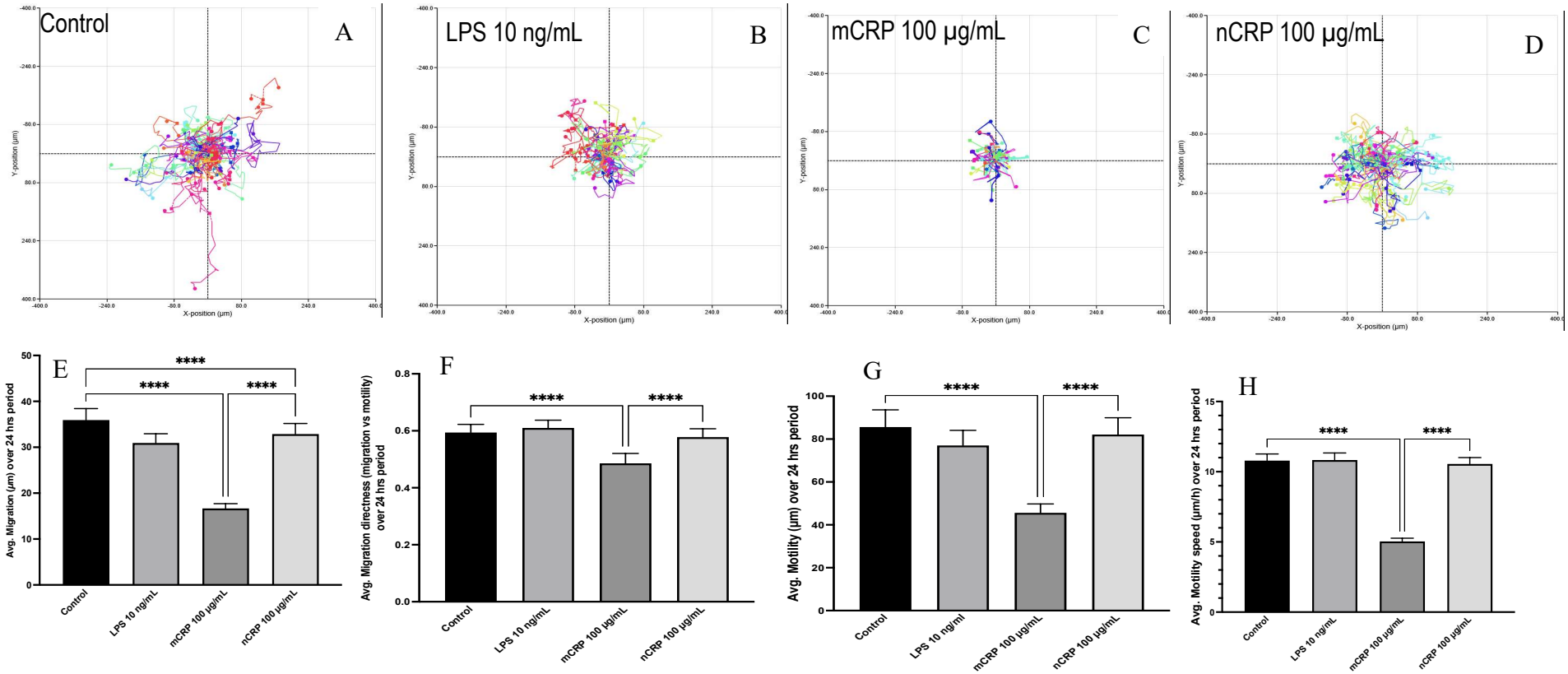

Figure 32 - Holographic imaging of cells reveal the impact of culture extracellular environment on cell migration and cell motility.

HMC-3 single cell tracking analysis performed with the integrated software from the phase shift holographic images. HMC-3 cells were grown and treated with 1) Control, 2) LPS 10 ng/mL positive control, 3) mCRP and 4 nCRP as described in chapter 2 (2.2.3.3). A-D) Single cell 2D movement trajectories from 50 cells chosen at random per field of view were displayed in a rose plot. Original units for cell movement parameters are displayed on the x and Y axis by means of logarithmic scale. E) Migration directness, G) cell motility and H) speed. Cell was tracked over a 24-hour period and quantified from single cell tracking data in which 50 random cells were chosen. Graphs represent Mean ± SEM (two – way ANOVA multi-comparison (turkey)) (p =< 0.05, p**** <0.0001. 3 fields of view per a well were measured and repeated n=3.*

4.3.3 Determine the kinetic dose response for GW3965.

The kinetic dose response for GW3965 was performed using the live cell imager (holo-monitor) with the integrated analysis software. An in-depth analysis can be performed on the single cell tracking cell morphology and further looking into cell count, confluence, and mean cell volume to determine the effects that the drug compound is having upon the cells. A range of doses was selected based on the literature search and a kinetic dose-response assay was performed to determine if there are any adverse effects of this agonist on microglial HMC3 cells. Several measurement outputs were analysed during this experiment, which included cell count, confluence, mean volume, and migration versus directness. Finally, a rose plot was used to determine the trajectories after the dose responses of GW3965. Looking at Figure 33 A-E, there were no differences within the trajectories. Looking at Figures 34 A and B, the cell count was tracked over 24 hours and showed no adverse effects in the dosage response. Interestingly, the cell count did increase at all concentrations of GW3965 when compared to the control group. Control vs GW3965 (1.25 μM) CI 95% -3484 to -287.1 p = 0.0145, Control vs GW3965 (2.5 μM) CI 95% -6313 to – 3254 p = <0.0001, Control vs GW3965 (5 μM) CI 95% -4673 to -1615 p = <0.0001, Control vs GW3965 (10 μM) CI 95% -4988 to -1929 p = <0.0001. Secondly, looking at Figures 34 C and D, which are looking at the confluence of the cells. Again, there are no adverse effects on the cell confluence after treatment with GW3965 at varying dosages. Interestingly, the dosage of GW3965 at 2.5 μM (CI 95% -5.117 to -3.029) p = <0.0001, 5 μM (CI 95% -2.929 to -0.8412) p = <0.0001 and 10 μM (CI 95% -3.971 to 1.883) p = <0.0001 caused a significant increase within the confluence compared to the control. Thirdly, Figure 34 E and F were looking at the mean cell volume of HMC3 microglial cells and was used to determine if HMC-3 cells were affected by the dose response of GW3965. Only a significant effect was found within the 10 □m dosage (CI 95% -207.6 to -78.58) p = <0.0001. All other doses were found not to be significant. Overall, no adverse side effects were presented. Going forward a dose of 2.5 μm was used for future experiments based on these results and literature-based searches.

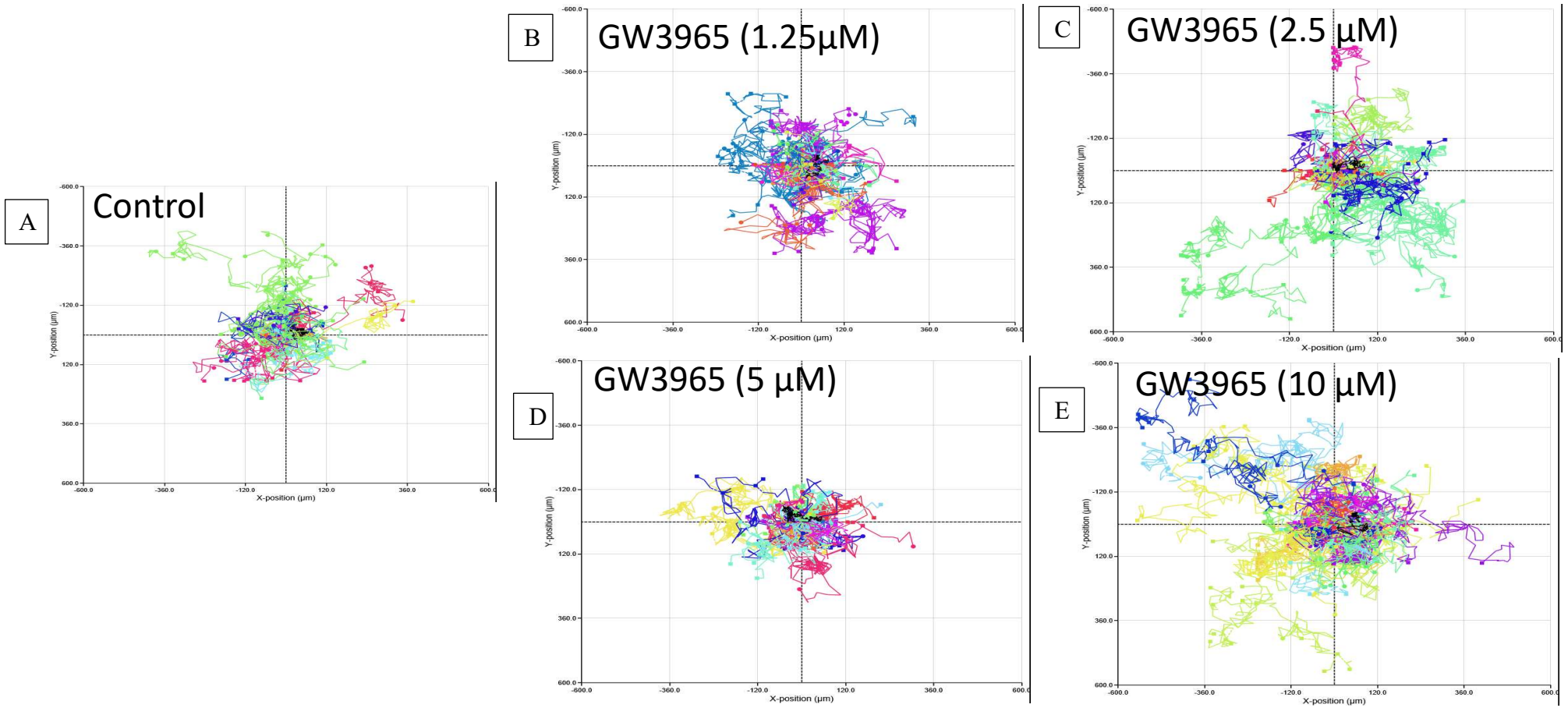

Figure 33 – HMC-3 single cell 2D movement trajectories after GW3965 drug treatment displayed as a rose plot.

Single cell 2D movement trajectories from 160 cells chosen at random per field of view were displayed in a rose plot. Original units for cell movement parameters are displayed on the X and Y axis by means of logarithmic scale. Each plot represents the migration pathway over the 24-hour period.

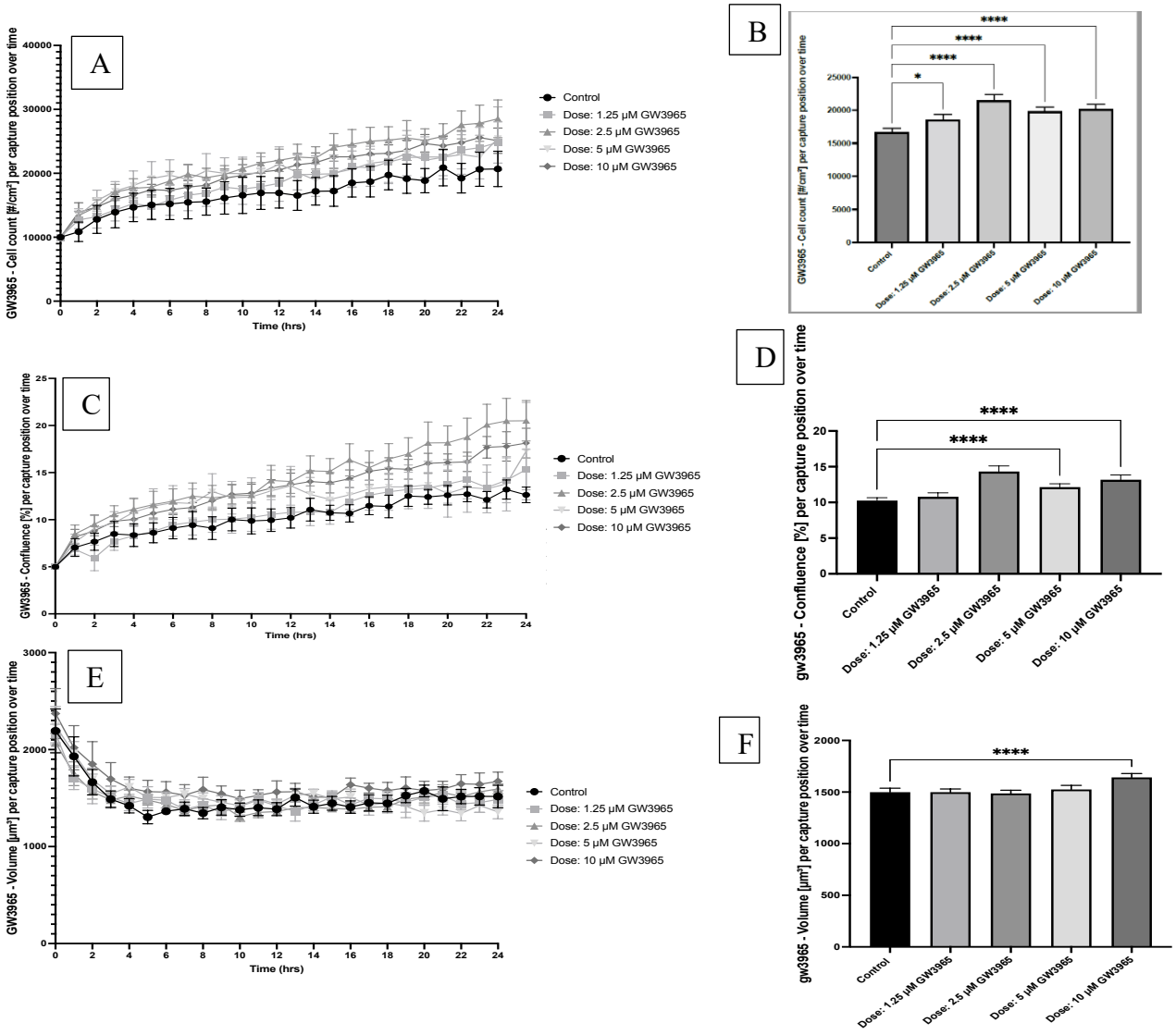

Figure 34 – Kinetic response of GW3965 treated HMC-3 microglia cells for 24-hour period.

*The effects of GW3965 varying dosages were investigated using live cell imaging kinetic response analysis. 4 concentrations (10 µm, 5 µm, 2.5 µm 1.25 µm) were observed and negative control included. A and B) Cell count monitoring of HMC-3 cells treated with varying dosages of GW3965, C and D) Cell confluence monitoring of HMC-3 cells treated with varying dosages of GW3965, E and F) Cell volume monitoring of HMC-3 cells treated with varying dosages of GW3965. Data presented as Mean ± SEM (2-way ANOVA) p = * P<0.05, P<0.001, P=<0.0001 n=3.*

4.3.4 Determine the kinetic dose response for GSK4112.

Another potential compound was analysed, using the kinetic analysis of the holo-monitor, and that was GSK4112. A range of doses was selected based on the literature search and a kinetic dose-response assay was performed to determine if there are any adverse effects of GSK4112 on microglial (HMC-3) cells. Several measurement outputs were analysed during this experiment, which included cell count, confluence, and mean volume. Finally, a rose plot was used to determine the trajectories as seen in Figure 35 A-D. When visually looking at the rose plots generated from the internal software, a difference was observed in the migration compared to the control. Looking at Figures 36A and B were looking at cell count. There was a significant increase in cell count at dosage 2.5 μM compared to the control group in cell count compared to the control (CI 95% -3402 to -464.8) p = 0.0058. Interestingly at dosage 10 μM there is a significant decrease in cell count compared to the control group (CI 95% 3936 to 6873) p = <0.0001. Again, when looking at the confluence of the cells figure 36 C and D, there was a significant reduction in confluence as dosages 2.5 μM (CI 95% -2.143 to -4.529) p = <0.0001, 5 μM (CI 95% -2.065 to -4.452) p = <0.0001 and 10 μM (CI 95% -2.757 to -5.143) p = <0.0001 compared to the control. Figure 36 E-F represents the volume [μm^3] per capture position over time. The volume is significantly decreasing in dosages 2.5μM (CI 95% 457.7 to -646.8) p = <0.0001, 5 μM (CI 95% 255.9 to 447.1) p = <0.0001 and 10 μM (CI 95% 52.13 to 243.3) p = 0.0009 in relation to the control group.

From this point onwards GW3965 was carried forward as a potential compound for treatment in neuroinflammation.

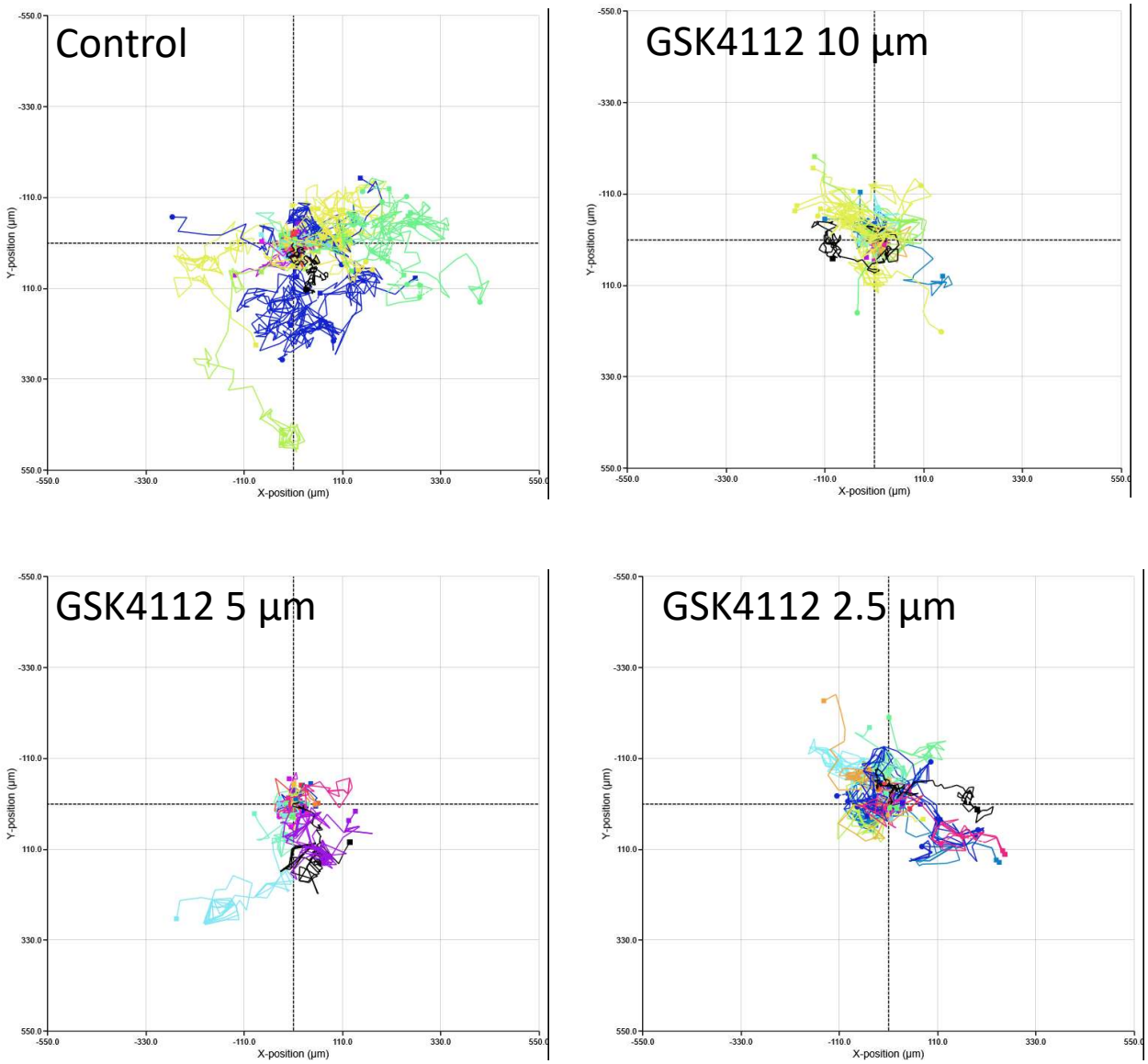

Figure 35 - HMC-3 single cell 2D movement trajectories after GSK4112 drug treatment displayed as a rose plot.

Single-cell 2D movement trajectories from 160 cells chosen at random per field of view were displayed in a rose plot. Original units for cell movement parameters are displayed on the X and Y axis using a logarithmic scale. Each plot represents the migration pathway over the 24 hours. Single-cell 2D movement trajectories from 160 cells chosen at random per field of view were displayed in a rose plot. Original units for cell movement parameters are displayed on the x and Y axis using a logarithmic scale. Each plot represents to migration pathway over the 24 hours. From the plot, GSK4112 does influence cell movement when compared to the control.

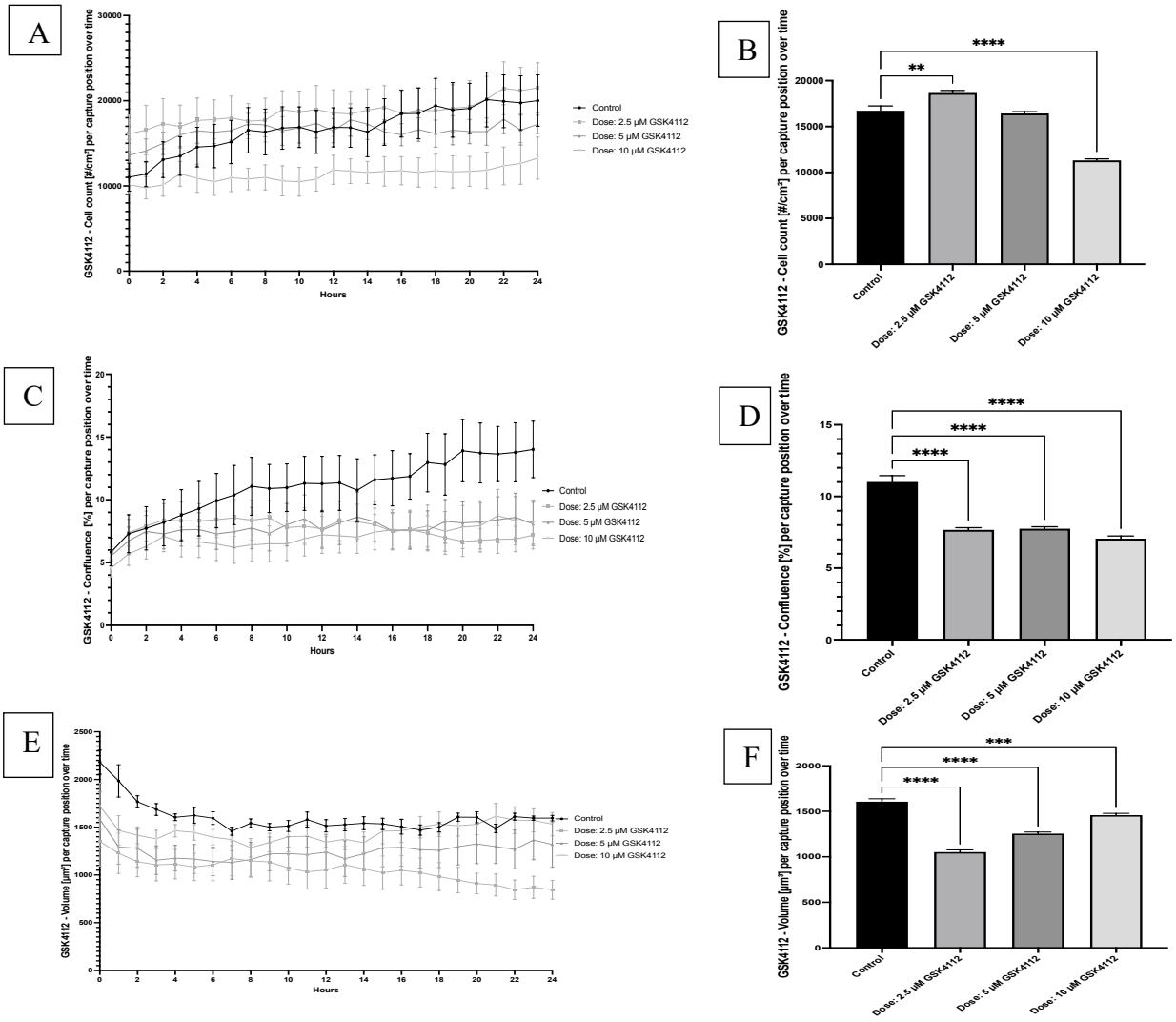

Figure 36 - Kinetic response of GSK4112 over 24-hour period.

*The effects of GSK4112 varying dosages were investigated using live cell imaging kinetic response analysis. 3 concentrations (10 µm, 5 µm, and 2.5 µm) were observed and negative control was included. A and B) Cell count monitoring of HMC-3 cells treated with varying dosages of GSK4112, C and D) Cell confluence monitoring of HMC-3 cells treated with varying dosages of GSK4112, E and F) Cell volume monitoring of HMC-3 cells treated with varying dosages of GSK4112. Data presented as Mean ± SEM (2-way ANOVA) p = * P<0.05, P= *** <0.001, P = **** <0.0001 n=3*

4.3.5 LPS and mCRP modulated IL-6 protein levels in HMC-3 microglia cells.

HMC-3 cells were seeded in a 12-well plate and the experiment was set when a confluence of 80% was reached. HMC-3 cells were pre-treated with GW3965 µm, 30 minutes before mCRP was added. LPS 10 ng/mL was used as an inflammatory control and complete media was used as the negative control for no inflammatory stimulation. To determine the effects of LPS and mCRP on the expression of inflammatory mediators, HMC-3 microglia cells were exposed for 6 and 24 hr to 100 µg/ml mCRP and LPS 10 ng/mL and secreted protein levels of several different markers were measured in the supernatant using ELISA or multiplex analysis. As shown in Figure 37 A, at the 6 hours mark the negative control presented with Low levels of IL-6 protein. LPS 10 ng/ml presented with increased levels of IL-6 above 1500 µg/ml, and this was significantly different compared to negative control 484.0 ± 36.43 vs LPS 10 ng/ml 1507 ± 86.20 (95% CI -1411 to -634.8) p=<0.0001. mCRP 100 µg/ml presented with levels above 1000 mg/ml of IL-6 and significantly different from the control 484 ± 36.43 vs mCRP 100 mg/ml 1172 ± 12.35 (95% CI -1076 to -299.8), p= 0.0007. mCRP showed a similar response to LPS inflammatory mediator. GW3965 2.5 mM significantly reduced IL-6 protein which was increased due to the inflammatory stimulant LPS at a concentration of 10 ng/ml. LPS 10 ng/ml 1507 ± 86.20 vs 810 ± 66.19 (308.5 to 1084) p=0.0007. This is a similar representation to HMC-3 cells treated with mCRP and GW3965 in which levels were reduced compared to the pro-inflammatory mediator protein mCRP. mCRP 1172 ± 12.35 vs GW3965 + mCRP 775.3 ± 79.87 (95% CI -8.502 to 784.3) p=0.0442, however, levels did not decrease to the baseline levels detected in the control. As shown in Figure 37 B, at the 24-hour mark the negative control presented with Low levels of IL-6 protein. LPS 10 ng/ml presented with increased levels of IL-6 above 2500 µg/ml, and this was significantly different compared to negative control p=<0.0001. mCRP 100 µg/ml presented with levels above 2000 µg/ml of IL-6 and significantly different from the control p=<0.0001. mCRP showed a similar response to LPS inflammatory mediator. Interestingly when treating HMC-3 with GW3965 and LPS, levels of IL-6 were not significantly decreased compared to LPS p=<0.0001. This is a similar representation to HMC-3 cells treated with mCRP and GW3965 in which levels were reduced compared to the pro-inflammatory mediator protein mCRP p=<0.0001, however levels did not decease to the baseline levels detected in the control.

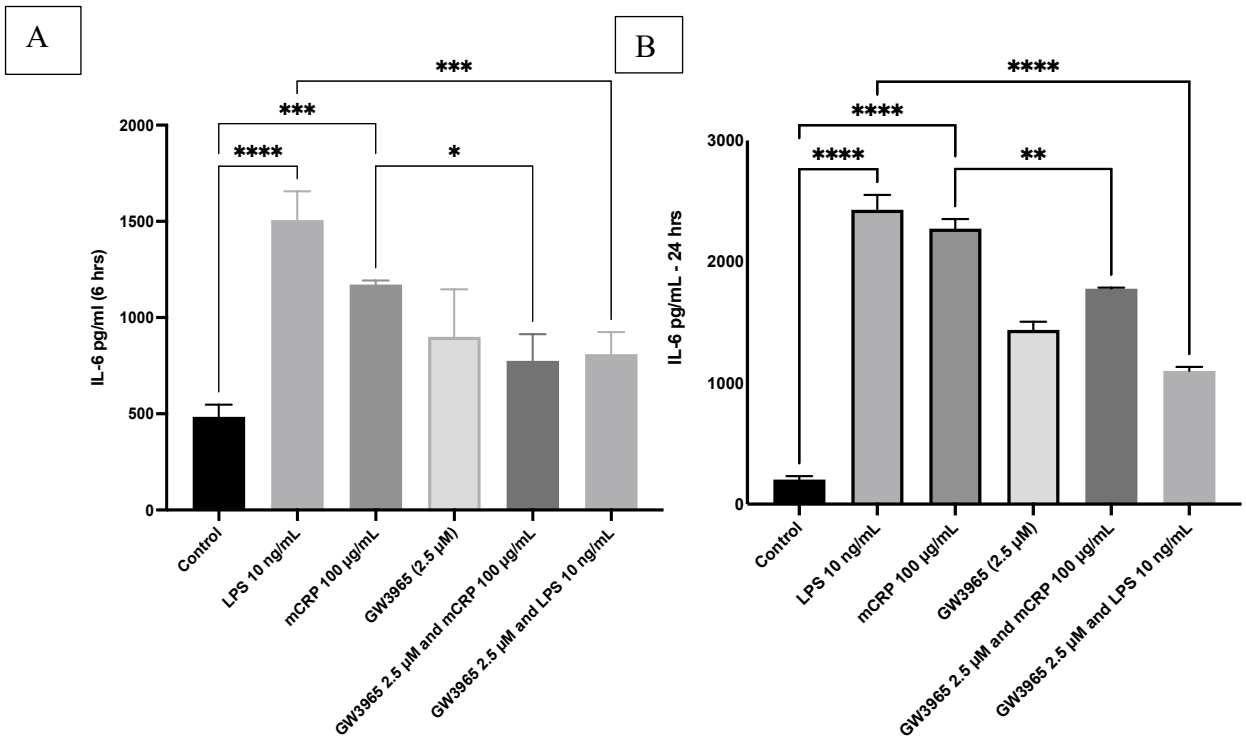

Figure 37 -GW3965 2.5 µM significantly reduces IL-6 protein levels after treatment with pro-inflammatory mediators (LPS and mCRP)

IL-6 protein levels measured after LPS 10 ng/ml and mCRP 100 µg/ml treatment of HMC-3 plus or minus agonist GW3965 µM. A) IL-6 protein levels at 6 hours. B) IL-6 protein levels at 24 hours. Data presented as Mean ± SEM - One-way anova (p = < 0.05 p **= <0.01, p*** = < 0.001, p**** <0.0001. (n=3)*

4.3.6 mCRP activated IL-6 and regulated through NfKb signalling pathway.

HMC-3 cells were treated and prepared as described in chapter 2. Immunofluorescence microscopy was used to look at levels of IL-6 (red) and activation of the NfKb p65 signalling pathway (green) in microglia cells treated with varying conditions (figure 38A). Microglia cells were treated with control (complete media) (222.2 ± 42.38), LPS 10 ng/ml (282.2 ± 33.53), mCRP 100 mg/ml (338 ± 74.95), nCRP mg/ml (247.4 ± 30.44), GW3965 2.5 µM (176.3 ± 2.975), LPS 10 ng/ml with GW3965 2.5 µM (160.9 ± 1.957) and mCRP 100 mg/ml with GW3965 2.5 µM (294.9 ± 31.82). Present in figure 38B, IL-6 Levels did not significantly increase in LPS-treated samples compared to the control - 95% CI -142.0 to 4.286 (p= 0.4970) whereas mCRP-treated caused a significant increase in IL-6 (95% CI -156.4 to -10.09) p=<0.0001. mCRP caused a significant increase in IL-6 compared to nCRP (95% CI - 61.95 to 208.2) p = <0.0001. GW3965 agonist significantly reduced levels of IL-6 which were increased after LPS (95% CI 83.65 to 229.9) p=<0.0001. Further to this, the agonist was able to significantly decrease levels of IL-6 which were increased due to mCRP treatment (95% CI 13.11 to 159.4) p=0.0082. NFkB Levels did not significantly increase in LPS treated samples compared to the control - 95% CI -142.0 to 4.286 (p=0.0854) whereas mCRP treated caused a significant increase in IL-6 (95% CI -156.4 to -10.09) p=0.0127.

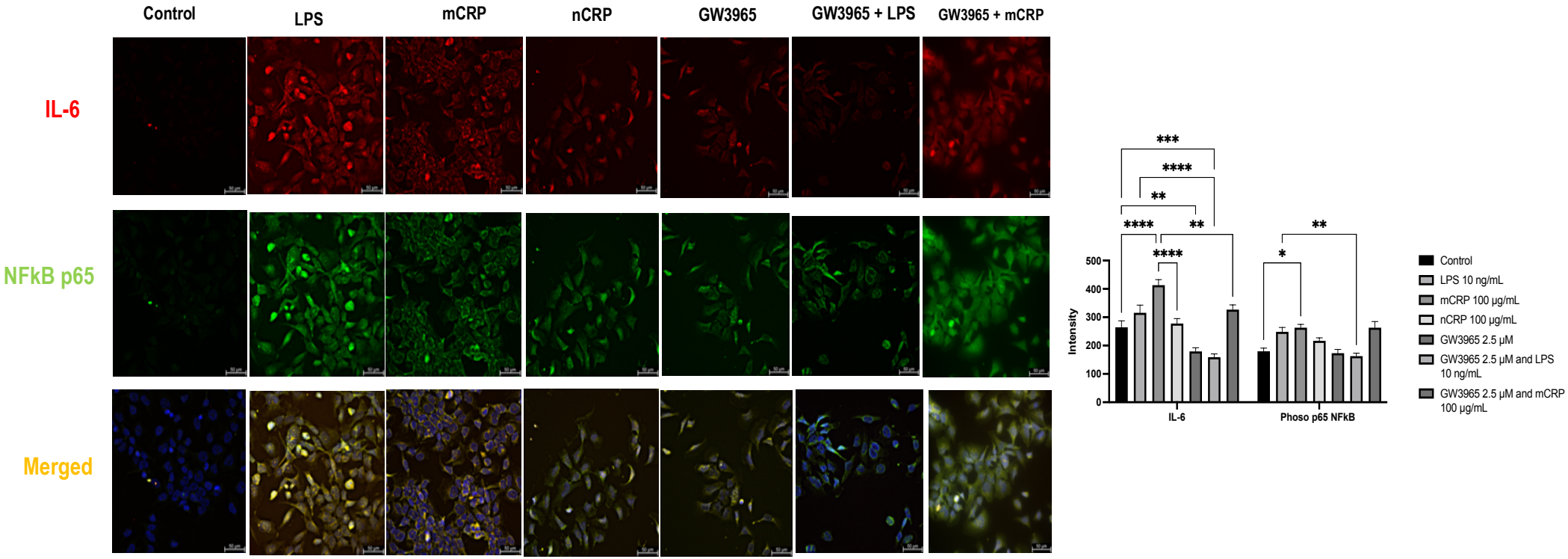

Figure 38 - GW3965 (2.5 µM) reduced pro-inflammatory IL-6 levels in inflammatory mediator stimulated HMC-3 microglia cells.

A) Immunofluorescent staining results for microglia (HMC-3 cell) stained for anti-mouse IL-6 with secondary IgG 568 goat anti mouse (Red) and Anti-rabbit NfKb (Green) with secondary Alexafluro 488 goat anti-rabbit IgG and Nucleus staining (Dapi - Blue) before and after stimulation with LPS and mCRP and treated with GW3965 2.5 µM. Samples were view under 10 x 63 magnification with oil (n3).

4.3.7 LPS and mCRP modulated IL-1β protein levels in HMC-3 microglia cells but not TNFα.

As shown in Figure 39 A, at the 6-hour mark the negative control presented with low levels of IL-1β protein. LPS 10 ng/ml presented with increased levels of IL-1β above 40 μg/ml, and this was significantly different compared to negative control (CI 95% -64.66 to -6.258) p = 0.0182. mCRP 100 μg/ml presented with levels above 40 μg/ml of IL-1β which was significantly different from the control (CI 95% -58.26 to -4.947) p = 0.0207. mCRP showed a similar response to LPS inflammatory meditator. Interestingly when treating HMC-3 cells with GW3965 2.5 μM and LPS 10 ng/mL, levels of IL-1β were significantly decreased compared to LPS (CI 95% 13.69 to 72.09) p = 0.0059. This is a similar result to HMC-3 cells treated with mCRP and GW3965 in which levels were reduced compared to the pro-inflammatory mediator protein mCRP (CI 95% 3.517 to 51.20) p = <0.0248, however, levels did not decrease to the baseline levels detected in the control. As shown in Figure 39B at the 6-hour mark the negative control presented with low levels of TNFα. LPS 10 ng/ml presented with increased levels of TNF-α but this was not deemed significant to the control group (CI 95% -2760 to 525.5) p = 0.1843. mCRP 100 μg/ml presented with increased levels of TNFα but levels were not significant compared to the control (CI 95% -2862 to -424.1) p = 0.1417. Interestingly when treating HMC-3 cells with GW3965 2.5 μM and LPS 10 ng/mL, levels of TNFα were not significantly decreased compared to LPS (CI 95% -1335 to 1348) p = >0.9999. This is a similar result to HMC-3 cells treated with mCRP and GW3965 (CI 95% -945.6 to 1737) p = 0.7957.

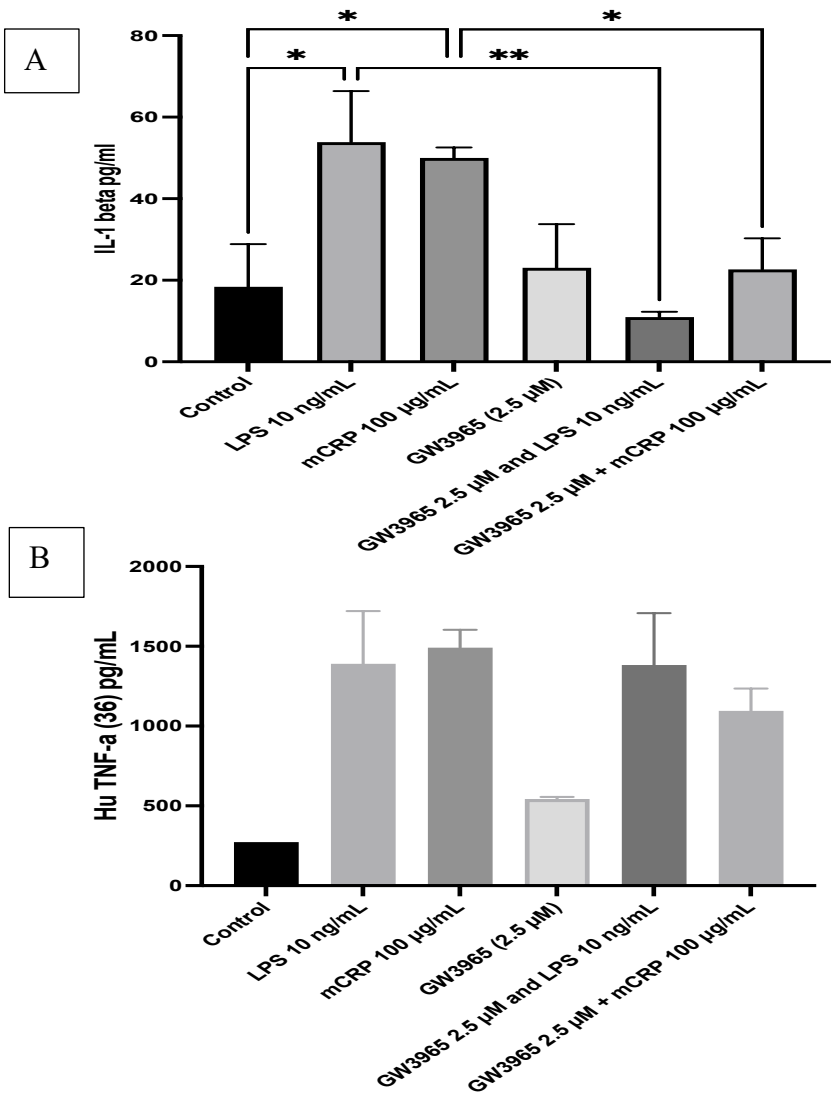

Figure 39 – GW3965 agonist reduced IL-1β levels but not TNF alpha after treatment with LPS and mCRP.

Following the treatment of HMC-3 microglia cells with LPS 10 ng/ml or mCRP 100 µg/ml plus or minus GW3965 2.5µM for 6 hours, supernatant was collected to measure IL-1β (ELISA) and TNFα protein (Multiplex panel). A) IL-1β protein levels at 6 hours and B) TNFα protein levels 6-hours. Data presented as Mean ± SEM (pg/ml) - One-way anova (p = < 0.05 p **= <0.01, p*** = < 0.001, p**** <0.0001. (n=3)*

4.3.8 The Effects of the GW3965 on LPS/mCRP-Stimulated HMC3 microglia cells expression of chemokines

Figure 40A presented RANTES protein levels after microglial cells were treated with mCRP and LPS to induce an inflammatory response plus or minus GW3965 (2.5 μM). When comparing the control to LPS-treated cells, levels of RANTES was significantly increased GW3965 (CI 95% -3138 to -1563) p = 0.0004. Interestingly, mCRP had an increase in RANTES protein levels and was significantly different to the control (CI 95% -2240 to -954.1) p = 0.0009. After HMC-3 cells were treated with LPS plus GW9365 levels of RANTES were significantly decreased after anti-inflammatory agonist drug treatment (CI 95% 1242 to 2817) p = 0.0008. After HMC-3 cells were treated with mCRP plus GW9365 levels of RANTES were significantly decreased after anti-inflammatory agonist drug treatment (CI 95% 498.6 to 1785) p = 0.0044. Figure 40B, presents the Exotoxin protein levels. Control levels were at baseline, with LPS-stimulated cells significantly increasing protein levels CI 95% (-123.3 to – 15.62). mCRP levels were increased compared to the control CI 95% (-98.00 to – 9.661) but they were not significantly different. After HMC-3 cells were treated with either LPS/mCRP plus or minus GW9365 (2.5 μM), there was no significant decrease in the Exotoxin protein levels. Finally, in figure 40C, HMC-3 cells treated with LPS 10 ng/ml showed no significant increase in VEGF levels compared to the control (CI 95% -3708 to 879.9) p = 0.2695. Whereas mCRP treated cells caused a significant increase in VEGF protein levels (CI 95% -4840 to -252.1) p = 0.0318. When cells were treated with mCRP 100 μg/ml or LPS 10 ng/ml plus or minus GW3965 (2.5 μM) levels of VEGF were not significantly altered. Figure 40D represents IFN-g protein levels which were not significantly increased after stimulation with LPS (CI 95% -271.0 to 147.4) p = 0.9710 or mCRP (CI 95% -271 to 89.62) p = 0.4334 and drug treatment had no effect on VEGF protein expression levels over 6-hour period.

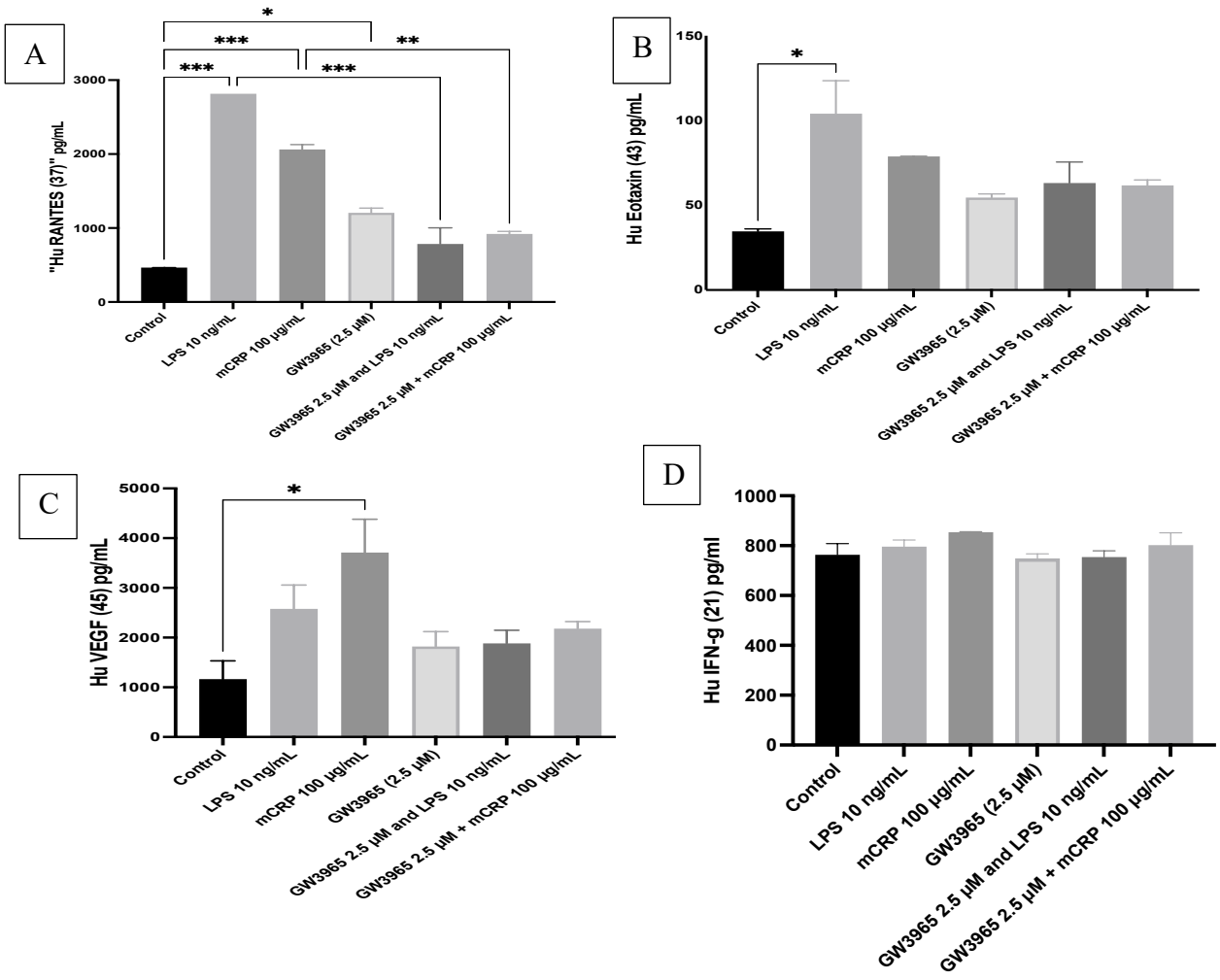

Figure 40 – Chemokine protein analysis after treatment with LPS or mCRP plus or minus GW3965

Following HMC-3 microglia cell treatment with LPS 10 ng/ml or mCRP 100 µg/ml plus or minus GW3965 2.5µM for 6 hours, supernatant was collected for multiplex analysis. A) RANTES protein levels, B) Eotaxin, C) VEGF protein level and D) IFN-g protein levels. Data presented as Mean ± SEM (pg/ml) - One-way anova (p = < 0.05 p **= <0.01, p*** = < 0.001, p**** <0.0001. (n=3)*

Figure 41A shows the measurement of MIP1 α protein levels. No significance was found within any of the treated samples. Looking at MIP1β protein results from the multiplex panel in Figure 41B, LPS treated microglia cells increased levels of MIP1 β significantly compared to the control (CI 95% -1422 to -173.1) p = 0.0166. Interestingly, cells treated with mCRP 100 μg/ml increased levels of MIP1 β compared to the control group but was not deemed significant. Treatment with either mCRP or LPS plus or minus GW3965 showed no difference in protein levels. Finally, in Figure 41 C, LPS levels were significantly increased compared to the control (CI 95% -1196 to -135.4) p = 0.0180. Interestingly, MCP-1 protein level se created by into supernatant by microglia cells were increased but significantly compared to the control (CI 95% -935.7 to 125.1) p = 0.1399. When HMC 3 microglial cells were treated with GW3965 and stimulated with LPS, there was a significant decrease in MCP-1 levels (CI 95% 38.07 to 1099) p = 0.0371. Whereas when mCRP-treated cells were treated with GW965, there was no significant decline when compared to mCRP on its own.

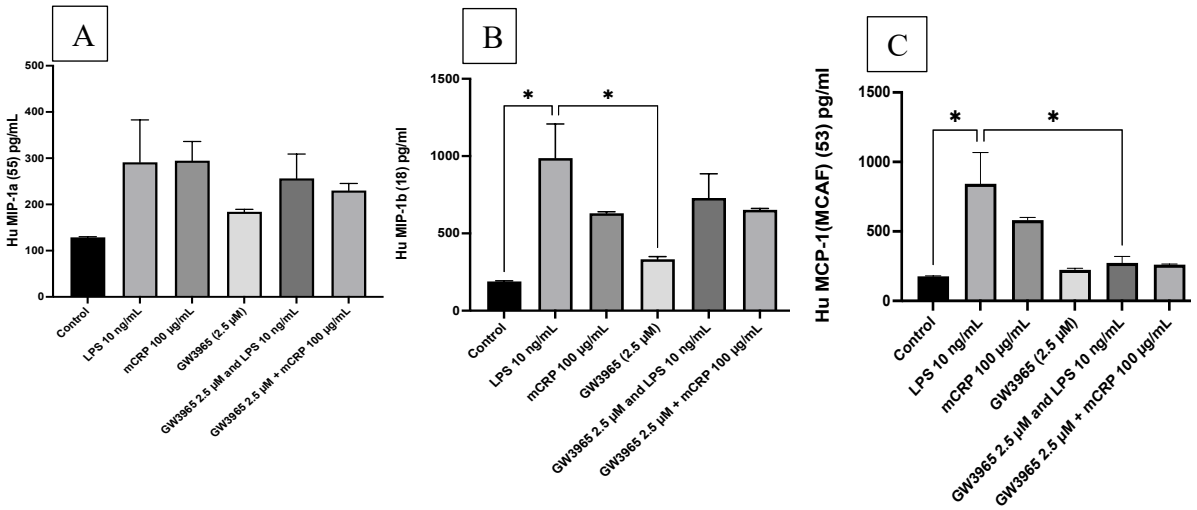

Figure 41 – Regulation of monocyte and macrophage chemokines after microglia cells treated with LPS or mCRP.

HMC-3 were treated with either LPS or mCRP with or without GW3965 for 6 hours before supernatant collection for multiplex analysis. Protein levels of MCP-1 were not significantly altered after the treatment of either LPS or mCRP with or without GW3965. A) MIP1, B) MIP-β and C) MCP-1. Data presented as Mean ± SEM - One-way anova (p = < 0.05 p **= <0.01, p*** = < 0.001, p**** <0.0001. (n=3)*

4.3.9 Inflammatory mediators LPS/mCRP significantly increase key anti-inflammatory cytokines levels with GW3965 agonist have no effect.

Figure 42A represents the anti-inflammatory protein expression levels of IL-4 after microglia cells were treated with either LPS or mCRP plus or minus agonist GW3965 (2.5 μM). After treatment with LPS there was an increase in IL-4 protein levels when compared to the control group CI 95% (-86.37 to 18.50) p = 0.0064. A similar increased effect was observed when cells were treated with mCRP compared to the control group CI 95% (-86.35 to 18.47) p = 0.0065. Microglia cells treated with inflammatory mediator mCRP + GW3965 (2.5 μM) did not decrease levels of IL-4 compared to cells treated with mCRP alone (CI 95% (-22.88 to 45.02) p = 0.7790). Microglia cells treated with inflammatory mediator LPS + GW3965 (2.5 μM) had no effect on reducing levels of the anti-inflammatory cytokine IL-4 with CI 95% (-24.17 to 43.70) p = 0.8472. Figure 42B is representing IL-9 protein levels after treatment of microglial cells (HMC-3) with either control, LPS 10 ng/ml and mCRP 100 μg/ml plus or minus GW3965 (2.5 μM). IL-9 levels in LPS (CI 95% -1073 to -398.5) p = 0.0011. HMC-3 cell treated with mCRP for 6 hours showed a significant increase in IL-9 levels compared to the control (CI 95% -934.8 to -257.6) p = 0.0033. Interestingly, when cells are treated with LPS in conjunction with GW3965 (2.5 μM), levels of IL-9 expressed into the collected supernatant are significantly reduced (CI 95% -195.7 to 872.9) p = 0.0058. This was also the case for cells treated with mCRP and GW3965 (CI 95% 76.93 to 754.1) p = 0.0200. Figure 42C represents IL-17 protein levels after microglial cells (HMC-3) were treated with LPS or mCRP for 6 hours plus or minus agonist GW3965 (2.5 μM). LPS treated cells increased expression levels of IL-17 compared to the control (CI 95% -1885 to -250.3) p = 0.0149. mCRP stimulated microglia cells increased levels of IL-17 compared to the control (CI 95% -1919 to -285.1) p = 0.0127 but agonist GW3965 (2.5 μM) in conjunction with LPS or mCRP did not decrease levels of IL-17 secreted into the supernatant.

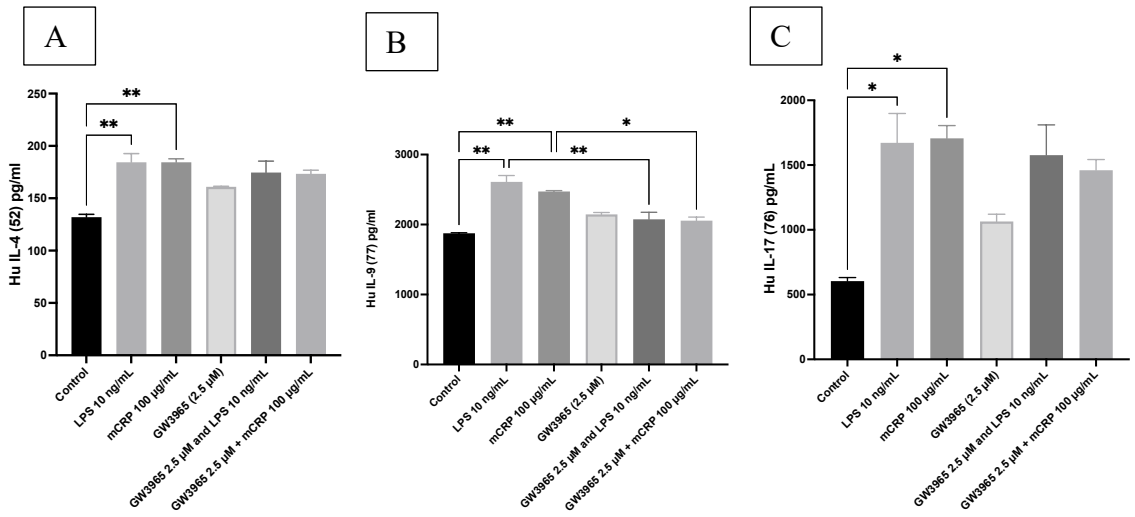

Figure 42 – LPS and mCRP pro inflammatory mediators increases key anti-inflammatory protein expression levels in microglia cells

Anti-inflammatory cytokine analysis through multiplex after microglia cells with stimulated with key pro-inflammatory mediators (LPS and mCRP) with or without anti-inflammatory therapeutic (GW3965 2.5 µm). A) IL-4 protein levels, B) IL-9 protein levels, C) IL-17 protein levels. Data presented as Mean± SEM - One-way anova (p = < 0.05 p **= <0.01, p*** = < 0.001, p**** <0.0001. (n=3)*

4.3.10 Inflammatory mediators have no effect on IL-1β, IL-6 and TNFα gene expression levels over time course.

Figure 43A presents the housekeeping gene stability in which it was determined that the housekeeping genes were stable and ideal for analysis. Three housekeeping genes were used during this analysis, and they were TBP, RPLPO and PABC4. Figure 43B, TNFα data presented showed no significant increase or decrease in TNFα gene expression levels when stimulated with inflammatory mediators mCRP and LPS nor was reduction observed after treatment with anti – inflammatory LXR agonist GW3965 (2.5 µM). As shown in figure 43C, levels of IL-6 were also measured after the stimulation of microglia cells with mCRP, and interestingly levels of IL-6 showed no change to the control compared to LPS which up regulation of IL-6 when compared to the control. Figure 43D, Interestingly, when observing gene expression levels of IL-1β, LPS and mCRP down regulated expression when compared to control levels. When mCRP stimulated microglia, cells were treated with GW3965, levels of IL-1β were seen to be up - regulated.

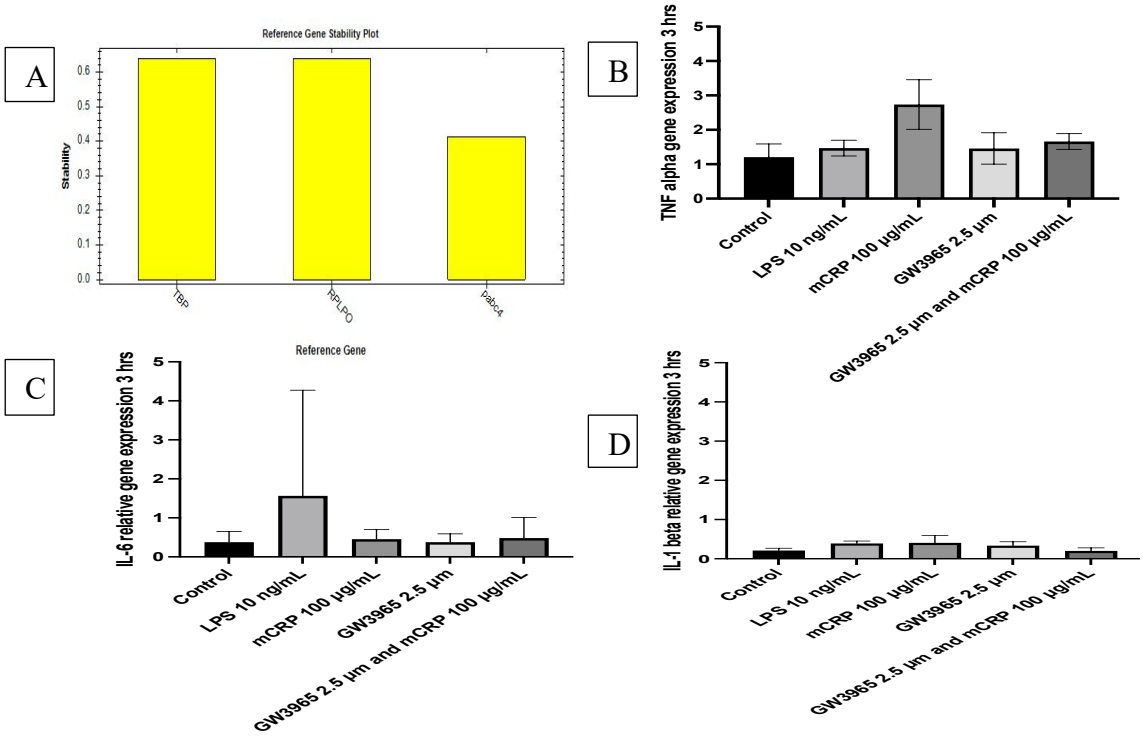

Figure 43 - Gene expression analysis of HMC-3 cells at 3 hrs.

A) Housekeeping gene expression stability was ideal, B) TNF alpha gene expression, IL-6 gene expression and C) IL-1 beta gene expression. Data presented as Mean ± SEM - One-way anova (p = < 0.05 p **= <0.01, p*** = < 0.001, p**** <0.0001. (n=3)*

Microglial cells which were stimulated for 6 hrs with LPS or mCRP inflammatory mediator plus or minus GW3965 were measured for several different pro-inflammatory cytokine expression levels. Figure 44A represents 3 selected housekeeping genes which were a stability test. Green indicates the housekeepers are stable and red not ideal unless in combination with more than one other ideal housekeeper. Figures 44B, C and D represent the statical analysis of gene expression (IL-1β, IL-6 and TNFα) which is present as relative gene expression. Figure B, IL-1β gene expression levels were measured at the 6 hrs mark after microglia cells were treated with LPS or mCRP plus or minus GW3965 (2.5 M). Interestingly, mCRP compared to the control showed downregulation in IL-1β expression (CI 95% -11.45 to 11.29) p = >0.9999 but not deemed significant. Whereas the agonist GW3965 increased levels of IL-1β compared to the control (CI 95% -27.64 to -4.900) p = 0.0058. Figure C, IL-6 gene expression levels were measured at the 6 hrs mark after microglia cells were treated with LPS or mCRP plus or minus GW3965 (2.5 μM). Interestingly, mCRP compared to the control showed no difference in IL-6 expression (CI 95% -1.648 to 1.623) p = >0.9999. GW3965 showed no increase nor decrease compared to the control (CI 95% -1.167 to -2.103) p = 0.8740. Figure D, TNFα gene expression levels were measured at the 6 hrs mark after microglia cells were treated with LPS or mCRP plus or minus GW3965 (2.5 μM). Interestingly, mCRP compared to the control showed a downregulation in TNFα expression (CI 95% -15.11 to 16.53) p = >0.9999. Whereas the agonist GW3965 increased levels of TNFα compared to the control (CI 95% -34.09 to -2.458) p = 0.0273.

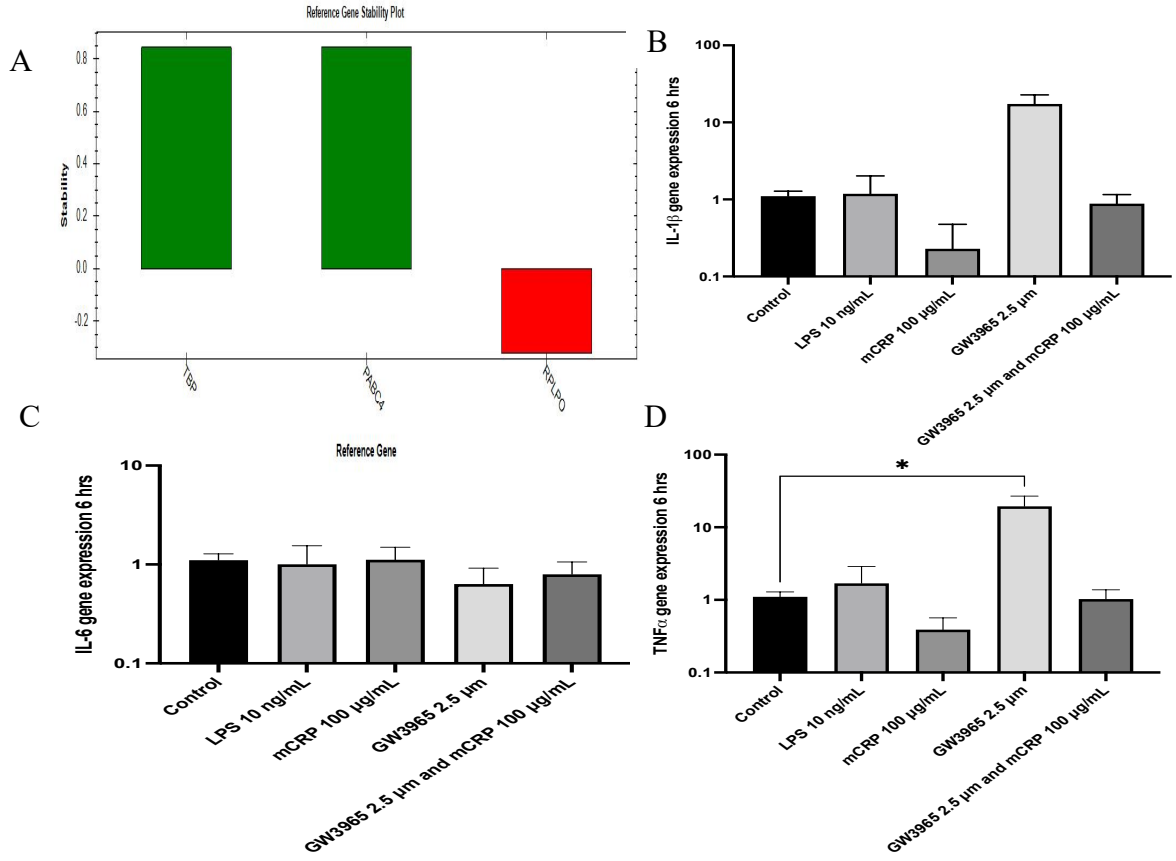

Figure 44 – Pro-inflammatory gene expression analysis after 6 hr treatment with inflammatory mediators and anti-inflammatory agonist.

HMC-3 cells were pre-treated for 6 hrs with and without GW3965 (2.5 μM) and then in conjunction stimulated with and with LPS or mCRP to induced a pro inflammatory response to observe therapeutic effect of GW3965. A Gene stability analysis of housekeeping genes (TBP, RPLPO and PABC4) in which they were deemed suitable. B, IL-1β gene expression levels, B, IL-6 gene expression analysis and D, TNFα gene expression. Data presented as Mean ± SEM - One-way anova (p = < 0.05 p **= <0.01, p*** = < 0.001, p**** <0.0001. (n=3)*

Microglial cells which were stimulated for 24 hrs with LPS or mCRP inflammatory mediator with and without the treatment of GW3965 were measured for several different pro-inflammatory cytokine expression levels. Figure 45A is a representation of the gene stability plot which measured the housekeeping gene stability in which they were established as stable (green). Figure 45B, represents TNFα gene expression and shows no significant up regulation or down-regulation in gene expression after the stimulation with either LPS (CI 95% -1.553 to 0.8462) p = 0.8629 or mCRP (CI 95% -1.463 to 0.9363) p = 0.9465 compared to the control group. Figure 45C represents the expression levels of IL-6. Interestingly the treatment with mCRP compared to the control showed no increase or decrease in expression levels (CI 95% -0.9528 to 0.9439) p = >0.9999. This was also the case when HMC-3 cells were treated with known inflammatory mediator LPS (CI 95% -0.9226 to 0.9741) p = >0.9999. Figure 45D represents the expression levels of IL-1β. Interestingly the treatment with mCRP compared to the control showed no increase or decrease in expression levels (CI 95% -0.8018 to 0.9102) p = 0.9995. This was also the case when HMC-3 cells were treated with known inflammatory mediator LPS (CI 95% -1.395 to 0.3167) p = 0.3015.

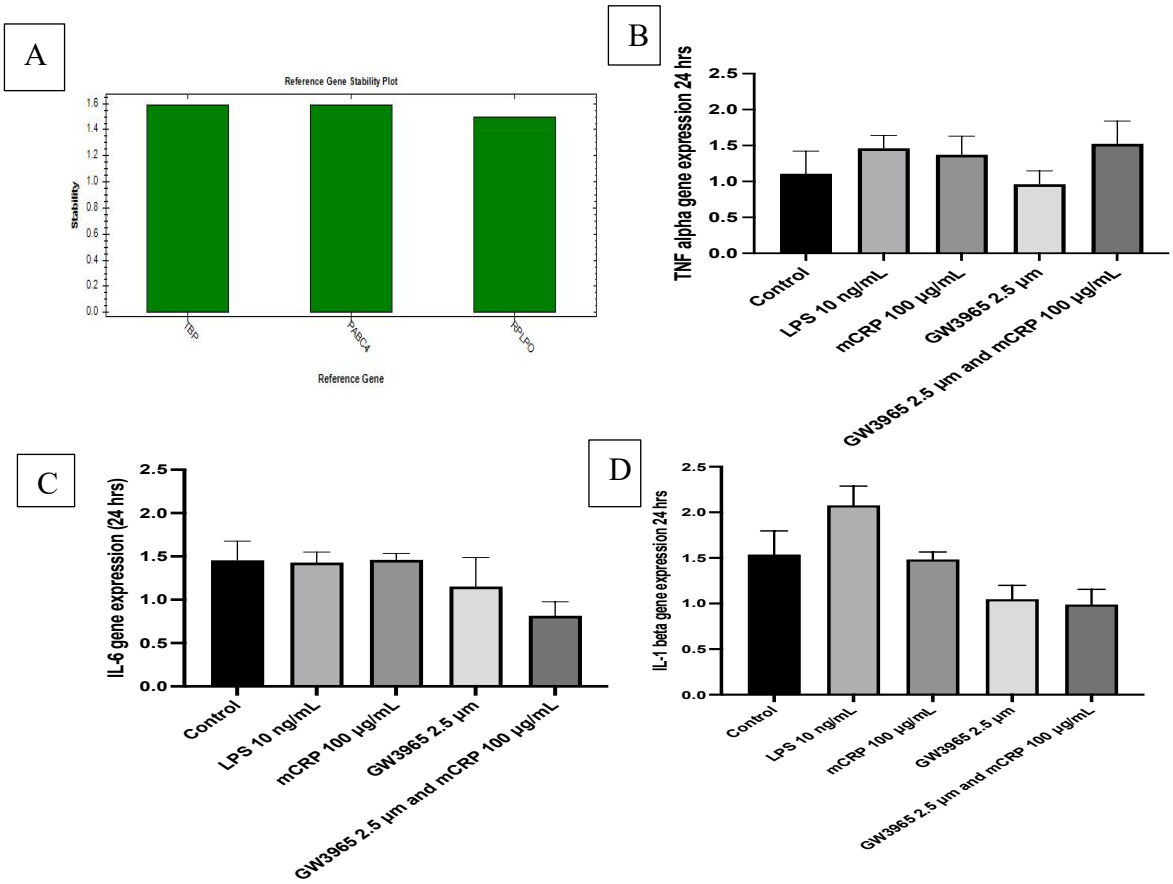

Figure 45 - gene expression analysis of HMC-3 microglial cells stimulated with LPS and mCRP for 24 hrs to induce an inflammatory in which to test GW3965 as a potential anti-inflammatory therapeutic target.

HMC-3 cells were pre-treated for 24 hrs with and without GW3965 and then in conjunction stimulated with and with LPS or mCRP to induce a pro-inflammatory response to observing therapeutic effect of GW3965. A) Gene stability analysis of housekeeping genes (TBP, RPLPO and PABC4) in which they were deemed suitable, B) TNFα gene expression levels, C, IL-6 gene expression analysis and D, IL-1β gene expression. Data presented as Mean ± SEM - One-way anova (p = < 0.05 p **= <0.01, p*** = < 0.001, p**** <0.0001. (n=3).*

4.4 Discussion

4.4.1 mCRP promotes morphological changes with resident microglia brain cells

mCRP has previously been identified as a pro-inflammatory with the ability to have negative effects. Firstly, it was important to establish how mCRP interacts with microglia cells which are the resident macrophage in the brain. Microglia cells have been shown to be constantly mobile even without inflammation and infection. When microglia cells become activated, the morphological changes and the bodies enlarge, become round and their synapses become shorter or disappear which enhance their phagocytic and migratory abilities (Yu et al., 2020).

The morphological and functional changes of microglia activated under different stimulations are not completely clear (Wu et al., 2018). As described in chapter 3, mCRP has morphological effects on U937 monocytes and human coronary artery cells. During this research, it was observed that mCRP causes morphological effects on microglia cells (HMC-3 cells) but also alters the way the cells migrate and halters the motility of the microglia cells. Interestingly, this effect was not seen when microglia cells were treated with nCRP. Scanning electron microscope observation of mCRP treated microglia cells showed membrane morphology and integrity changes, losing microvilli, budding, swelling, formation of apoptotic body, and total cell rupture. Motility and migration are important and microglia cells control this through filaments which form a structure known as lamellipodia and filopodia (Franco-Bocanegra et al., 2019). Holo monitor microscope system was used to observe and analysis the effects of CRP isoforms (mCRP and nCRP) on HMC-3 microglia cells. Microglia cells can change migration when stimulated by inflammation. It is well established that different receptors have different effects on the migration of microglia cells. For example, LPS has been seen to inhibited microglia migration. The mechanism remains elusive to how LPS can inhibited migration of microglia cells, but evidence does suggest it could be due to the down regulation of the purinergic receptor P2Y12. As previously described, migration is important as when microglia cells become activated, they move towards the injury site. In turn, this activation leads to a cascade of events in which inflammatory cytokines and chemokines are release causing more damage (Yu et al., 2020). Further to this, mCRP was also found to affect the motility and motility vs directness. Migration and motility go hand in hand with a significance important in the human

body and especially the resident brain cell which move towards sites of inflammation and important in neuroinflammation. It is vital to find the mechanism by which mCRP is inhibiting HMC-3 motility and migration as this could affect the way microglia cells to neuroinflammation after an ischemic event. In this case, mCRP is seen to accumulated after an ischemic event and the significant importance of microglia cells in ischemic injury.

4.4.2 mCRP causes pro-inflammatory cytokine to increase with GW3965 potentially acting as an inhibiting compound.

mCRP has been shown to have pro-inflammatory properties whereas nCRP does not. Not only is mCRP seen as an inflammatory mediator it is also bound to several different cell types including endothelial cells, neutrophils, and macrophages(Fujita et al., 2014). During this research, mCRP was used to induce an inflammatory response in HMC-3 microglia cells and had a similar stimulatory effect to LPS which is a well-known inflammatory mediator in inflammatory in vitro studies (Lively and Schlichter, 2018). mCRP was seen to significantly increase pro-inflammatory cytokines levels IL-6 over 6- and 24-hour periods. Further to this, levels of IL-1β were significantly increased over 6 hours but returned to normal after 24 hours. Interestingly, TNFα levels did increase and were in line with LPS, but the levels were not deemed significant when compared to the control. In the current research, mCRP is demonstrated to be a molecule that is critical to inflammation, plus the results display the damage on different cell types and causing aggregation formation it is vital to research the pro-inflammatory mechanisms and therapeutic target to reduce this response to aid in neuroinflammation treatment after ischemic events (Sproston and Ashworth, 2018; Sproston et al., 2018). In a previous study, levels of TNFα and IL-1β were seen to be induced in macrophages and glial cells by mCRP through induction of NO. This showcases the pro-inflammatory effect of mCRP and perpetuating damage (Al-Baradie et al., 2021). Through the stimulation of mCRP, it has also been shown that other pro-inflammatory markers are upregulated including IL-6, IL-8, and MCP-1 with the association through the NF-kB transcription factor (Zeinolabediny et al., 2021). Interestingly when MCP-1 cytokines levels were analysed, LPS caused a significant increase however mCRP did show an increase, but this was not significant in line with LPS. As levels were measured at the 6-hour mark as this period was important due to acute inflammation response, it could be that the peak of MCP-1 was not

observed in this period. This is a possibility as levels did increase but not significantly to the control. For example, a study showed that peak MCP-1 levels in mouse brain and serum were reached at the 6-hour mark after LPS stimulation (Thompson et al., 2008). However, it must be noted levels can be altered slightly depending on if tissue or fluid is measured. MCP-1 is a vital cytokine to research as IL-6 can induce this cytokine (Viedt et al., 2002). IL-6 can regulate CRP and with the dissociation to mCRP and the increased levels of IL-6, there is clear evidence a cascade of events occurs that interplay with each other in response to inflammatory events (Biswas et al., 1998; Arendt et al., 2002; Strecker et al., 2011). Other cytokines and chemokines which were seen to be increased during this research included RANTES and IL-9. RANTES is an important pro-inflammatory chemokine which at sites of inflammation recruit leukocytes (Hu et al., 1999). As seen in this work and previous work to date, we understand that mCRP mediated an inflammatory response and increased levels of several important cytokines. There is a need to find a potential therapeutic which can reduce such a response after an ischemic event to prevent the long-term damage caused by prolonged inflammation. As we understand currently inflammation is vital in repair but can also be negative. One such target of interest as an anti-inflammatory and potential ischemic stroke treatment is GW3965 LXR agonist. HMC-3 microglia cells' inflammatory response was induced by mCRP. HMC-3 cells were also then treated with and without GW3965 (2.5 μm) to determine if the agonist has the potential to block the pro-inflammatory cytokine increase. HMC-3 cells were pre-treated for 30 minutes before the inclusion of mCRP 100 μg/ml. Indeed, GW3965 was seen to be able to reduce several key pro-inflammatory cytokine and chemokine levels (IL-6, MCP-1, IL-1β, IL-9 and RANTES) in HMC-3 microglia cells. Another study displayed that GW3965 has neuroprotective properties which were associated with the NfKb p65 subunit and overall decreased hippocampal expression of COX-2 and NfKb target gene presenting that LXR receptor could protect neuronal damage after an ischemic event (Cheng et al., 2010). Interestingly, during the current research immunofluorescent staining was employed and cells were stained with both IL-6 and NfKb p65 to determine the potential mechanism which is at play. LPS was seen to increase Il-6 inflammatory cytokine levels, and this was also the case for mCRP but not significantly. GW3965 (2.5 μM) was used as a therapeutic to determine if this anti-inflammatory could reduce the response of IL-6 in LPS and mCRP-treated microglia cells. Levels were significantly reduced when samples were pre-treated with GW3965 and then with LPS inflammatory mediator.

However, this was not the case for mCRP treatment HMC-3 cells with therapeutic target GW3965. This body of research shows that IL-6 have a play in inflammation and that GW3965 is a promising anti-inflammatory therapeutic. Nunomura et al. (2015) showed when activation of LXRα is caused by the agonist GW3965 the production of key cytokines (IL-1α and IL-1β) are suppressed in wild-type LXRα (−/−) BM-derived mouse mast cells. This research indicated this may be mediated by LXRβ. This finding indicates that IL-1α may cooperate with IL-1β to regulate interleukin networks (Nunomura et al., 2015).

4.4.3 mCRP does not alter gene expression is several markers at selected time points.

Some interesting results were presented when mCRP-stimulated microglia cells were analyzed for gene expression after protein levels were seen to be significantly upregulated. The control was set to establish a baseline for each gene of interest which were IL-1β, IL-6, and TNFα which are major players in neuroinflammation and ischemic stroke (Pawluk et al., 2020). LPS, which was used as the positive control was seen to upregulate IL-1β levels at the 3-hour mark, but no change was presented in the other cytokines and other time points of 6 and 24 hours. mCRP which is seen as a pro-inflammatory mediator down regulated gene expression of IL-1β levels at the 3-hour mark, but no change was noted in either IL-6 or TNFα at the 3-hour mark, or subsequently 6- and 24-hour time points. GW365 LXR agonist causes upregulation in gene expression of Il-1β at 3 hrs, IL-1β and TNFα at the 6-hour mark. LPS is a known inflammatory mediator which has been shown to cause a marked increase in the expression of several cytokines. For example, a study observed gene expression of levels of IL-6, −8, TNFα, MMP-9 and TIMP-1 after human airway epithelial cells were stimulated with LPS. They found that all these cytokines were significantly activated through the signaling pathways NF-κB, STAT3 or AP-1 (X. Liu et al., 2018). It must be noted that this study used different cells from the work presented above which used microglia cells. A study performed on microglia cells showed that LPS does indeed cause a marked increase in levels of IL-1β, IL-6, and TNFα in a dose-dependent manner (Minogue et al., 2012). Interestingly, during gene expression analysis in this work marked increase was only found in IL-1β and not any other cytokine as well as another time point. This can then lead to questioning what is happening. It would be increasing in significance to obverse a greater time point as the switching on of the genes and the peak levels could be missed. From the protein levels, we understand that there are increasing levels of several pro-

inflammatory cytokines caused by the stimulation of positive control LPS and mCRP which is also presented in the literature. As we are aware, mRNA plays a pivotal role in determining the protein amount (Y. Liu et al., 2016). This is important to note as we understand protein levels are increasing but mRNA was not seen to be upregulated by either mCRP or LPS.

Chapter 5 - Determine the potential anti – inflammatory potential of Adipose derided MSCs.

In this chapter, some data has been pre – published in Guo, B.; Sawkulycz, X.; Heidari, N.; Rogers, R.; Liu, D.; Slevin, M. Characterisation of Novel Angiogenic and Potent Anti-Inflammatory Effects of Micro-Fragmented Adipose Tissue. Int. J. Mol. Sci. 2021, 22, 3271. https://doi.org/10.3390/ijms22063271.

More work has been generated since publication which is outlined in chapter 5 of this PhD. Copy of the front page is in Appendix of the paper.

5.1 Introduction

5.1.1 Anti-inflammatory benefits of MSCs derived from micro-fragmented adipose tissue.

MSCs are multipotent and self-renew with the ability to repair damaged tissue. MSCs have anti-inflammatory properties and are immunomodulated, therefore making them potential candidates for cell-based therapies (Salari et al., 2020). MSCs can protect against cerebral ischemic injury by preventing neuronal damage via the inhibition of apoptosis (Y. Zhang et al., 2020). After the event of cell or tissue injury, MSCs can become activated by inflammatory cytokines and once activated they locate to sites of damage and induce tissue-regeneration. MSCs secrete numerous immune factors including IL-10, fibroblast FGF, vascular endothelial growth factors (VEGF), platelet-derived growth factor (PDGF), hepatocyte growth factor (HGF), TGF-β, and Insulin like Growth Factor 1 (IGF-1), and though much research has been conducted on these cells, the mechanisms by which MSCs are recruited and activated is still unclear (Salari et al., 2020). Fat tissue can be a major source of MSCs within the body, and therefore is of great interest especially as they also produce numerous immune and cell protective factors such as specific anti-inflammatory and immunosuppressive cytokines in addition to growth factors including iNOS, TGF-β and TSG 6 as examples. Other principal factors include extracellular vesicles that are important as they have been seen to have the ability to retain anti-inflammatory properties and therefore are also a target for research for cell-based therapist (Nava et al., 2019).

5.1.2 Current use of adipose-derived mesenchymal stem cell in a clinical setting

Fat tissue has several capabilities and a variety of physiological functions. Micro-fragmented adipose tissue (MFAT) has already been used in clinical setting with documentation of being a success. Some of the conditions which have benefited from the use of MFAT include osteoarthritis, post-menopausal vaginal atrophy, the repair of perianal fistulae and diabetic foot (Giordano et al., 2014; Cattaneo et al., 2018; Laureti et al., 2020). Several clinical trials have tested the role adipose-derived stem cells as a potential therapeutic and regenerative therapy in several different disease. Table 18 shows a breakdown of the current clinical trials using adipose derived stem cells which is broken into categories of disease to show the important of

research in this potential therapeutic. For example, adipose-derived stem cells have been used in clinical setting in patients with knee problems like osteoarthritis with promising recovery rates or reduced pain. A 2-year follow up study demonstrated that quality of life improved and functionally in elderly patient with knee osteoarthritis OA at grade between 2 and 4 (Gobbi et al., 2021).

Table 15 – The use of adipose derived stem cell in clinical trials.

NCT01649700	Completed	Treatment of Sequelae Caused by Severe Brain Injury with Autologous Adipose-derived Mesenchymal Stem Cells	Brain Injury	The efficacy and safety of autologous transplantation of ADMSC observed
NCT04063215	Active, not recruiting	A Clinical Trial to Determine the Safety and Efficacy of Hope Biosciences Autologous Mesenchymal Stem Cell Therapy for the Treatment of Traumatic Brain Injury and Hypoxic-Ischemic Encephalopathy	Traumatic brain injury	Biological: HB-adMSC
NCT04744051	Recruiting	ATCell™ Expanded Autologous, Adipose-Derived Mesenchymal Stem Cells Deployed Via Intravenous Infusion	Post-concussion syndrome	Drug delivery of 50, 150, 300 ADSC Infusion were given and Placebo Infusion

NCT04280003	Recruiting	Allogeneic Adipose Tissue-derived Mesenchymal Stem Cells in Ischemic Stroke	Allogeneic Adipose Tissue-derived Mesenchymal Stem Cells in Ischemic Stroke	Other: Alogenic adipose tissue-derived stem cells Drug: Placebo solution
NCT01678534	Completed	Reparative Therapy in Acute Ischemic Stroke with Allogenic Mesenchymal Stem Cells from Adipose Tissue, Safety Assessment, a Randomised, Double-Blind Placebo Controlled Single Center Pilot Clinical Trial (AMASCIS-01)	Ischemic stroke	Drug: Allogenic mesenchymal stem cells from adipose tissue Drug: Placebo
NCT02813512	Completed	Clinical Trial Study About Human Adipose-Derived Stem Cells in the Stroke	Stroke	Drug: ADSCs

Activate or completed looking at potential in traumatic brain injury and ischemic stroke. Information was obtained from the clinical trials website https://www.clinicaltrials.gov/

5.2 Aims and objectives.

To investigate the properties of MFAT as a potential anti-inflammatory therapeutic using in vitro based models and functional assays

1. Fully characterise and compare MFAT from 10 individual donors obtained from liposuction and processed by lipogems international spa processing device.
2. Elucidate the Inflammatory, chemokine and cytokine expression of MFAT cultured medium for the potential therapeutic use.
3. Observe the effects of MFAT cultured medium using LPS to induce inflammation in an in vitro model using U937 differentiated monocytes to macrophages.

5.3 Results

5.3.1 Characterisation of key cytokine, chemokine, and growth factor secretion from MFAT samples

Multiplex analysis was conducted to observe MFAT secretion of key markers of inflammation, regenerative responses, and anti-bacterial and vasculogenesis markers. This data was presented in a heat map overview with purple showing the least amount of secretion and yellow indicating elevated levels of different molecules secretions as seen in (Figure 46A). Most interestingly, there was a notable production of the IL-1Rα antagonist with a significant increase between 24 hrs and 5-day culturing in serum-free MEMα as seen in figure 45B 24 hours 1960 ± 723 (95% CI 292.6 – 3627) vs day 5 20969 ± 10776 (95% CI -3880 – 45817) p = 0.0039). Significant production of MIG (CXCL9) protein was produced with increasing levels between 24 hrs and 5-day culturing in serum-free MEMα as shown in figure 46 C (p = 0.0039). 24 hours 1844 ± 661.4 (95% CI 318.8 – 3369) vs day 5 4423 ± 755.7 (95% CI -2681– 6166) p = 0.0039). In Figure 45D, a slightly different profile for a hepatocyte-derived growth factor (HGF) was found with notable quantities of HGF produced even after 24 hrs and maintenance of secretion over 5 days. 24 hours 1635 ± 572.1 (95% CI 315.8 – 2954) vs day 5 1261 ± 299.7 (95% CI 569.6 – 1952) p = 0.6523.

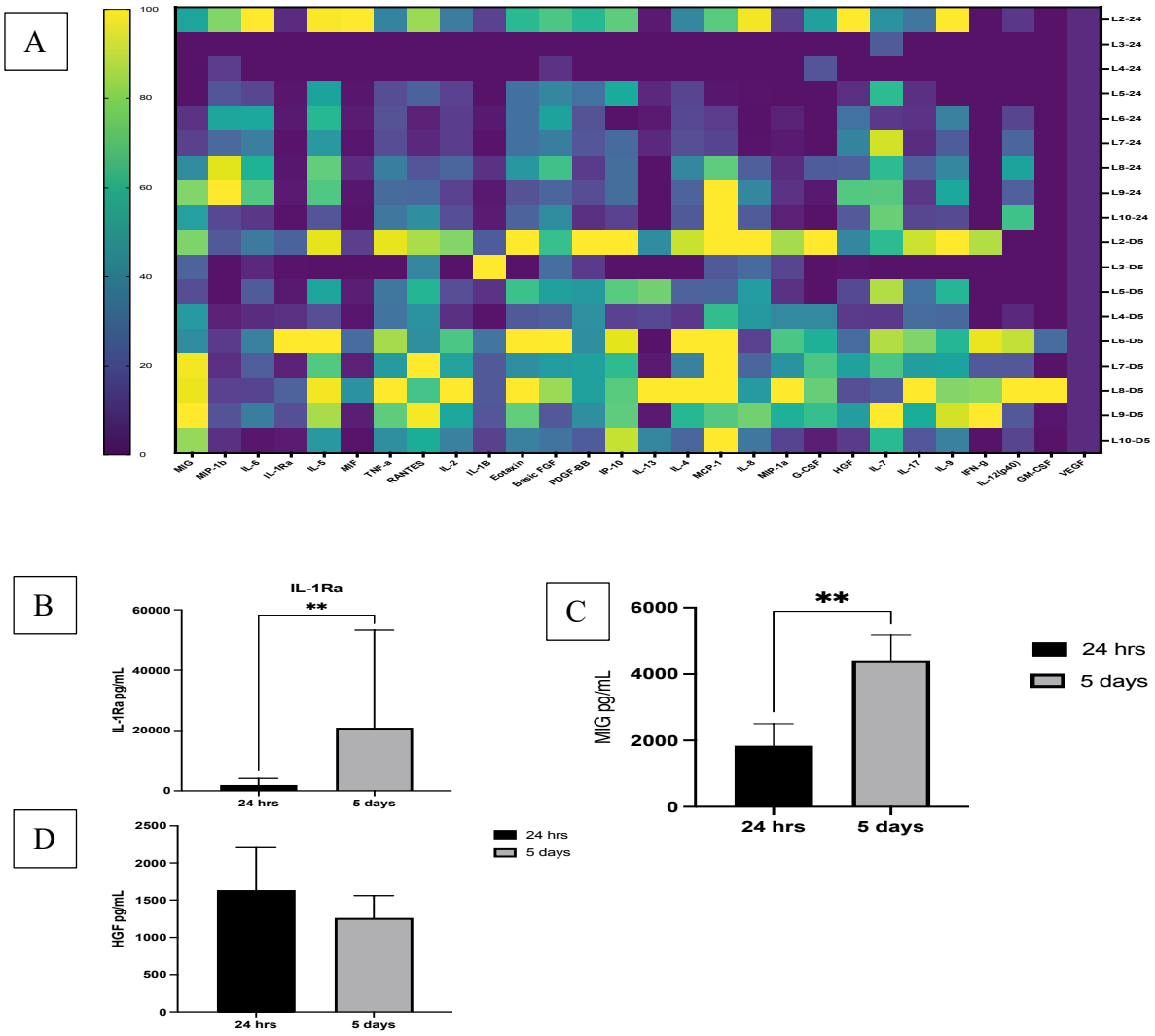

Figure 46 - Cytokines and growth factors in the MFAT condition medium in a serum free culture for 24hrs and 5 days.

24 hours and five days MFAT condition medium were measure for expression of cytokine, chemokine, and growth factors. A), Heat map of 32 factors. (B); IL-1Ra was significantly increased between 24 hours and 5-day MFAT culture medium (p= 0.0039). (C); There was a significant increase in MIG between one day and five-day culturing in serum free MEMα (p = 0.0039). (D); The expression of HGF was found but this remained stable between 24 hours and 5-day culturing (p = 0.6523). Data presented figure presented as Mean± SEM (CI 95%) and a Wilcoxon test performed (p = < 0.05 and p **= <0.01, (n=10)*

TGFβ1 and β3 were produced and secreted into the medium by MFAT and levels significantly increased over the five-day period. TGFβ1 protein levels were measured at 24 hours (57.80 ± 24.28) and day 5 (567.7 ± 158.8). Protein levels increased significantly at day 5 compared to 24 hours (CI 72.80 to 965.0, p = 0.0320) as displayed in figure 47A. TGFβ3 protein levels were also measured at the 24 hours (8.535 ± 1.904) and 5-day mark (24.96 ± 4.279). MFAT-conditioned media secretion levels of TGFβ3 were significantly increased at day 5 compared to 24 hrs (CI 95% 6.585 to 26.27, p = 0.0025) as displayed in figure 47B.

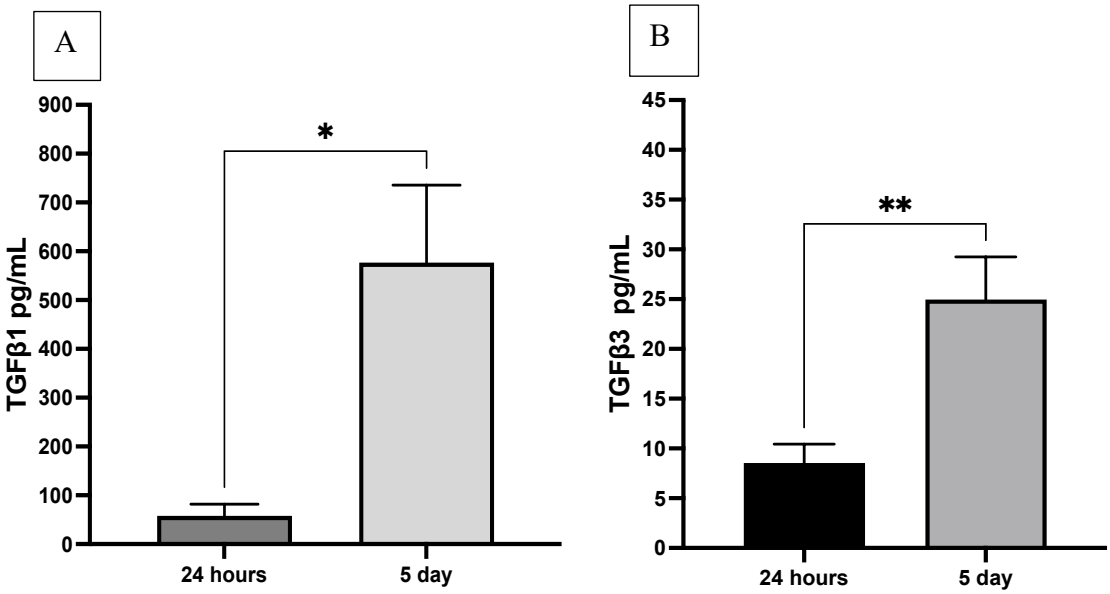

Figure 47 – MFAT secretion levels of TGFβ1-3 secretion

Levels of TGFβ1 and β3 protein secretion in MFAT conditioned media at 24 hrs and day 5 was measured ELISA. A) TGFβ 1 protein levels were significant increased at day 5 (p=0.0320) (n3). B) TGFβ3 secretion significantly increased at day 5 (p=0.0025) (n10). Unpaired T test with data presented as Mean ± SEM (p = < 0.05 p **= <0.01)*

Protein levels of several different cytokines and chemokines were significantly increased in an MFAT-conditioned medium in a serum-free culture. IL-1β levels were measured in the conditioned media at 24 hrs (2.614 ± 1.037) compared to 5 days (18.16 ± 6.655) with CI 95% (-19-23 to – 5.649) p = 0.0039. IL-6 secreted levels at 24 hrs (2925 ± 902.7) were higher compared to levels at day 5 (1480 ± 333.8) but were not deemed significant with CI 95% (-437.3 to 3568) p=0.0742. TNFα levels were significantly different between 24 hours (307.3 ± 69.26) and day 5 conditioned media (852.2 ± 171.9) with CI 95% (146.6 to 997.7) p = 0.0078. MIP-1 beta protein levels were significantly different between 24 hours and 5 days (p=0.0078). IL-4 protein levels were significantly increased from 24 hours and 5 days (p=0.0156).

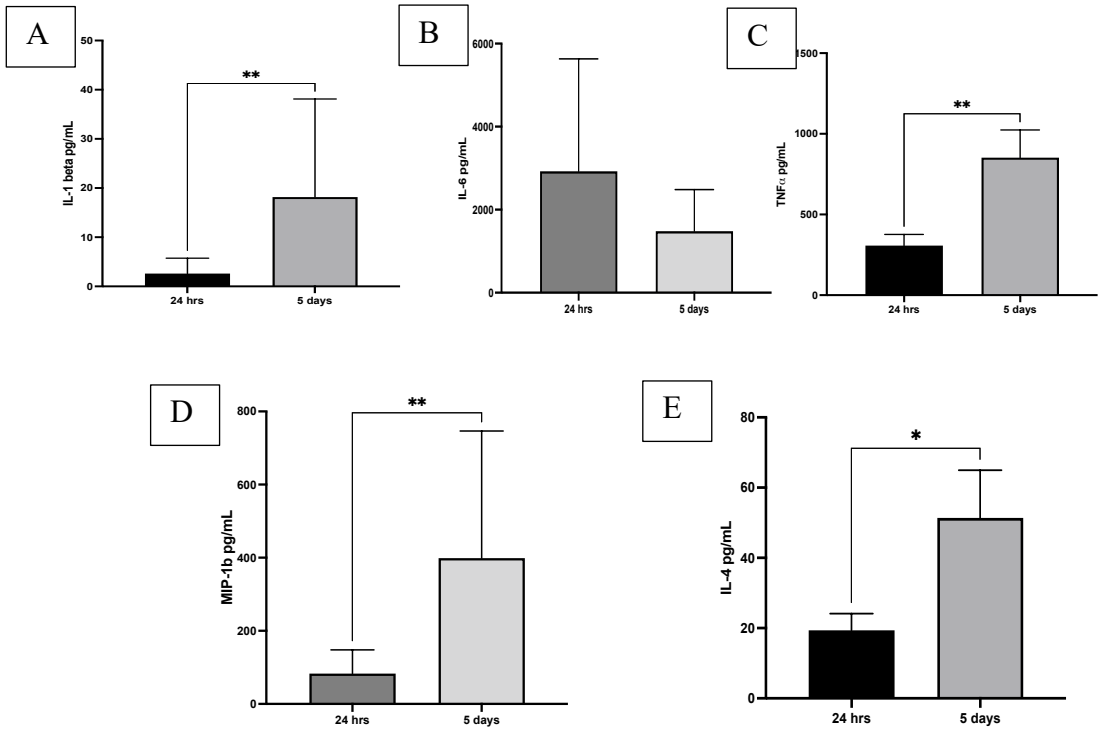

Figure 48 - Observation of 24 hour and day 5 culture MFAT media for secretion of several important cytokines and growth factors in culture media for one day and five days.

*A, B, C and D) There was a significant increase in TNFα IL-1β, IL-4 and MIP-1b between one day and five-day culturing in serum free MEMα (p < 0.05 *). E) IL-6 levels were not significantly different, but levels did drop by day 5. Wilcoxon matched – pairs signed rank test (n9)*

5.3.2 Differentiation of monocytes into M0 macrophage

Monocytes were transformed into macrophages using Phorbol 12-myristate 13-acetate (PMA) at a concentration of 50 ng/mL for 24 hours. Figure 49A represents monocytes which present as round floating cells in suspension. Figure 49B represents monocytes transformed into adherent macrophages and characterised by increased adhesion and formation of clumps.

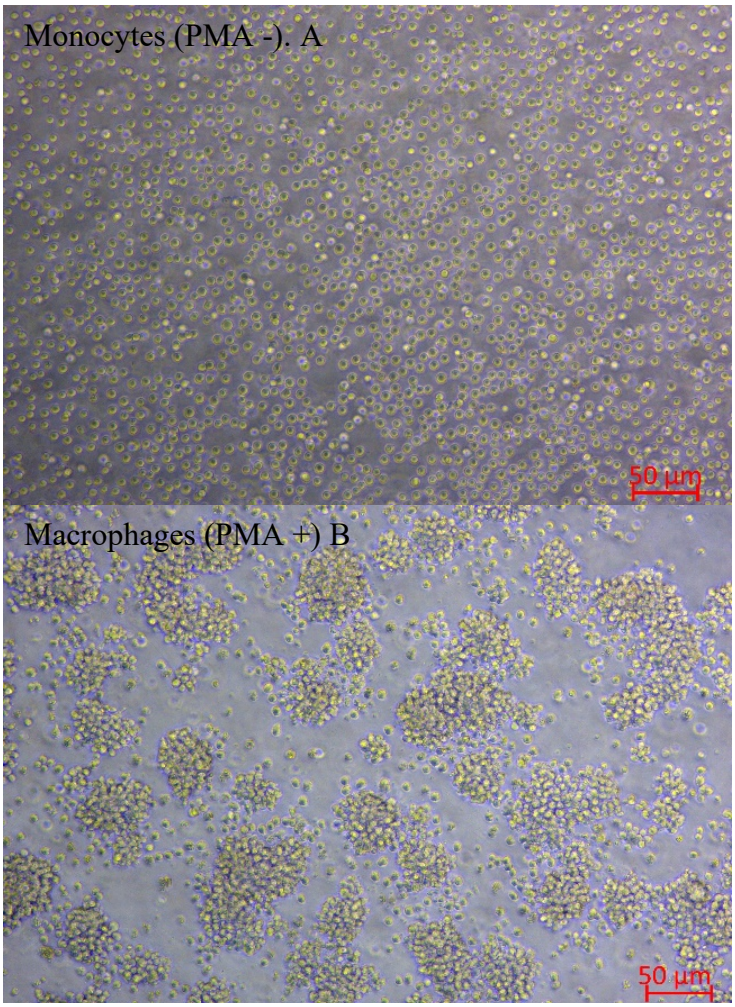

Figure 49 - Morphology of U937 cells before and after treatment with PMA at 50 ng/mL for 72 hours to differentiated monocytes to macrophages.

A) Cell appears to be rounded in shape and remain in suspension (floating). B) Cell have become adherent with the formation of clusters and cell presenting with ruffled membrane. Images taken using an axiovert 40C inverted phase contrast microscope at 4 x magnification.

The conversion of U937 monocytes into a distinct population of macrophages was confirmed via the detection of the FITC-conjugated anti-human CD11c surface marker (Rios de la Rosa et al., 2017) by flow cytometry figure 50. Untreated control U937 monocytes lacked the CD11c surface marker (17.52%) as well as stained monocytes (16.35). Whereas U937 PMA differentiated macrophages were 90.22% positively stained for CD11c+. Figure 50E shows an overlap in the 4 different conditions and differentiated macrophages (red) clearly show positive staining with a shift to the right. Green, yellow, and blue in the histogram represent control and present with no staining for CD11c. The red peak is presenting macrophages which have successfully been through PMA treatment and present with positive staining.

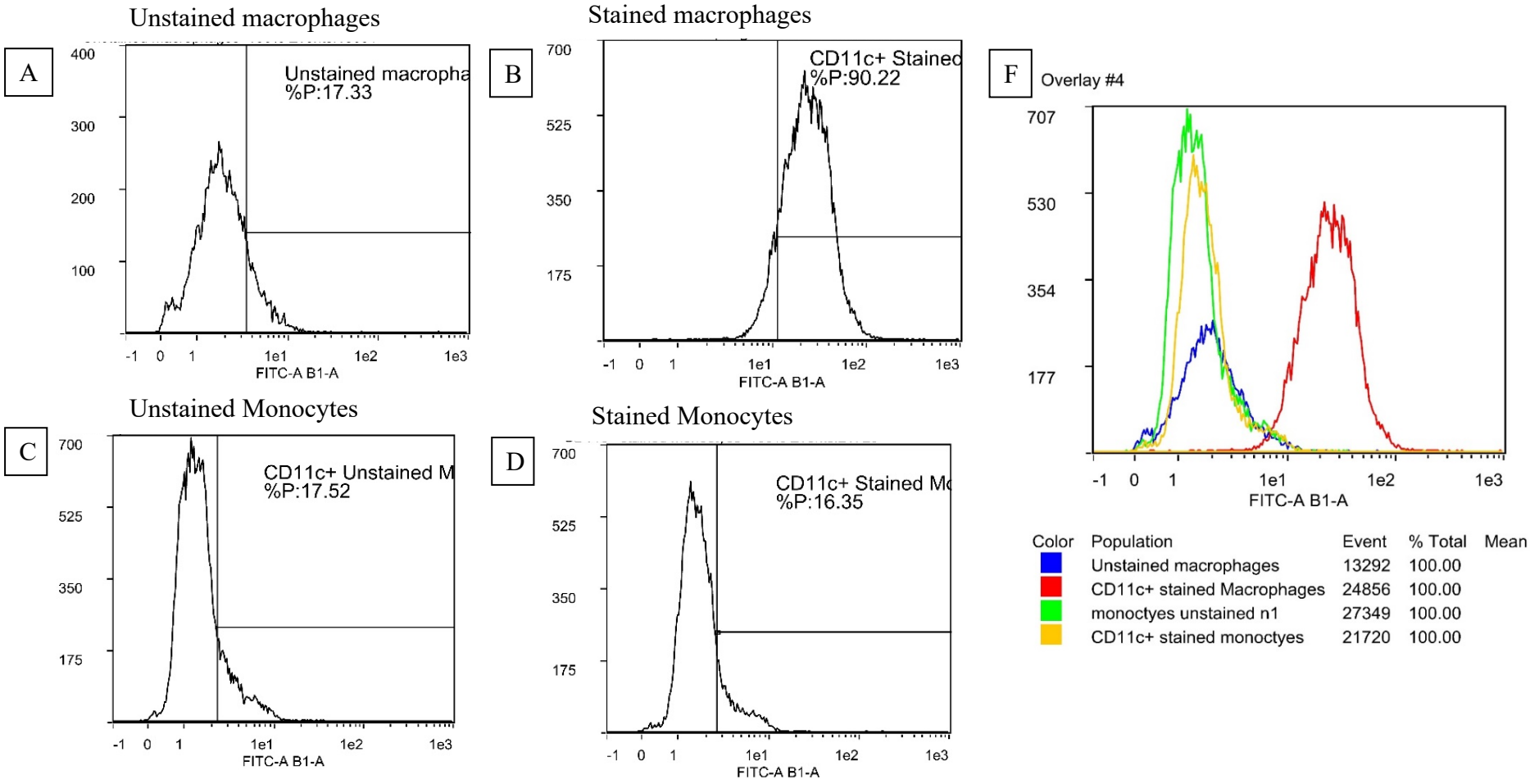

Figure 50 - Flow cytometry confirming U937 monocytes differentiation into M0 macrophages

CD11c surface mark was used to confirm the differentiation from monocytes to macrophages by flow cytometry. A) Unstained macrophages (- for CD11c, B, Stained Macrophage (+ for CD11c), C) Unstained monocytes (- for CD11c, D) stained monocytes (- for CD11c) and E, overlay of all condition to easy represent the shift in stained macrophages which is indicated by the red line. (n=3)

5.3.3 The Effects of the MFAT Conditioned Medium on the LPS-Stimulated Macrophage Expression of Pro-Inflammatory Cytokines

IL-1β protein levels were measured in the supernatant collected after U937 differentiated macrophages were stimulated with 10 ng/ml of LPS for 6 hours with and without MFAT-conditioned media (1/10). Figure 51A, IL-1β protein levels were significantly increased compared to the control baseline after treatment with the known inflammatory mediator LPS CI 95% (-35.26 to -14.38) p = <0.0001. LPS (10 ng/ml) treatment with MFAT conditioned media (1/10) showed a reduction in IL-1β protein levels compared to LPS treated samples CI 95% 15.36 to 36.23) p = (0.0001). Levels of IL-6 protein were significantly increased compared to the control baseline after stimulation with LPS inflammatory mediator CI 95% (-6166 to -4740) (p = <0.0001). LPS treatment with MFAT-conditioned media showed a reduction in IL-6 protein levels compared to LPS-treated samples CI 95% (4507 to 5933) p = 0.0001 (p=0.0001). Further observation shows levels nearing baseline.

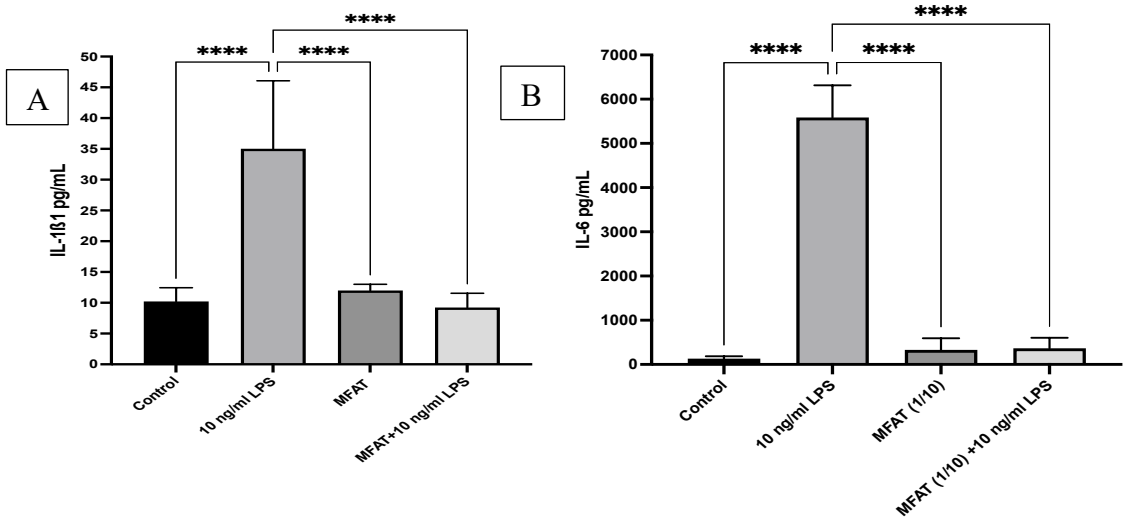

Figure 51 - MFAT condition medium attenuated LPS (10 ng/mL) mediated cytokines secretion of IL-1ß and IL-6

*(**A**)IL-1β protein expression levels; (**B**); IL-6 expression. 6-hour incubation of 10 ng/ml LPS with and without MFAT (1/10), samples tested from the day five conditioned medium of MFAT cultures by an ELISA. Data presented as Mean ± SEM - One-way anova (p**** <0.0001. (n=5)*

5.3.4 The Effects of the MFAT Conditioned Medium on the LPS-Stimulated Macrophage gene expression.

Figure 52 is a reference gene stability plot in which RPLPO and PABCP4 were deemed to be ideal as housekeeping gene for analysis of this gene expression analysis.

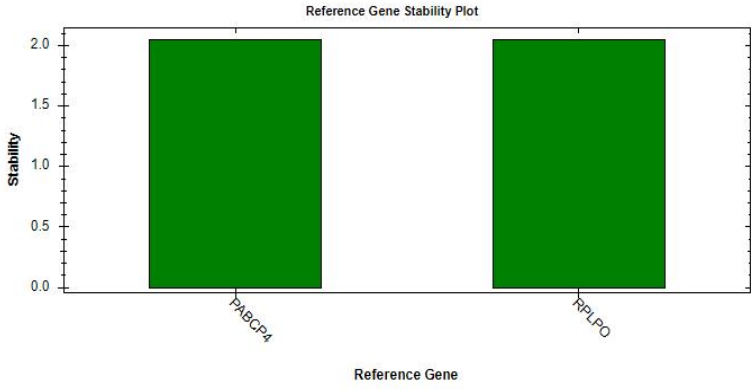

Figure 52 – Housekeeping gene stability plot for PABC4 and RPLPO

Figure 53A presents the IL-1β gene expression analysis in which the 6-hour treated LPS (10 ng/ml) simulated samples (0.04516 ± 0.007) caused a significant increase in IL-1β expression levels when comparing the control baseline group 2.328 ± 0.3634 with a CI 95% -3.106 to -1.459 (p = <0.0001). LPS 10 ng/ml in combination with MFAT conditioned media (0.06576 ± 0.009) significantly decreased levels of IL-1β expression when compared to LPS treated samples (2.328 ± 0.3634) with a CI 95% 1.438 to 3.085 (p = 0.0001). Figure 53B, presents the IL-6 gene expression analysis in which the 6-hour treated LPS (10 ng/ml) stimulated samples (0.01452 ± 0.003) caused a significant increase in IL-6 gene expression levels compared to the control baseline group (2.328 ± 0.2901) with a CI 95% -2.970 to -1.656 (p = <0.0001). LPS 10 ng/ml in combination with MFAT conditioned media (0.013 ± 0.0035) significantly decreased levels of IL-6 expression when compared to LPS treated samples (2.328 ± 0.2901) with a CI 95% 1.657 to 2.971 (p = 0.0001). Figure 53C presents a TNFα gene expression analysis in which the 6-hour treated LPS (10 ng/ml) stimulated samples (2.328 ± 0.2978) caused a significant increase in TNF gene expression levels compared to the control baseline group (0.1118 ± 0.007) with a CI 95% -2.892 to -1.540 (p = <0.0001). LPS 10 ng/ml in combination with MFAT conditioned media (0.1640 ± 0.082) significantly decreased levels of IL-6 expression when compared to LPS treated samples (2.328 ± 0.2978) with a CI 95% 1.488 to 2.9840 (p =<0.0001). Figure 53E presents IL-10 gene expression analysis in which the 6-hour treated LPS (10 ng/ml) stimulated samples

(1.760 ± 0.1678) caused a significant increase in gene expression levels compared to the control baseline group (1.000 ± 0.036) with a CI 95% -1.285 to -0.2347 (p = <0.0073). LPS 10 ng/ml in combination with MFAT conditioned media (0.9570 ± 0.1374) significantly decreased levels of IL-10 expression when compared to LPS treated samples (1.760 ± 0.1678) with a CI 95% 0.2777 to 1.328 (p =<0.0053).

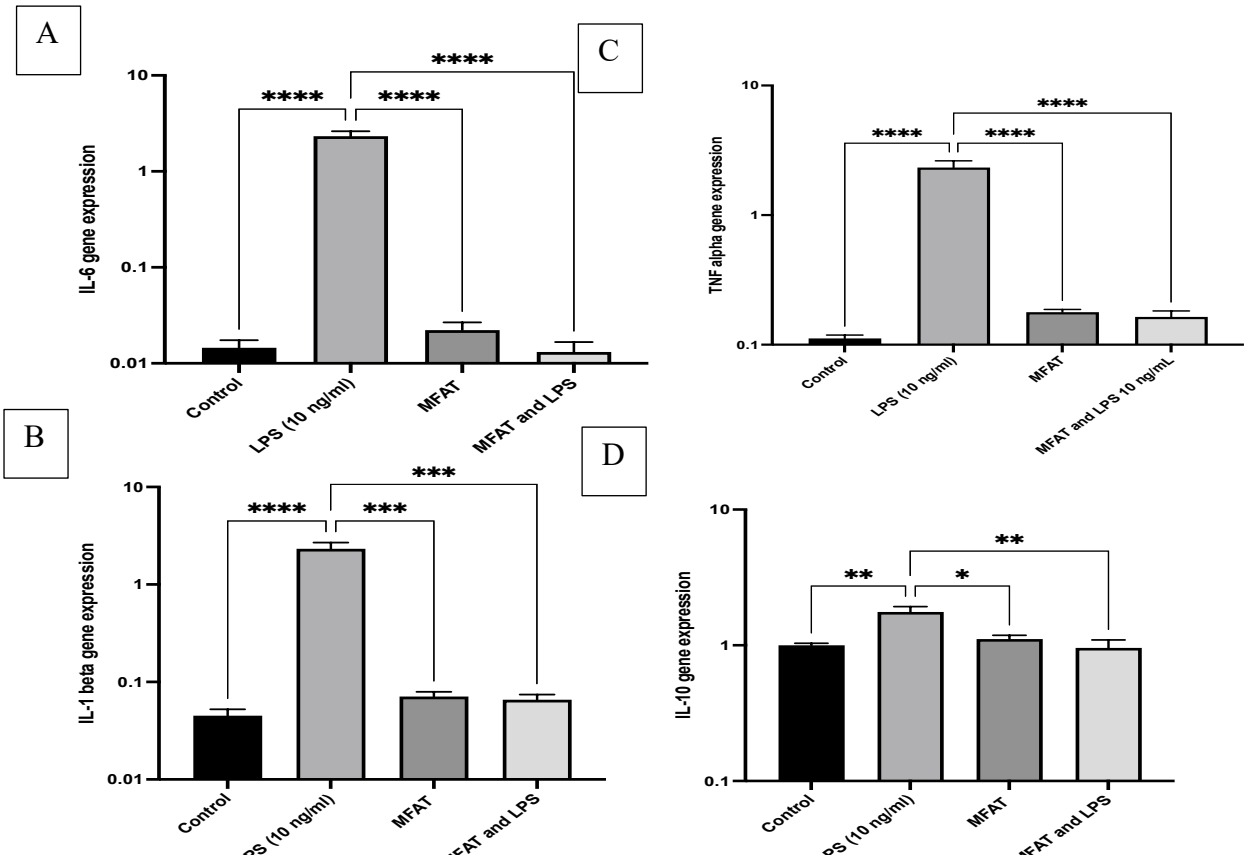

Figure 54 – MFAT conditioned media attenuates the upregulation of key-pro-inflammatory cytokines after LPS treatment.

(A)Reference gene housekeeper stability plot, B) IL-6 gene expression, C) TNFα gene expression, D) IL-1β gene expression and E) IL-10 gene expression, Data presented as Mean ± SEM - (p = < 0.05 p **= <0.01, p*** = < 0.001, p**** <0.0001. (n=5)*

5.4 Discussion

5.4.1 Characterisation of Cytokine Secretion from MFAT Samples

Cytokines and growth factors are present in the conditioned medium from MFAT cultures (in a serum free culture after one day and five days). Several key markers of inflammation, regeneration, anti-bacterial and vasculogenesis were looked at. IL-1Ra levels were increased in 5-day cultured MFAT conditioned media. IL-1Ra has immunosuppressive benefits as well as potential to reduce the inflammatory effects of IL-1, via stopping the binding of either IL-1α or IL-1β (Dinarello et al., 2012). There was also an increase in IL-1β levels from the 24-hour mark to the five-day mark. Interestingly, when looking at a previous study which indicates derived from macrophages could stimulate MSCs to secrete IL-1ra (Lu et al., 2021), there was a significant production of MIG protein (CXCL-9) in MFAT conditioned media which increased between 24 hours and day 5. This chemokine plays an essential role in the induction of chemotaxes to promote differentiation of leukocytes (Venetz et al., 2010). This protein also has anti-microbial benefits and is involved in immunoregulatory and inflammatory process. The antimicrobial benefits of this protein can help to protect against infection during or after treatments. CXCL- 9 has an extremely significant role in the regulation of cell recruitment to the sites of inflammation (Koper et al., 2018). Hepatocyte derived growth factor (HGF) was found with notable quantities of HGF produced even after 24 h and a maintenance of secretion over five days. HGF is secreted by MSCs, which plays an important role in MSC therapy. HGF has several different properties which include anti-apoptotic, immune regulation activities, which can prevent apoptosis inflammation and promote angiogenesis (Meng et al., 2022). There was production of TGFβ1 and β3 in MFAT conditioned media with levels significantly increasing between 24 hrs and 5 days. TGFβ1 and β3 are known to coordinate wound healing, control immune cell function, regulate differentiation, and cell growth in both epithelial and endothelial cells and finally maintain extracellular matrix (Kubiczkova et al., 2012). IL-4 was present in the conditioned media of the MFAT samples, levels significantly increased from 24 hrs to 5 days. IL-4 is an important cytokine in the CNS in which it provides neuroprotection and regeneration following an injury by inducing microglia and macrophages to a regenerative phenotype (Daines et al., 2021)

5.4.2 The Effects of the MFAT Conditioned Medium on the LPS-Stimulated Macrophage Expression of Pro-Inflammatory Cytokines

First, an in vitro inflammatory cell model was established with U937 differentiated macrophages. PMA treatment successfully induced the differentiation of U937 monocytes into M0 macrophages as seen in figure 48 and 49. The differentiation was confirmed by the expression of the CD11c surface marker which are expressed by macrophages and with monocytes lacking the marker.

An LPS in vitro model was used to test the anti-inflammatory properties of MFAT conditioned media. MFAT conditioned media was successfully able to reduce IL-1β and IL-6 protein levels which were significantly increased after U937 differentiated macrophages were treated with LPS. As previously described, MFAT has several different benefits and one include the secretion of many different cytokines and chemokines (B. Guo et al., 2021). As from the results, anti-inflammatory cytokines are released from the conditioned media. From the literature, it is known that pro-inflammatory cytokines, IL-1, IL-6 and TNF α can be inhibited by the anti-inflammatory cytokine like IL-4 and IL-10 in part via the transcriptional repression (Achsah D Keegan, 2014; Anovazzi et al., 2017). Gene expression levels were seen to be significantly upregulated after the treatment of LPS, which is a similar response in other studies that use LPS as a mediator (Suzuki et al., 2000). MFAT was able to significantly reduce levels of gene expression in several pro inflammatory cytokines. MFAT has been seen to reduce gene expression levels (Zhou et al., 2020). A study found that adipose derived cells were able to produce IL-6 in turn promoting osteogenesis (Huh and Lee, 2013). Another found that adipose derived stem cell can down regulate gene expression of CCL19, CCL5, TNFSF15 and IL-1β (Taha et al., 2020). MFAT is a promising tool for degeneration and has the potential to act as an inflammatory inhibitor which has been seen to down regulate important pro inflammatory cytokines and chemokines which were observed in this study.

Chapter 6 Conclusions and future work

6.1 Conclusion

It is well established that neuroinflammation has a significant role to play in ischemic stroke. Neuroinflammation has a positive role after an ischemic event to induce the healing process. However, inflammation is also detrimental and can cause long-term inflammation which subsequently causes further damage to the brain. Pro-inflammatory cytokines such as IL-6, TNFα and IL-1β play a role in neuroinflammation after the ischemic event. During this project, several different experiments were employed to elucidate the inflammatory role mCRP plays and the effects upon U937 monocytes or U937 differentiated macrophages and HMC-3 microglia cells. Selected LXR agonists and MFAT were also analysed to determine if they could be successful in attenuating increased pro-inflammatory cytokines production after inflammatory stimulation with mCRP or LPS. Determining the potential anti-inflammatory benefits of MFAT showed the ability of the tissue to secrete vital anti-inflammatory cytokines and chemokines into the conditioned medium. The next step was to employ an inflammatory in vitro model to determine if MFAT could significantly attenuate the inflammatory response within U937 differentiated macrophages. From the results, it was presented that MFAT does have anti-inflammatory properties and thus significantly attenuates the increased production of pro-inflammatory cytokines caused by LPS. This research has displayed the importance of continued research into different inflammatory therapeutics which could have the ability to regulate the inflammatory response for example after an ischemic event. These studies have shown the importance of ongoing research into mCRP to unlock the mechanisms this protein plays in different cells, inflammation and in ischemic stroke. Two different potential therapeutic targets show the promising result in reducing protein and gene expression levels. There are several areas which require further work.

Key outcomes

1. Demonstrated that mCRP is a pro-inflammatory risk factor and can morphologically manipulate microglia cells to prevent normal growth.
2. Assessed selected compounds of interest for therapeutic treatment and based on this screening identified GW3965, an LXR agonist, with potential to reduce inflammatory effects of LPS and mCRP.
3. Established cell line models of inflammation incorporating adipose-derived mesenchymal stem cells (AdMSC)
4. Demonstrated the protective properties of AdMSC mediated through the release of anti-inflammatory cytokines including IL-1ra.

6.2 Future work and limitations

Firstly, in this study, we established that mCRP is causing suspension monocytes to form aggregations which become increasingly prominent over 24 hours. mCRP can induce necrosis and cell death of U937 monocytes stimulated with mCRP over 24 hours with the effect taking place at the 6-hour mark. This was further shown with high-resolution imaging using the scanning electron microscope. It is possible to say that mCRP is having a negative impact. The next stage would be to determine by which mechanism this damage is occurring. Evaluating selected adhesion molecules would be beneficial to determine the mechanism by which aggregation formation is occurring. Ideally, this would be performed through ELISA, qPCR, and western blot analysis. It must be noted that research was only carried out on U937 monocytes alone, and it may have been beneficial to obverse the effect in differentiated macrophages.

It was clear that mCRP caused significant effects on the normal morphology and physiology of HMC-3 microglia cells. The data presented showed both migration and motility were affected. It was deemed that mCRP caused significant upregulation of several key pro-inflammatory markers and further to this LXR agonist GW3965 was deemed to attenuate this response. The

next logical step would be to determine the signalling pathway which is activating the inflammatory response. Several pathways of significant interest are NfKb and MAPK, which have previously been seen to regulate inflammatory signalling in mCRP-treated cells. Immortalised microglia cells were used during this work which has the limitation that they do not react in the same way as primary cells. Further to these primary cells you can gain true biological and technical repeats through specific donors. The main drawback of this experimental model is that it was based on a mono 2D culture. Using a 3D-based cell model of the neurovascular unit could be beneficial in answering questions about the inflammatory response after an ischemic event and testing potential therapeutic compounds.

It was determined that adMSC secrete vital anti–inflammatory cytokines and chemokines. It should be acknowledged that our data on the release of cytokines from MFAT was based on secretion in a neutral serum-free culture environment and that this may not reflect their activity and secretion in vivo. Further to this, using the MFAT in the LPS inflammatory in vitro cell model, showed that MFAT has the potential to be able to reduce key pro-inflammatory cytokine protein levels and further can regulate gene expression of these several markers. A direction for further work would be to test the ability of MFAT and its anti-inflammatory properties using an inflammatory model using primary-based glial cells. To establish a better understanding and knowledge of how this could be beneficial in neuroinflammation. It is also important to determine the mechanism by which the reduction is occurring and which signalling pathway is activated. It is known that NfKb is an essential signalling pathway which is at play in inflammation and neuroinflammation.

Al-Baradie, R. S., Pu, S., Liu, D. H., Zeinolabediny, Y., Ferris, G., Sanfeli, C., Corpas, R., Garcia-Lara, E., et al. (2021) 'Monomeric C-Reactive Protein Localized in the Cerebral Tissue of Damaged Vascular Brain Regions Is Associated With Neuro-Inflammation and Neurodegeneration-An Immunohistochemical Study.' *Frontiers in Immunology*, 12, Mar 16,

Ali, R. A., Wuescher, L. M. and Worth, R. G. (2015) 'Platelets: essential components of the immune system.' *Curr Trends Immunol*, 16 pp. 65-78.

Anovazzi, G., Medeiros, M. C., Pigossi, S. C., Finoti, L. S., Moreira, T. M. S., Mayer, M. P. A., Zanelli, C. F., Valentini, S. R., et al. (2017) 'Functionality and opposite roles of two interleukin 4 haplotypes in immune cells.' *Genes and Immunity*, 18(1), Jan-Feb, pp. 33-41.

Arboix, A. and Alio, J. (2010) 'Cardioembolic stroke: clinical features, specific cardiac disorders and prognosis.' *Curr Cardiol Rev*, 6(3), Aug, pp. 150-161.

Arendt, B. K., Velazquez-Dones, A., Tschumper, R. C., Howell, K. G., Ansell, S. M., Witzig, T. E. and Jelinek, D. F. (2002) 'Interleukin 6 induces monocyte chemoattractant protein-1 expression in myeloma cells.' *Leukemia*, 16(10), Oct, pp. 2142-2147.

Asada, Y., Yamashita, A., Sato, Y. and Hatakeyama, K. (2020) 'Pathophysiology of atherothrombosis: Mechanisms of thrombus formation on disrupted atherosclerotic plaques.' *Pathology International*, 70(6), Jun, pp. 309-322.

Badimon, L., Pena, E., Arderiu, G., Padro, T., Slevin, M., Vilahur, G. and Chiva-Blanch, G. (2018) 'C-Reactive Protein in Atherothrombosis and Angiogenesis.' *Frontiers in Immunology*, 9, Mar 2,

Baman, J. R., Cox, J. L., McCarthy, P. M., Kim, D., Patel, R. B., Passman, R. S. and Wilcox, J. E. (2021) 'Atrial fibrillation and atrial cardiomyopathies.' *Journal of Cardiovascular Electrophysiology*, 32(10), Oct, pp. 2845-2853.

Bhavsar, I., Miller, C. S. and Al-Sabbagh, M. (2015) 'Macrophage Inflammatory Protein-1 Alpha (MIP-1 alpha)/CCL3: As a Biomarker.' *General Methods in Biomarker Research and their Applications.*, Jun 1, pp. 223–249.

BHF. (2022) *Watch: What are ACE inhibitors and what do they do in your body?* : [Online] [Accessed on 16/11/22] bhf.org.uk/informationsupport/heart-matters-magazine/medical/drug-cabinet/ace-inhibitors

Biehl, J. K. and Russell, B. (2009) 'Introduction to stem cell therapy.' *J Cardiovasc Nurs*, 24(2), Mar-Apr, pp. 98-103; quiz 104-105.

Bilotta, M. T., Petillo, S., Santoni, A. and Cippitelli, M. (2020) 'Liver X Receptors: Regulators of Cholesterol Metabolism, Inflammation, Autoimmunity, and Cancer.' *Frontiers in Immunology*, 11, Nov 3,

Bio-techne. (2023a) *IL-6 Signaling Pathways*. [Online] [Accessed on 17/02/23] https://www.rndsystems.com/pathways/il-6-family-signaling-pathways

Bio-techne. (2023b) 'IL-4 Signaling Pathways.'

Biswas, P., Delfanti, F., Bernasconi, S., Mengozzi, M., Cota, M., Polentarutti, N., Mantovani, A., Lazzarin, A., et al. (1998) 'Interleukin-6 induces monocyte chemotactic protein-1 in peripheral blood mononuclear cells and in the U937 cell line.' *Blood*, 91(1), Jan 1, pp. 258-265.

Boehme, A. K., Esenwa, C. and Elkind, M. S. V. (2017) 'Stroke Risk Factors, Genetics, and Prevention.' *Circulation Research*, 120(3), Feb 3, pp. 472-495.

Boncler, M., Wu, Y. and Watala, C. (2019) 'The Multiple Faces of C-Reactive ProteinPhysiological and Pathophysiological Implications in Cardiovascular Disease.' *Molecules*, 24(11), Jun 1,

Bonecchi, R. and Graham, G. J. (2016) 'Atypical Chemokine Receptors and Their Roles in the Resolution of the inflammatory Response.' *Frontiers in Immunology*, 7, Jun 10,

Boras, E., Slevin, M., Alexander, M. Y., Aljohi, A., Gilmore, W., Ashworth, J., Krupinski, J., Potempa, L. A., et al. (2014) 'Monomeric C-reactive protein and Notch-3 co-operatively increase angiogenesis through PI3K signalling pathway.' *Cytokine*, 69(2), Oct, pp. 165-179.

Bradley, J. R. (2008) 'TNF-mediated inflammatory disease.' *Journal of Pathology*, 214(2), Jan, pp. 149-160.

Camilleri, E. T., Gustafson, M. P., Dudakovic, A., Riester, S. M., Garces, C. G., Paradise, C. R., Takai, H., Karperien, M., et al. (2016) 'Identification and validation of multiple cell surface markers of clinical-grade adipose-derived mesenchymal stromal cells as novel release criteria for good manufacturing practice-compliant production.' *Stem Cell Research & Therapy*, 7, Aug 11,

Camporeale, A. and Poli, V. (2012) 'IL-6, IL-17 and STAT3: a holy trinity in auto-immunity?' *Front Biosci (Landmark Ed)*, 17(6), Jun 1, 20120601, pp. 2306-2326.

Candelario-Jalil, E., Dijkhuizen, R. M. and Magnus, T. (2022) 'Neuroinflammation, Stroke, Blood-Brain Barrier Dysfunction, and Imaging Modalities.' *Stroke*, 53(5), May, pp. 1473-1486.

Caprio, V., Badimon, L., Di Napoli, M., Fang, W. H., Ferris, G. R., Guo, B. Q., Iemma, R. S., Liu, D. H., et al. (2018) 'pCRP-mCRP Dissociation Mechanisms as Potential Targets for the Development of Small-Molecule Anti-Inflammatory Chemotherapeutics.' *Frontiers in Immunology*, 9, May 28,

Cattaneo, G., De Caro, A., Napoli, F., Chiapale, D., Trada, P. and Camera, A. (2018) 'Micro-fragmented adipose tissue injection associated with arthroscopic procedures in patients with symptomatic knee osteoarthritis.' *BMC Musculoskelet Disord*, 19(1), May 30, 20180530, p. 176.

Chen, H. and Zhou, L. (2022) 'Treatment of ischemic stroke with modified mesenchymal stem cells.' *Int J Med Sci*, 19(7) 20220627, pp. 1155-1162.

Chen, R., Ovbiagele, B. and Feng, W. W. (2016) 'Diabetes and Stroke: Epidemiology, Pathophysiology, Pharmaceuticals and Outcomes.' *American Journal of the Medical Sciences*, 351(4), Apr, pp. 380-386.

Chen, S., Shao, L. and Ma, L. (2021) 'Cerebral Edema Formation After Stroke: Emphasis on Blood-Brain Barrier and the Lymphatic Drainage System of the Brain.' *Front Cell Neurosci*, 15 20210816, p. 716825.

Cheng, O., Ostrowski, R. P., Liu, W. and Zhang, J. H. (2010) 'ACTIVATION OF LIVER X RECEPTOR REDUCES GLOBAL ISCHEMIC BRAIN INJURY BY REDUCTION OF NUCLEAR FACTOR-kappa B.' *Neuroscience*, 166(4), Apr 14, pp. 1101-1109.

Chevilley, A., Lesept, F., Lenoir, S., Ali, C., Parcq, J. and Vivien, D. (2015) 'Impacts of tissue-type plasminogen activator (tPA) on neuronal survival.' *Front Cell Neurosci*, 9 20151016, p. 415.

Chiu, S. and Bharat, A. (2016) 'Role of monocytes and macrophages in regulating immune response following lung transplantation.' *Curr Opin Organ Transplant*, 21(3), Jun, pp. 239-245.

Christiaens, V. and Lijnen, H. R. (2010) 'Angiogenesis and development of adipose tissue.' *Molecular and Cellular Endocrinology*, 318(1-2), Apr 29, pp. 2-9.

Chugh, C. (2019) 'Acute Ischemic Stroke: Management Approach.' *Indian Journal of Critical Care Medicine*, 23, Jun, pp. S140-S146.

Daines, J. M., Schellhardt, L. and Wood, M. D. (2021) 'The Role of the IL-4 Signaling Pathway in Traumatic Nerve Injuries.' *Neurorehabil Neural Repair*, 35(5), May, 20210323, pp. 431-443.

Dayem, A. A., Choi, H. Y., Yang, G. M., Kim, K., Saha, S. K., Kim, F. H. and Cho, S. G. (2016) 'The potential of nanoparticles in stem cell differentiation and further therapeutic applications.' *Biotechnology Journal*, 11(12), Dec, pp. 1550-1560.

De La Torre, R., Pena, E., Vilahur, G., Slevin, M. and Badimon, L. (2013) 'Monomerization of C-reactive protein requires glycoprotein IIb-IIIa activation: pentraxins and platelet deposition.' *Journal of Thrombosis and Haemostasis*, 11(11), Nov, pp. 2048-2058.

Denes, A., Pinteaux, E., Rothwell, N. J. and Allan, S. M. (2011) 'Interleukin-1 and stroke: biomarker, harbinger of damage, and therapeutic target.' *Cerebrovasc Dis*, 32(6) 20111118, pp. 517-527.

Diener, H. C., Sacco, R. L., Easton, J. D., Granger, C. B., Bar, M., Bernstein, R. A., Brainin, M., Brueckmann, M., et al. (2020) 'Antithrombotic Treatment of Embolic Stroke of Undetermined Source: RE-SPECT ESUS Elderly and Renally Impaired Subgroups.' *Stroke*, 51(6), Jun, 20200514, pp. 1758-1765.

Dinarello, C. A., Simon, A. and van der Meer, J. W. M. (2012) 'Treating inflammation by blocking interleukin-1 in a broad spectrum of diseases.' *Nature Reviews Drug Discovery*, 11(8), Aug, pp. 633-652.

DiSabato, D. J., Quan, N. and Godbout, J. P. (2016) 'Neuroinflammation: the devil is in the details.' *Journal of Neurochemistry*, 139, Oct, pp. 136-153.

Doll, D. N., Barr, T. L. and Simpkins, J. W. (2014) 'Cytokines: Their Role in Stroke and Potential Use as Biomarkers and Therapeutic Targets.' *Aging and Disease*, 5(5), Oct, pp. 294-306.

Dong, R., Huang, R. X., Wang, J. Q., Liu, H. Y. and Xu, Z. X. (2021) 'Effects of Microglial Activation and Polarization on Brain Injury After Stroke.' *Frontiers in Neurology*, 12, Jul 1,

Donkor, E. S. (2018) 'Stroke in the 21(st) Century: A Snapshot of the Burden, Epidemiology, and Quality of Life.' *Stroke Res Treat*, 2018 20181127, p. 3238165.

Dusing, R., Waeber, B., Destro, M., Santos Maia, C. and Brunel, P. (2017) 'Triple-combination therapy in the treatment of hypertension: a review of the evidence.' *J Hum Hypertens*, 31(8), Aug, 20170223, pp. 501-510.

El-Ansary, M., Abdel-Aziz, I., Mogawer, S., Abdel-Hamid, S., Hammam, O., Teaema, S. and Wahdan, M. (2012) 'Phase II Trial: Undifferentiated Versus Differentiated Autologous Mesenchymal Stem Cells Transplantation in Egyptian Patients with HCV Induced Liver Cirrhosis.' *Stem Cell Reviews and Reports*, 8(3), Sep, pp. 972-981.

ElAli, A. and Jean LeBlanc, N. (2016) 'The Role of Monocytes in Ischemic Stroke Pathobiology: New Avenues to Explore.' *Front Aging Neurosci*, 8 20160222, p. 29.

Eldahshan, W., Fagan, S. C. and Ergul, A. (2019) 'Inflammation within the neurovascular unit: Focus on microglia for stroke injury and recovery.' *Pharmacological Research*, 147, Sep,

Erta, M., Quintana, A. and Hidalgo, J. (2012) 'Interleukin-6, a Major Cytokine in the Central Nervous System.' *International Journal of Biological Sciences*, 8(9) pp. 1254-1266.

Fadini, G. P. and Cosentino, F. (2018) 'Diabetes and ischaemic stroke: a deadly association.' *European Heart Journal*, 39(25), Jul 1, pp. 2387-2389.

Fields, J. K., Gunther, S. and Sundberg, E. J. (2019) 'Structural Basis of IL-1 Family Cytokine Signaling.' *Front Immunol*, 10 20190620, p. 1412.

Filep, J. G. (2009) 'Platelets Affect the Structure and Function of C-Reactive Protein.' *Circulation Research*, 105(2), Jul 17, pp. 109-111.

Fluri, F., Schuhmann, M. K. and Kleinschnitz, C. (2015) 'Animal models of ischemic stroke and their application in clinical research.' *Drug Design Development and Therapy*, 9 pp. 3445-3454.

Franco-Bocanegra, D. K., McAuley, C., Nicoll, J. A. R. and Boche, D. (2019) 'Molecular Mechanisms of Microglial Motility: Changes in Ageing and Alzheimer's Disease.' *Cells*, 8(6), Jun,

Fujita, M., Takada, Y. K., Izumiya, Y. and Takada, Y. (2014) 'The Binding of Monomeric C-Reactive Protein (mCRP) to Integrins alpha v beta 3 and alpha 4 beta 1 Is Related to Its Pro-Inflammatory Action.' *Plos One*, 9(4), Apr 2,

Galderisi, U., Peluso, G. and Di Bernardo, G. (2022) 'Clinical Trials Based on Mesenchymal Stromal Cells are Exponentially Increasing: Where are We in Recent Years?' *Stem Cell Rev Rep*, 18(1), Jan, 20210816, pp. 23-36.

Garcia-Lara, E., Aguirre, S., Clotet, N., Sawkulycz, X., Bartra, C., Almenara-Fuentes, L., Sunol, C., Corpas, R., et al. (2021) 'Antibody Protection against Long-Term Memory Loss Induced by Monomeric C-Reactive Protein in a Mouse Model of Dementia.' *Biomedicines*, 9(7), Jul 16, 20210716,

Gershov, D., Kim, S., Brot, N. and Elkon, K. B. (2000) 'C-Reactive protein binds to apoptotic cells, protects the cells from assembly of the terminal complement components, and sustains an antiinflammatory innate immune response: implications for systemic autoimmunity.' *J Exp Med*, 192(9), Nov 6, pp. 1353-1364.

Gertz, K., Kronenberg, G., Kalin, R. E., Baldinger, T., Werner, C., Balkaya, M., Eom, G. D., Hellmann-Regen, J., et al. (2012) 'Essential role of interleukin-6 in post-stroke angiogenesis.' *Brain*, 135, Jun, pp. 1964-1980.

Gesta, S., Tseng, Y. H. and Kahn, C. R. (2007) 'Developmental origin of fat: Tracking obesity to its source.' *Cell*, 131(2), Oct 19, pp. 242-256.

Gezmu, T., Schneider, D., Demissie, K., Lin, Y. and Gizzi, M. S. (2014) 'Risk Factors for Acute Stroke among South Asians Compared to Other Racial/Ethnic Groups.' *Plos One*, 9(9), Sep 30,

Giordano, A., Smorlesi, A., Frontini, A., Barbatelli, G. and Cinti, S. (2014) 'White, brown and pink adipocytes: the extraordinary plasticity of the adipose organ.' *Eur J Endocrinol*, 170(5), May, 20140410, pp. R159-171.

Gobbi, A., Dallo, I., Rogers, C., Striano, R. D., Mautner, K., Bowers, R., Rozak, M., Bilbool, N., et al. (2021) 'Two-year clinical outcomes of autologous microfragmented adipose tissue in elderly patients with knee osteoarthritis: a multi-centric, international study.' *Int Orthop*, 45(5), May, 20210302, pp. 1179-1188.

Griffin, P., Dimitry, J. M., Sheehan, P. W., Lananna, B. V., Guo, C., Robinette, M. L., Hayes, M. E., Cedeno, M. R., et al. (2019) 'Circadian clock protein Rev-erbalpha regulates neuroinflammation.' *Proc Natl Acad Sci U S A*, 116(11), Mar 12, 20190221, pp. 5102-5107.

Guo, B., Sawkulycz, X., Heidari, N., Rogers, R., Liu, D. and Slevin, M. (2021) 'Characterisation of Novel Angiogenic and Potent Anti-Inflammatory Effects of Micro-Fragmented Adipose Tissue.' *Int J Mol Sci*, 22(6), Mar 23, 20210323,

Guo, B. Q., Sawkulycz, X., Heidari, N., Rogers, R., Liu, D. H. and Slevin, M. (2021) 'Characterisation of Novel Angiogenic and Potent Anti-Inflammatory Effects of Micro-Fragmented Adipose Tissue.' *International Journal of Molecular Sciences*, 22(6), Mar,

Guo, D. K., Zhu, Y., Sun, H. Y., Xu, X. Y., Zhang, S., Hao, Z. B., Wang, G. H., Mu, C. C., et al. (2019) 'Pharmacological activation of REV-ERBalpha represses LPS-induced microglial activation through the NF-kappaB pathway.' *Acta Pharmacol Sin*, 40(1), Jan, 20180627, pp. 26-34.

Guo, X. and Miao, Z. (2021) 'Advances in mechanical thrombectomy for acute ischaemic stroke from large vessel occlusions.' *Stroke Vasc Neurol*, 6(4), Dec, 20210720, pp. 649-657.

Han, D., Liu, H. and Gao, Y. (2020) 'The role of peripheral monocytes and macrophages in ischemic stroke.' *Neurol Sci*, 41(12), Dec, 20201003, pp. 3589-3607.

Han, Y., Li, X., Zhang, Y., H., Y, Chang, F. and Ding, J. (2019) 'Mesenchymal Stem Cells for Regenerative Medicine.' *Cells*, 8(8) p. 886.

Holloway, P. M. and Gavins, F. N. E. (2016) 'Modeling Ischemic Stroke In Vitro: Status Quo and Future Perspectives.' *Stroke*, 47(2), Feb, pp. 561-569.

Hu, S., Chao, C. C., Ehrlich, L. C., Sheng, W. S., Sutton, R. L., Rockswold, G. L. and Peterson, P. K. (1999) 'Inhibition of microglial cell RANTES production by IL-10 and TGF-beta.' *J Leukoc Biol*, 65(6), Jun, pp. 815-821.

Hughes, C. E. and Nibbs, R. J. B. (2018) 'A guide to chemokines and their receptors.' *Febs Journal*, 285(16), Aug, pp. 2944-2971.

Huh, J. E. and Lee, S. Y. (2013) 'IL-6 is produced by adipose-derived stromal cells and promotes osteogenesis.' *Biochimica Et Biophysica Acta-Molecular Cell Research*, 1833(12), Dec, pp. 2608-2616.

Huilcaman, R., Venturini, W., Fuenzalida, L., Cayo, A., Segovia, R., Valenzuela, C., Brown, N. and Moore-Carrasco, R. (2022) 'Platelets, a Key Cell in Inflammation and Atherosclerosis Progression.' *Cells*, 11(6), Mar 17, 20220317,

Hurford, R., Sekhar, A., Hughes, T. A. T. and Muir, K. W. (2020) 'Diagnosis and management of acute ischaemic stroke.' *Practical Neurology*, 20(4), Aug, pp. 306-318.

Idriss, H. T. and Naismith, J. H. (2000) 'TNF alpha and the TNF receptor superfamily: Structure-function relationship(s).' *Microscopy Research and Technique*, 50(3), Aug 1, pp. 184-195.

Im, S. S. and Osborne, T. F. (2011) 'Liver x receptors in atherosclerosis and inflammation.' *Circ Res*, 108(8), Apr 15, pp. 996-1001.

Iyer, S. S. and Cheng, G. H. (2012) 'Role of Interleukin 10 Transcriptional Regulation in Inflammation and Autoimmune Disease.' *Critical Reviews in Immunology*, 32(1) pp. 23-63.

Jayaraj, R. L., Azimullah, S., Beiram, R., Jalal, F. Y. and Rosenberg, G. A. (2019) 'Neuroinflammation: friend and foe for ischemic stroke.' *Journal of Neuroinflammation*, 16, Jul 10,

Jeon, S. W. and Kim, Y. K. (2016) 'Neuroinflammation and cytokine abnormality in major depression: Cause or consequence in that illness?' *World Journal of Psychiatry*, 6(3), Sep 22, pp. 283-293.

Jesus, S. M. O. D. (2022) Thrombectomy. In: [Internet], I. S. Treasure Island (FL): StatPearls Publishing.

Jin, R., Yang, G. and Li, G. (2010) 'Inflammatory mechanisms in ischemic stroke: role of inflammatory cells.' *J Leukoc Biol*, 87(5), May, 20100203, pp. 779-789.

Junttila, I. S. (2018) 'Tuning the Cytokine Responses: An Update on Interleukin (IL)-4 and IL-13 Receptor Complexes.' *Front Immunol*, 9 20180607, p. 888.

Jurcau, A. and Simion, A. (2021) 'Neuroinflammation in Cerebral Ischemia and Ischemia/Reperfusion Injuries: From Pathophysiology to Therapeutic Strategies.' *Int J Mol Sci*, 23(1), Dec 21, 20211221,

Jurga, A. M., Paleczna, M. and Kuter, K. Z. (2020) 'Overview of General and Discriminating Markers of Differential Microglia Phenotypes.' *Front Cell Neurosci*, 14 20200806, p. 198.

Keane, M. P., Belperio, J. A., Moore, T. A., Moore, B. B., Arenberg, D. A., Smith, R. E., Burdick, M. D., Kunkel, S. L., et al. (1999) 'Neutralization of the CXC chemokine, macrophage inflammatory protein-2, attenuates bleomycin-induced pulmonary fibrosis.' *J Immunol*, 162(9), May 1, pp. 5511-5518.

Keegan, A. D. (2014) 'IL-4 Receptor.'

Keegan, A. D., Leonard, W. J. and Zhu, J. (2021) 'Recent advances in understanding the role of IL-4 signaling.' *Fac Rev*, 10 20210907, p. 71.

Kelly-Welch, A., Hanson, E. M. and Keegan, A. D. (2005) 'Interleukin-4 (IL-4) pathway.' *Sci STKE*, 2005(293), Jul 19, 20050719, p. cm9.

Kempuraj, D., Thangavel, R., Selvakumar, G. P., Zaheer, S., Ahmed, M. E., Raikwar, S. P., Zahoor, H., Saeed, D., et al. (2017) 'Brain and Peripheral Atypical Inflammatory Mediators Potentiate Neuroinflammation and Neurodegeneration.' *Front Cell Neurosci*, 11 20170724, p. 216.

Kes, V. B., Simundic, A. M., Nikolac, N., Topic, E. and Demarin, V. (2008) 'Pro-inflammatory and anti-inflammatory cytokines in acute ischemic stroke and their relation to early neurological deficit and stroke outcome.' *Clinical Biochemistry*, 41(16-17), Nov, pp. 1330-1334.

Khreiss, T., Jozsef, L., Potempa, L. A. and Filep, J. G. (2004) 'Opposing effects of C-reactive protein isoforms on shear-induced neutrophil-platelet adhesion and neutrophil aggregation in whole blood.' *Circulation*, 110(17), Oct 26, pp. 2713-2720.

Khreiss, T., Jozsef, L., Hossain, S., Chan, J. S. D., Potempa, L. A. and Filep, J. G. (2002) 'Loss of pentameric symmetry of C-reactive protein is associated with delayed apoptosis of human neutrophils.' *Journal of Biological Chemistry*, 277(43), Oct 25, pp. 40775-40781.

Kim, Y., Ryu, J., Ryu, M. S., Lim, S., Han, K. O., Lim, I. K. and Han, K. H. (2014) 'C-reactive protein induces G2/M phase cell cycle arrest and apoptosis in monocytes through the upregulation of B-cell translocation gene 2 expression.' *Febs Letters*, 588(4), Feb 14, pp. 625-631.

King, D., Wittenberg, R., Patel, A., Quayyum, Z., Berdunov, V. and Knapp, M. (2020) 'The future incidence, prevalence and costs of stroke in the UK.' *Age and Ageing*, 49(2), Mar, pp. 277-282.

Koper, O. M., Kaminska, J., Sawicki, K. and Kemona, H. (2018) 'CXCL9, CXCL10, CXCL11, and their receptor (CXCR3) in neuroinflammation and neurodegeneration.' *Advances in Clinical and Experimental Medicine*, 27(6), Jun, pp. 849-856.

Kostulas, N., Kivisakk, P., Huang, Y. M., Matusevicius, D., Kostulas, V. and Link, H. (1998) 'Ischemic stroke is associated with a systemic increase of blood mononuclear cells expressing interleukin-8 mRNA.' *Stroke*, 29(2), Feb, pp. 462-466.

Kratofil, R. M., Kubes, P. and Deniset, J. F. (2017) 'Monocyte Conversion During Inflammation and Injury.' *Arteriosclerosis Thrombosis and Vascular Biology*, 37(1), Jan, pp. 35-+.

Kubiczkova, L., Sedlarikova, L., Hajek, R. and Sevcikova, S. (2012) 'TGF-beta - an excellent servant but a bad master.' *J Transl Med*, 10, Sep 3, 20120903, p. 183.

Kuriakose, D. and Xiao, Z. C. (2020) 'Pathophysiology and Treatment of Stroke: Present Status and Future Perspectives.' *International Journal of Molecular Sciences*, 21(20), Oct,

Lambertsen, K. L., Biber, K. and Finsen, B. (2012) 'Inflammatory cytokines in experimental and human stroke.' *Journal of Cerebral Blood Flow and Metabolism*, 32(9), Sep, pp. 1677-1698.

Lambertsen, K. L., Finsen, B. and Clausen, B. H. (2019) 'Post-stroke inflammation-target or tool for therapy?' *Acta Neuropathologica*, 137(5), May, pp. 693-714.

Land, W. G. (2015) 'The Role of Damage-Associated Molecular Patterns (DAMPs) in Human Diseases: Part II: DAMPs as diagnostics, prognostics and therapeutics in clinical medicine.' *Sultan Qaboos Univ Med J*, 15(2), May, 20150528, pp. e157-170.

Laureti, S., Gionchetti, P., Cappelli, A., Vittori, L., Contedini, F., Rizzello, F., Golfieri, R., Campieri, M., et al. (2020) 'Refractory Complex Crohn's Perianal Fistulas: A Role for Autologous Microfragmented Adipose Tissue Injection.' *Inflamm Bowel Dis*, 26(2), Jan 6, pp. 321-330.

Law, M., Wald, N. and Morris, J. (2003) 'Lowering blood pressure to prevent myocardial infarction and stroke: a new preventive strategy.' *Health Technol Assess*, 7(31) pp. 1-94.

Li, Y., Zhu, Z. Y., Huang, T. T., Zhou, Y. X., Wang, X., Yang, L. Q., Chen, Z. A., Yu, W. F., et al. (2018) 'The peripheral immune response after stroke-A double edge sword for blood-brain barrier integrity.' *CNS Neurosci Ther*, 24(12), Dec, 20181101, pp. 1115-1128.

Liu , M.-X. P., Jun-Chun Tang , Ya Zhang , Hua-Bao Liao , Yang Zhuang , Dan Zhao , Qi Wan. (2017) 'Role of neuroinflammation in ischemic strokie.' *Neuroimmunol Neuroinflammation*, (4) pp. 158-166.

Liu, X., Yin, S., Chen, Y., Wu, Y., Zheng, W., Dong, H., Bai, Y., Qin, Y., et al. (2018) 'LPSinduced proinflammatory cytokine expression in human airway epithelial cells and macrophages via NFkappaB, STAT3 or AP1 activation.' *Mol Med Rep*, 17(4), Apr, 20180202, pp. 5484-5491.

Liu, Y., Beyer, A. and Aebersold, R. (2016) 'On the Dependency of Cellular Protein Levels on mRNA Abundance.' *Cell*, 165(3), Apr 21, pp. 535-550.

Lively, S. and Schlichter, L. C. (2018) 'Microglia Responses to Pro-inflammatory Stimuli (LPS, IFNgamma+TNFalpha) and Reprogramming by Resolving Cytokines (IL-4, IL-10).' *Front Cell Neurosci*, 12 20180724, p. 215.

Lopes, R. O. P., Barbosa, G. S., Leite, K. R., Merces, C., Santana, R. F. and Brandao, M. A. G. (2021) 'Risk factors for hyperglycemia and hypoglycemia in adults with pharmacologically treated type 2 diabetes mellitus: a quantitative systematic review protocol.' *JBI Evid Synth*, 19(1), Jan, pp. 163-169.

Losy, J. and Zaremba, J. (2001) 'Monocyte chemoattractant protein-1 is increased in the cerebrospinal fluid of patients with ischemic stroke.' *Stroke*, 32(11), Nov, pp. 2695-2696.

Lu, D., Xu, Y., Liu, Q. and Zhang, Q. (2021) 'Mesenchymal Stem Cell-Macrophage Crosstalk and Maintenance of Inflammatory Microenvironment Homeostasis.' *Front Cell Dev Biol*, 9 20210625, p. 681171.

Ma, R., Xie, Q., Li, Y., Chen, Z., Ren, M., Chen, H., Li, H., Li, J., et al. (2020) 'Animal models of cerebral ischemia: A review.' *Biomed Pharmacother*, 131, Nov, 20200913, p. 110686.

Mao, P., Joshi, K., Li, J. F., Kim, S. H., Li, P. P., Santana-Santos, L., Luthra, S., Chandran, U. R., et al. (2013) 'Mesenchymal glioma stem cells are maintained by activated glycolytic metabolism involving aldehyde dehydrogenase 1A3.' *Proceedings of the National Academy of Sciences of the United States of America*, 110(21), May 21, pp. 8644-8649.

Marimuthu, R., Francis, H., Dervish, S., Li, S. C. H., Medbury, H. and Williams, H. (2018) 'Characterization of Human Monocyte Subsets by Whole Blood Flow Cytometry Analysis.' *J Vis Exp*, (140), Oct 17, 20181017,

Marko, M., Posekany, A., Szabo, S., Scharer, S., Kiechl, S., Knoflach, M., Serles, W., Ferrari, J., et al. (2020) 'Trends of r-tPA (Recombinant Tissue-Type Plasminogen Activator) Treatment and Treatment-Influencing Factors in Acute Ischemic Stroke.' *Stroke*, 51(4), Apr, 20200302, pp. 1240-1247.

McGurgan, I. J., Ziai, W. C., Werring, D. J., Al-Shahi Salman, R. and Parry-Jones, A. R. (2020) 'Acute intracerebral haemorrhage: diagnosis and management.' *Pract Neurol*, 21(2), Dec 7, 20201207, pp. 128-136.

McVoy, J. R. S., Oughli, H. A. and Oh, U. (2015) 'Liver X receptor-dependent inhibition of microglial nitric oxide synthase 2.' *Journal of Neuroinflammation*, 12, Feb 10,

Melnikov, I., Kozlov, S., Saburova, O., Avtaeva, Y., Guria, K. and Gabbasov, Z. (2023) 'Monomeric C-Reactive Protein in Atherosclerotic Cardiovascular Disease: Advances and Perspectives.' *Int J Mol Sci*, 24(3), Jan 20, 20230120,

Meng, H. F., Jin, J., Wang, H., Wang, L. S. and Wu, C. T. (2022) 'Recent advances in the therapeutic efficacy of hepatocyte growth factor gene-modified mesenchymal stem cells in multiple disease settings.' *J Cell Mol Med*, 26(18), Sep, 20220803, pp. 4745-4755.

Michael, D. R., Ashlin, T. G., Buckley, M. L. and Ramji, D. P. (2012) 'Liver X receptors, atherosclerosis and inflammation.' *Curr Atheroscler Rep*, 14(3), Jun, pp. 284-293.

Migdady, I., Russman, A. and Buletko, A. B. (2021) 'Atrial Fibrillation and Ischemic Stroke: A Clinical Review.' *Semin Neurol*, 41(4), Aug, 20210413, pp. 348-364.

Minogue, A. M., Barrett, J. P. and Lynch, M. A. (2012) 'LPS-induced release of IL-6 from glia modulates production of IL-1beta in a JAK2-dependent manner.' *J Neuroinflammation*, 9, Jun 14, 20120614, p. 126.

Molins, B., Pena, E., de la Torre, R. and Badimon, L. (2011) 'Monomeric C-reactive protein is prothrombotic and dissociates from circulating pentameric C-reactive protein on adhered activated platelets under flow.' *Cardiovascular Research*, 92(2), Nov 1, pp. 328-337.

Moradi, S., Mahdizadeh, H., Saric, T., Kim, J., Harati, J., Shahsavarani, H., Greber, B. and Moore, J. B. t. (2019) 'Research and therapy with induced pluripotent stem cells (iPSCs): social, legal, and ethical considerations.' *Stem Cell Res Ther*, 10(1), Nov 21, 20191121, p. 341.

Morales, J. R., Ballesteros, I., Deniz, J. M., Hurtado, O., Vivancos, J., Nombela, F., Lizasoain, I., Castrillo, A., et al. (2008) 'Activation of liver X receptors promotes neuroprotection and reduces brain inflammation in experimental stroke.' *Circulation*, 118(14), Sep 30, pp. 1450-1459.

Muldoon, L. L., Alvarez, J. I., Begley, D. J., Boado, R. J., Del Zoppo, G. J., Doolittle, N. D., Engelhardt, B., Hallenbeck, J. M., et al. (2013) 'Immunologic privilege in the central nervous system and the blood-brain barrier.' *J Cereb Blood Flow Metab*, 33(1), Jan, 20121017, pp. 13-21.

Murray, K. N., Parry-Jones, A. R. and Allan, S. M. (2015) 'Interleukin-1 and acute brain injury.' *Frontiers in Cellular Neuroscience*, 6(9) p. 18.

Musial-Wysocka, A., Kot, M. and Majka, M. (2019) 'The Pros and Cons of Mesenchymal Stem Cell-Based Therapies.' *Cell Transplantation*, 28(7), Jul, pp. 801-812.

Nava, S., Sordi, V., Pascucci, L., Tremolada, C., Ciusani, E., Zeira, O., Cadei, M., Soldati, G., et al. (2019) 'Long-Lasting Anti-Inflammatory Activity of Human Microfragmented Adipose Tissue.' *Stem Cells Int*, 2019 20190219, p. 5901479.

Ngwa, D. N. and Agrawal, A. (2019) 'Structure-Function Relationships of C-Reactive Protein in Bacterial Infection.' *Frontiers in Immunology*, 10, Feb 26,

Nogueira, G. O., Garcez, P. P., Bardy, C., Cunningham, M. O. and Sebollela, A. (2022) 'Modeling the Human Brain With ex vivo Slices and in vitro Organoids for Translational Neuroscience.' *Front Neurosci*, 16 20220224, p. 838594.

Nunomura, S., Okayama, Y., Matsumoto, K., Hashimoto, N., Endo-Umeda, K., Terui, T., Makishima, M. and Ra, C. (2015) 'Activation of LXRs using the synthetic agonist GW3965 represses the production of pro-inflammatory cytokines by murine mast cells.' *Allergology International*, 64, Sep, pp. S11-S17.

Orihuela, R., McPherson, C. A. and Harry, G. J. (2016) 'Microglial M1/M2 polarization and metabolic states.' *Br J Pharmacol*, 173(4), Feb, 20150511, pp. 649-665.

Parameswaran, N. a. P., S. (2010) 'Tumor necrosis factor-a signaling in macrophages.' *Critical Reviews in Eukaryotic Gene Expression*, Begell House Inc. pp. 87–103.

Park, A., Kim, W. K. and Bae, K. H. (2014) 'Distinction of white, beige and brown adipocytes derived from mesenchymal stem cells.' *World J Stem Cells*, 6(1), Jan 26, pp. 33-42.

Park, J., Chang, J. Y., Kim, J. Y. and Lee, J. E. (2020) 'Monocyte Transmodulation: The Next Novel Therapeutic Approach in Overcoming Ischemic Stroke?' *Front Neurol*, 11 20201022, p. 578003.

Pawluk, H., Wozniak, A., Grzesk, G., Kolodziejska, R., Kozakiewicz, M., Kopkowska, E., Grzechowiak, E. and Kozera, G. (2020) 'The Role of Selected Pro-Inflammatory Cytokines in Pathogenesis of Ischemic Stroke.' *Clinical Interventions in Aging*, 15 pp. 469-484.

Pittenger, M. F., Discher, D. E., Peault, B. M., Phinney, D. G., Hare, J. M. and Caplan, A. I. (2019) 'Mesenchymal stem cell perspective: cell biology to clinical progress.' *Npj Regenerative Medicine*, 4(1), Dec 2,

Poeta, V. M., Massara, M., Capucetti, A. and Bonecchi, R. (2019) 'Chemokines and Chemokine Receptors: New Targets for Cancer Immunotherapy.' *Frontiers in Immunology*, 10, Mar 6,

Porro, C., Cianciulli, A. and Panaro, M. A. (2020) 'The Regulatory Role of IL-10 in Neurodegenerative Diseases.' *Biomolecules*, 10(7), Jul,

Prud'homme, G. J. (2007) 'Pathobiology of transforming growth factor beta in cancer, fibrosis and immunologic disease, and therapeutic considerations.' *Lab Invest*, 87(11), Nov, 20070827, pp. 1077-1091.

Rajab, I. M., Hart, P. C. and Potempa, L. A. (2020) 'How C-Reactive Protein Structural Isoforms With Distinctive Bioactivities Affect Disease Progression.' *Frontiers in Immunology*, 11, Sep 10,

Rajkovic, O., Potjewyd, G. and Pinteaux, E. (2018) 'Regenerative Medicine Therapies for Targeting Neuroinflammation After Stroke.' *Front Neurol*, 9 20180903, p. 734.

Ramesh, G., MacLean, A. G. and Philipp, M. T. (2013) 'Cytokines and Chemokines at the Crossroads of Neuroinflammation, Neurodegeneration, and Neuropathic Pain.' *Mediators of Inflammation*, 2013

Ramon-Vazquez, A., de la Rosa, J. V., Tabraue, C., Lopez, F., Diaz-Chico, B. N., Bosca, L., Tontonoz, P., Alemany, S., et al. (2019) 'Common and Differential Transcriptional Actions of Nuclear Receptors Liver X Receptors alpha and beta in Macrophages.' *Mol Cell Biol*, 39(5), Mar 1, 20190215,

Randelli, P., Menon, A., Ragone, V., Creo, P., Bergante, S., Randelli, F., De Girolamo, L., Montrasio, U. A., et al. (2016) 'Lipogems Product Treatment Increases the Proliferation Rate of Human Tendon Stem Cells without Affecting Their Stemness and Differentiation Capability.' *Stem Cells International*, 2016

Ren, K. and Torres, R. (2009) 'Role of interleukin-1beta during pain and inflammation.' *Brain Res Rev*, 60(1), Apr, 20081231, pp. 57-64.

Rolski, F. and Blyszczuk, P. (2020) 'Complexity of TNF-alpha Signaling in Heart Disease.' *J Clin Med*, 9(10), Oct 12, 20201012,

Rossi, C., Cusimano, M., Zambito, M., Finardi, A., Capotondo, A., Garcia-Manteiga, J. M., Comi, G., Furlan, R., et al. (2018) 'Interleukin 4 modulates microglia homeostasis and attenuates the early slowly progressive phase of amyotrophic lateral sclerosis.' *Cell Death & Disease*, 9, Feb,

Salari, V., Mengoni, F., Del Gallo, F., Bertini, G. and Fabene, P. F. (2020) 'The Anti-Inflammatory Properties of Mesenchymal Stem Cells in Epilepsy: Possible Treatments and Future Perspectives.' *Int J Mol Sci*, 21(24), Dec 18, 20201218,

Sanchis, P., Fernandez-Gayol, O., Comes, G., Escrig, A., Giralt, M., Palmiter, R. D. and Hidalgo, J. (2020) 'Interleukin-6 Derived from the Central Nervous System May Influence the Pathogenesis of Experimental Autoimmune Encephalomyelitis in a Cell-Dependent Manner.' *Cells*, 9(2), Jan 31, 20200131,

Shao, Z., Tu, S. and Shao, A. (2019) 'Pathophysiological Mechanisms and Potential Therapeutic Targets in Intracerebral Hemorrhage.' *Front Pharmacol*, 10 20190919, p. 1079.

Slevin, M., Matou-Nasri, S., Turu, M., Luque, A., Rovira, N., Badimon, L., Boluda, S., Potempa, L., et al. (2010) 'Modified C-Reactive Protein Is Expressed by Stroke Neovessels and Is a Potent Activator of Angiogenesis In Vitro.' *Brain Pathology*, 20(1), Jan, pp. 151-165.

Slevin, M., Iemma, R. S., Zeinolabediny, Y., Liu, D. H., Ferris, G. R., Caprio, V., Phillips, N., Di Napoli, M., et al. (2018) 'Acetylcholine Inhibits Monomeric C-Reactive Protein Induced Inflammation, Endothelial Cell Adhesion, and Platelet Aggregation; A Potential Therapeutic?' *Frontiers in Immunology*, 9, Sep 26,

Smadja, D. M., d'Audigier, C., Guerin, C. L., Mauge, L., Dizier, B., Silvestre, J. S., Dal Cortivo, L., Gaussem, P., et al. (2012) 'Angiogenic potential of BM MSCs derived from patients with critical leg ischemia.' *Bone Marrow Transplantation*, 47(7), Jul, pp. 997-1000.

Sochocka, M., Diniz, B. S. and Leszek, J. (2017) 'Inflammatory Response in the CNS: Friend or Foe?' *Mol Neurobiol*, 54(10), Dec, 20161126, pp. 8071-8089.

Sproston, N. R. and Ashworth, J. J. (2018) 'Role of C-Reactive Protein at Sites of Inflammation and Infection.' *Frontiers in Immunology*, 9, Apr 13,

Sproston, N. R., El Mohtadi, M., Slevin, M., Gilmore, W. and Ashworth, J. J. (2018) 'The effect of C-reactive Protein Isoforms on nitric Oxide Production by U937 Monocytes/Macrophages.' *Frontiers in Immunology*, 9, Jul 2,

Spyridon, M., Moraes, L. A., Jones, C. I., Sage, T., Sasikumar, P., Bucci, G. and Gibbins, J. M. (2011) 'LXR as a novel antithrombotic target.' *Blood*, 117(21), May 26, pp. 5751-5761.

Strecker, J. K., Minnerup, J., Gess, B., Ringelstein, E. B., Schabitz, W. R. and Schilling, M. (2011) 'Monocyte chemoattractant protein-1-deficiency impairs the expression of IL-6, IL-1beta and G-CSF after transient focal ischemia in mice.' *PLoS One*, 6(10) 20111021, p. e25863.

Strioga, M., Viswanathan, S., Darinskas, A., Slaby, O., & Michalek, J. (2012) 'Same or not the same? Comparison of adipose tissue-derived versus bone marrow-derived mesenchymal stem and stromal cells.' *Stem cells and development*, 21(14) pp. 2724–2752.

Suzuki, T., Hashimoto, S., Toyoda, N., Nagai, S., Yamazaki, N., Dong, H. Y., Sakai, J., Yamashita, T., et al. (2000) 'Comprehensive gene expression profile of LPS-stimulated human monocytes by SAGE.' *Blood*, 96(7), Oct 1, pp. 2584-2591.

Taha, S., Volkmer, E., Haas, E., Alberton, P., Straub, T., David-Rus, D., Aszodi, A., Giunta, R., et al. (2020) 'Differences in the Inflammatory Response of White Adipose Tissue and Adipose-Derived Stem Cells.' *Int J Mol Sci*, 21(3), Feb 6, 20200206,

Takata, F., Nakagawa, S., Matsumoto, J. and Dohgu, S. (2021) 'Blood-Brain Barrier Dysfunction Amplifies the Development of Neuroinflammation: Understanding of Cellular Events in Brain Microvascular Endothelial Cells for Prevention and Treatment of BBB Dysfunction.' *Front Cell Neurosci*, 15 20210913, p. 661838.

Tanaka, T., Narazaki, M. and Kishimoto, T. (2014) 'IL-6 in inflammation, immunity, and disease.' *Cold Spring Harb Perspect Biol*, 6(10), Sep 4, 20140904, p. a016295.

Tawil, S. E. and Muir, K. W. (2017) 'Thrombolysis and thrombectomy for acute ischaemic stroke.' *Clin Med (Lond)*, 17(2), Apr, pp. 161-165.

Thompson, W. L., Karpus, W. J. and Van Eldik, L. J. (2008) 'MCP-1-deficient mice show reduced neuroinflammatory responses and increased peripheral inflammatory responses to peripheral endotoxin insult.' *Journal of Neuroinflammation*, 5, Aug 15,

Tiryaki, T., Conde-Green, A., Cohen, S. R., Canikyan, S. and Kocak, P. (2020) 'A 3-step Mechanical Digestion Method to Harvest Adipose-derived Stromal Vascular Fraction.' *Plast Reconstr Surg Glob Open*, 8(2), Feb, 20200227, p. e2652.

Tremolada, C., Colombo, V. and Ventura, C. (2016) 'Adipose Tissue and Mesenchymal Stem Cells: State of the Art and Lipogems (R) Technology Development.' *Current Stem Cell Reports*, 2(3), Sep, pp. 304-312.

Turner, M. D., Nedjai, B., Hurst, T. and Pennington, D. J. (2014) 'Cytokines and chemokines: At the crossroads of cell signalling and inflammatory disease.' *Biochimica Et Biophysica Acta-Molecular Cell Research*, 1843(11), Nov, pp. 2563-2582.

Ullah, I., Subbarao, R. B. and Rho, G. J. (2015) 'Human mesenchymal stem cells - current trends and future prospective.' *Bioscience Reports*, 35, Apr 1,

Van Breedam, E. and Ponsaerts, P. (2022) 'Promising Strategies for the Development of Advanced In Vitro Models with High Predictive Power in Ischaemic Stroke Research.' *International Journal of Molecular Sciences*, 23(13), Jul,

Venetz, D., Ponzoni, M., Schiraldi, M., Ferreri, A. J., Bertoni, F., Doglioni, C. and Uguccioni, M. (2010) 'Perivascular expression of CXCL9 and CXCL12 in primary central nervous system lymphoma: T-cell infiltration and positioning of malignant B cells.' *Int J Cancer*, 127(10), Nov 15, pp. 2300-2312.

Verma, R., Balakrishnan, L., Sharma, K., Khan, A. A., Advani, J., Gowda, H., Tripathy, S. P., Suar, M., et al. (2016) 'A network map of Interleukin-10 signaling pathway.' *J Cell Commun Signal*, 10(1), Mar, 20150808, pp. 61-67.

Viedt, C., Vogel, J., Athanasiou, T., Shen, W., Orth, S. R., Kubler, W. and Kreuzer, J. (2002) 'Monocyte chemoattractant protein-1 induces proliferation and interleukin-6 production in human smooth muscle cells by differential activation of nuclear factor-kappaB and activator protein-1.' *Arterioscler Thromb Vasc Biol*, 22(6), Jun 1, pp. 914-920.

Wajngarten, M. and Silva, G. S. (2019) 'Hypertension and Stroke: Update on Treatment.' *European Cardiology Review*, 14(2), Sum, pp. 111-115.

Wang Q, T. X., Yenari MA. (2007) 'The inflammatory response in stroke.' *J Neuroimmunol*, 1(2) pp. 53-68.

Wang, Q. W., Zhu, X. J., Xu, Q., Ding, X., Chen, Y. E. and Song, Q. (2005) 'Effect of C-reactive protein on gene expression in vascular endothelial cells.' *American Journal of Physiology-Heart and Circulatory Physiology*, 288(4), Apr, pp. H1539-H1545.

Webster, J. D. and Vucic, D. (2020) 'The Balance of TNF Mediated Pathways Regulates Inflammatory Cell Death Signaling in Healthy and Diseased Tissues.' *Front Cell Dev Biol*, 8 20200521, p. 365.

Wevers, N. R., Nair, A. L., Fowke, T. M., Pontier, M., Kasi, D. G., Spijkers, X. M., Hallard, C., Rabussier, G., et al. (2021) 'Modeling ischemic stroke in a triculture neurovascular unit on-a-chip.' *Fluids and Barriers of the Cns*, 18(1), Dec 14,

Wouters, E., de Wit, N. M., Vanmol, J., van der Pol, S. M. A., Hof, B. V., Sommer, D., Loix, M., Geerts, D., et al. (2019) 'Liver X Receptor Alpha Is Important in Maintaining Blood-Brain Barrier Function.' *Frontiers in Immunology*, 10, Jul 31,

Wu, X., Yu, T., Xu, H., Sun, X., Kou, D. and Li, L. (2018) 'Morphological and functional changes of microglia cultured under different oxygen concentrations and the analysis of related mechanisms.' *Exp Ther Med*, 15(2), Feb, 20171205, pp. 2015-2019.

Yang, C., Hawkins, K. E., Dore, S. and Candelario-Jalil, E. (2019) 'Neuroinflammatory mechanisms of blood-brain barrier damage in ischemic stroke.' *Am J Physiol Cell Physiol*, 316(2), Feb 1, 20181031, pp. C135-C153.

Yao, Z., Zhang, Y. and Wu, H. (2019) 'Regulation of C-reactive protein conformation in inflammation.' *Inflamm Res*, 68(10), Oct, 20190716, pp. 815-823.

Yao, Z. Y., Zhang, Y. M. and Wu, H. B. (2019) 'Regulation of C-reactive protein conformation in inflammation.' *Inflammation Research*, 68(10), Oct, pp. 815-823.

Youssef, B. B. (2016) 'Chapter 19 - Cellular Automata-Based Modeling of Three-Dimensional Multicellular Tissue Growth.' *In* Quoc Nam Tran, H. R. A., Computing, I. E. T. i. C. S. a. A., Emerging Trends in Applications and Infrastructures for Computational Biology, B., and Systems Biology, and Morgan Kaufmann (eds.) *Systems and Applications*
Emerging Trends in Computer Science and Applied Computing. Vol. 287-303.

Yu, L. T., Su, X. J., Li, S. P., Zhao, F. Y., Mu, D. Z. and Qu, Y. (2020) 'Microglia and Their Promising Role in Ischemic Brain Injuries: An Update.' *Frontiers in Cellular Neuroscience*, 14, Jul 10,

Zakrzewski, W., Dobrzynski, M., Szymonowicz, M. and Rybak, Z. (2019) 'Stem cells: past, present, and future.' *Stem Cell Research & Therapy*, 10, Feb 26,

Zeinolabediny, Y., Kumar, S. and Slevin, M. (2021) 'Monomeric C-Reactive Protein - A Feature of Inflammatory Disease Associated With Cardiovascular Pathophysiological Complications?' *In Vivo*, 35(2), Mar-Apr, pp. 693-697.

Zhang, J. M. and An, J. (2007) 'Cytokines, inflammation, and pain.' *Int Anesthesiol Clin*, 45(2), Spring, pp. 27-37.

Zhang, S. X. (2019) 'Microglial activation after ischaemic stroke.' *Stroke and Vascular Neurology*, 4(2), Jun, pp. 71-74.

Zhang, Y. and Cao, H. (2020) 'Monomeric C-reactive protein affects cell injury and apoptosis through activation of p38 mitogen-activated protein kinase in human coronary artery endothelial cells.' *Bosn J Basic Med Sci*, 20(4), Nov 2, 20201102, pp. 487-494.

Zhang, Y., Deng, Z., Li, Y., Yuan, R., Yang, M., Zhao, Y., Wang, L., Zhou, F., et al. (2020) 'Mesenchymal Stem Cells Provide Neuroprotection by Regulating Heat Stroke-Induced Brain Inflammation.' *Front Neurol*, 11 20200505, p. 372.

Zhang, Z., Yang, Y., Hill, M. A. and Wu, J. (2012) 'Does C-reactive protein contribute to atherothrombosis via oxidant-mediated release of pro-thrombotic factors and activation of platelets?' *Frontiers in physiology*, 3(433) pp. 1-6.

Zhao, L., Lei, W., Deng, C., Wu, Z., Sun, M., Jin, Z., Song, Y., Yang, Z., et al. (2021) 'The roles of liver X receptor alpha in inflammation and inflammation-associated diseases.' *J Cell Physiol*, 236(7), Jul, 20201210, pp. 4807-4828.

Zhao, S. C., Ma, L. S., Chu, Z. H., Xu, H., Wu, W. Q. and Liu, F. D. (2017) 'Regulation of microglial activation in stroke.' *Acta Pharmacologica Sinica*, 38(4), Apr, pp. 445-458.

Zheng, H., Zhang, B., Chhatbar, P. Y., Dong, Y., Alawieh, A., Lowe, F., Hu, X. and Feng, W. (2018) 'Mesenchymal Stem Cell Therapy in Stroke: A Systematic Review of Literature in Pre-Clinical and Clinical Research.' *Cell Transplant*, 27(12), Dec, 20181022, pp. 1723-1730.

Zhong, Y., Li, S. H., Liu, S. M., Szmitko, P. E., He, X. Q., Fedak, P. W. M. and Verma, S. (2006) 'C-reactive protein upregulates receptor for advanced glycation end products expression in human endothelial cells.' *Hypertension*, 48(3), Sep, pp. 504-511.

Zhou, X., Zhang, F., Wang, D., Wang, J., Wang, C., Xia, K., Ying, L., Huang, X., et al. (2020) 'Micro Fragmented Adipose Tissue Promotes the Matrix Synthesis Function of Nucleus Pulposus Cells and Regenerates Degenerated Intervertebral Disc in a Pig Model.' *Cell Transplant*, 29, Jan-Dec, p. 963689720905798.

Zhu, H., Guo, Z. K., Jiang, X. X., Li, H., Wang, X. Y., Yao, H. Y., Zhang, Y. and Mao, N. (2010) 'A protocol for isolation and culture of mesenchymal stem cells from mouse compact bone.' *Nature Protocols*, 5(3) pp. 550-560.

Zhu, H., Hu, S. P., Li, Y. T., Sun, Y., Xiong, X. X., Hu, X. Y., Chen, J. J. and Qiu, S. (2022) 'Interleukins and Ischemic Stroke.' *Frontiers in Immunology*, 13, Jan 31,

Zuk, P. A., Zhu, M., Ashjian, P., De Ugarte, D. A., Huang, J. I., Mizuno, H., Alfonso, Z. C., Fraser, J. K., et al. (2002) 'Human adipose tissue is a source of multipotent stem cells.' *Molecular Biology of the Cell*, 13(12), Dec, pp. 4279-4295.

Appendix

Laser-Capture Microdissection for Measurement of Angiogenesis After Stroke

Mark Slevin, Xenia Sawkulycz, Laura Combes, Baoqiang Guo, Wen-Hui Fang, Yasmin Zeinolabediny, Donghui Liu, Glenn Ferris, and Anna Ludlaim

Abstract

Laser capture microdissection has been around for almost a decade now. It has shown great promise for identification and determination of differences between activity and health of cells or even a single cell compared with its neighboring, local, or adjacent tissue inhabitants. Here we will provide a background to its use in neurological and cardiovascular fields and indicate a detailed methodological approach for successful RNA capture and analysis by one of the many current profiling systems available for pattern recognition.

Key words Laser capture microdissection, Stroke, RNA/DNA, Angiogenesis

biomedicines

MDPI

Article

Antibody Protection against Long-Term Memory Loss Induced by Monomeric C-Reactive Protein in a Mouse Model of Dementia

Elisa García-Lara [1], Samuel Aguirre [1], Núria Clotet [1], Xenia Sawkulycz [2], Clara Bartra [1], Lidia Almenara-Fuentes [1], Cristina Suñol [1], Rubén Corpas [1], Peter Olah [3], Florin Tripon [3], Andrei Crauciuc [3], Mark Slevin [2,3,*] and Coral Sanfeliu [1,*]

[1] Institut d'Investigacions Biomèdiques de Barcelona (IIBB), CSIC and IDIBAPS, 08036 Barcelona, Spain; elisaglara21@gmail.com (E.G.-L.); samuelaguirreinfantes@gmail.com (S.A.); nuria.cg07@gmail.com (N.C.); clara.bartra@iibb.csic.es (C.B.); almenara.lidia.22@gmail.com (L.A.-F.); cristina.sunol@iibb.csic.es (C.S.); rubencorpas@gmail.com (R.C.)

[2] School of Life Sciences, John Dalton Building, Manchester Metropolitan University, Manchester M15 6BH, UK; XENIA.SAWKULYCZ@stu.mmu.ac.uk

[3] Genetics Department, George Emil Palade University of Medicine, Pharmacy, Science and Technology of Targu Mures, 540142 Targu Mures, Romania; olah_peter@yahoo.com (P.O.); tripon.florin.2010@gmail.com (F.T.); andrei.crauciuc@gmail.com (A.C.)

* Correspondence: M.A.Slevin@mmu.ac.uk (M.S.); coral.sanfeliu@iibb.csic.es (C.S.); Tel.: +44-(0)-161-247-1172 (M.S.); +34-93-363-8338 (C.S.)

check for updates

Citation: García-Lara, E.; Aguirre, S.; Clotet, N.; Sawkulycz, X.; Bartra, C.; Almenara-Fuentes, L.; Suñol, C.; Corpas, R.; Olah, P.; Tripon, F.; et al. Antibody Protection against Long-Term Memory Loss Induced by Monomeric C-Reactive Protein in a Mouse Model of Dementia. *Biomedicines* **2021**, *9*, 828. https://doi.org/10.3390/biomedicines9070828

Academic Editors: Arnab Ghosh and Masaru Tanaka

Received: 6 May 2021
Accepted: 12 July 2021
Published: 16 July 2021

Publisher's Note: MDPI stays neutral with regard to jurisdictional claims in published maps and institutional affiliations.

Abstract: Monomeric C-reactive protein (mCRP), the activated isoform of CRP, induces tissue damage in a range of inflammatory pathologies. Its detection in infarcted human brain tissue and its experimentally proven ability to promote dementia with Alzheimer's disease (AD) traits at 4 weeks after intrahippocampal injection in mice have suggested that it may contribute to the development of AD after cerebrovascular injury. Here, we showed that a single hippocampal administration of mCRP in mice induced memory loss, lasting at least 6 months, along with neurodegenerative changes detected by increased levels of hyperphosphorylated tau protein and a decrease of the neuroplasticity marker *Egr1*. Furthermore, co-treatment with the monoclonal antibody 8C10 specific for mCRP showed that long-term memory loss and tau pathology were entirely avoided by early blockade of mCRP. Notably, 8C10 mitigated *Egr1* decrease in the mouse hippocampus. 8C10 also protected against mCRP-induced inflammatory pathways in a microglial cell line, as shown by the prevention of increased generation of nitric oxide. Additional in vivo and in vitro neuroprotective testing with the anti-inflammatory agent TPPU, an inhibitor of the soluble epoxide hydrolase enzyme, confirmed the predominant involvement of neuroinflammatory processes in the dementia induced by mCRP. Therefore, locally deposited mCRP in the infarcted brain may be a novel biomarker for AD prognosis, and its antibody blockade opens up therapeutic opportunities for reducing post-stroke AD risk.

Keywords: monomeric C-reactive protein (mCRP); biomarker; Alzheimer's disease; mouse model of mCRP dementia

1. Introduction

Sustained neuroinflammation is a risk factor for age-related diseases, including cerebrovascular injuries and Alzheimer's disease (AD) [1,2]. Systemic inflammatory conditions may trigger or aggravate a range of cardiovascular and metabolic diseases that also contribute to brain dysfunction and dementia [3,4]. Indeed, inflammatory processes are increasingly being considered the culprits of frailty and disease in the elderly. As a result, the search for reliable inflammatory biomarkers and intervention targets to combat dementia and other disabling conditions has intensified.

C-reactive protein (CRP) is a widely used peripheral marker of inflammatory processes. It was identified by Tillet and Francis in 1930 in the blood of patients with pneumococcal

> Neurobiol Aging. 2020 Aug;92:75-81. doi: 10.1016/j.neurobiolaging.2020.04.008.
Epub 2020 Apr 15.

Regulation of interleukin 6 by a polymorphic CpG within the frontal cortex in Alzheimer's disease

Xenia Sawkulycz [1], Steven Bradburn [1], Andrew Robinson [2], Antony Payton [3], Neil Pendleton [3], Chris Murgatroyd [4]

Affiliations + expand

PMID: 32408055 DOI: 10.1016/j.neurobiolaging.2020.04.008

Abstract

The cytokine interleukin 6 (IL-6) has been linked to the pathogenesis of Alzheimer's disease (AD). This is the first study to investigate the genetic and epigenetic interactions in the control of IL-6 in human brain and its relation to AD neuropathology in prefrontal cortex tissues from AD and controls genotyped for the SNP -174 C/G rs1800795, a polymorphic CpG in which the G allele creates a CpG site. Within CC homozygotes there were significantly higher brain levels of IL-6 protein compared to G allele carriers. The C allele that resulted in an absence of methylation at a CpG was also associated with significant changes in methylation at neighboring CpGs. Furthermore, there were significant differences in methylation between CC and CG/GG at CpG sites in the AD and control groups. That DNA methylation was altered in the brains by the presence of rs1800795, which further correlated with protein levels suggests the presence of a polymorphic CpG and genetic-epigenetic interactions in the regulation of IL-6 in the prefrontal cortex within AD brains.

Keywords: Alzheimer's disease; DNA methylation; Epigenetic; Interleukin-6; Neuroinflammation; Prefrontal cortex.

Article Navigation > Biophysics Reports > 2021 > 7(2): 81-90

Citation: Combes Laura, Sawkulycz Xenia, Fang Wen-Hui, Guo Baoqiang, Slevin Mark. Potential of adipose derived stem cell preparations in neurological repair and regeneration[J]. *Biophysics Reports*, 2021, 7(2): 81-90. doi: 10.52601/bpr.2021.200025

Potential of adipose derived stem cell preparations in neurological repair and regeneration

doi: 10.52601/bpr.2021.200025

Combes Laura[1], Sawkulycz Xenia[1], Fang Wen-Hui[2], Guo Baoqiang[1], Slevin Mark[1]

1. Department of Life Sciences, Manchester Metropolitan University, Manchester, UK
2. Department of Biological and Geographical Sciences University of Huddersfield, Huddersfield, UK

+More Information

Abstract

Stem cell therapy is a promising treatment for neurogenerative disease as well as inflammatory and immune mediated diseases. Decades of preclinical research has demonstrated stem cell ability to differentiate into multiple cell lineages and be utilised in regeneration and repair with their immunomodulatory and immunosuppressive properties. This work has provided the fundamental scientific knowledge needed to launch various clinical trials studying stem cell therapy in autoimmune disorders, stroke, and other tissue injury. Despite the early success many of these promising therapies are yet to breakthrough into clinical use. In this review, we highlight the recent developments in the use of stem cells as therapeutic agents for neurological conditions as well as their failures and how the clinical translation can be improved.

Keywords: Adipose derived mesenchymal stem cells, Micro-fragmented adipose tissue, Suicide gene therapy